TNIK, A NOVEL ANDROGEN RECEPTOR-REPRESSED GENE, IS A POTENTIAL BIOMARKER FOR NEUROENDOCRINE PROSTATE CANCER

by

Ka Mun Nip

B.Sc., Simon Fraser University, 2009

A THESIS SUBMITTED IN PARTIAL FULFILLMENT OF

THE REQUIREMENTS FOR THE DEGREE OF

MASTER OF SCIENCE

in

THE FACULTY OF GRADUATE AND POSTDOCTORAL STUDIES

(Experimental Medicine)

THE UNIVERSITY OF BRITISH COLUMBIA

(Vancouver)

December 2017

Abstract

Traf2- and Nck-interacting kinase (TNIK) is a serine/threonine kinase upregulated and amplified in pancreatic and gastric cancer respectively. TNIK has also been identified as a potential therapeutic target of colorectal cancer. However, the role of TNIK in prostate cancer (PCa) has not been investigated.

Interrogating public human PCa patient data, we found that TNIK expression is associated with an aggressive form of PCa termed neuroendocrine prostate cancer (NEPC). Treatment-induced NEPC can arise as a consequence of strong selective pressure from androgen receptor (AR) pathway inhibition. Clinically, TNIK expression is positively correlated with neuroendocrine (NE) markers and inversely correlated with androgen regulated genes. In agreement, our *in vitro* studies reveal that TNIK expression is increased under AR pathway inhibition. We found that TNIK is transcriptionally repressed by androgen via direct binding of the AR at the TNIK locus.

Through gain of function studies, we demonstrated that TNIK is not required for NE differentiation. Likewise, loss of function studies using siRNA or small molecule inhibitors targeting TNIK did not have significant effect on the growth of Enzalutamide-resistant cells with NE phenotype *in vitro*. Overall, our results indicate that TNIK may serve as a possible biomarker for NEPC.

Lay Summary

Prostate cancer (PCa) cells are dependent on the androgen receptor (AR) for growth and survival; therefore, treatments for PCa are focused on targeting AR. With the clinical integration of highly potent AR-targeted drugs, more aggressive and treatment resistant forms of PCa have emerged in patients. Accordingly, new strategies and effective therapies are needed for targeting this disease. In this study, we found that a gene, *TNIK*, was highly expressed in a lethal type of treatment-resistant PCa termed neuroendocrine prostate cancer (NEPC). Therefore, we performed experiments to study the role of TNIK in NEPC. Results from this study indicate that TNIK could be used as a biomarker for NEPC.

Preface

This thesis is composed of my original work that was carried out during the completion of my MSc program. The research work presented in this thesis will be submitted in a manuscript for publication:

TNIK, a novel androgen receptor-repressed gene, is a potential biomarker for neuroendocrine prostate cancer. Ka Mun Nip, Alastair Davies, Daksh Thaper, Sepideh Vahid, Kirsi Ketola, Jennifer Bishop, Amina Zoubeidi.

The concept and design of this work were conceived by myself and my supervisor, Dr. Amina Zoubeidi. All experiments and data analysis were performed by myself throughout the course of my thesis. Public data mining was performed by myself with the guidance of Dr. Alastair Davies and Mr. Daksh Thaper. Dr. Alastair Davies, Mr. Daksh Thaper, Ms. Sepideh Vahid provided valuable feedbacks on experimental design and results. Dr. Kirsi Ketola and Dr. Jennifer Bishop also provided helpful comments during the early stage of this study. The manuscript was drafted by myself and reviewed by Dr. Alastair Davies and Dr. Amina Zoubeidi.

Table of Contents

List of Tables

List of Figures

List of Abbreviations

Adeno	Prostatic adenocarcinoma
ADT	Androgen deprivation therapy
APC	Adenomatous polyposis coli
AR	Androgen receptor
ARE	Androgen response element
bp	Base pair
ChIP	Chromatin immunoprecipitation
CRPC	Castration-resistant prostate cancer
CSC	Cancer stem cell
CSS	Charcoal stripped serum
DHT	Dihydrotestosterone
EMT	Epithelial-mesenchymal transition
ENZ	Enzalutamide
ENZR	Enzalutamide-resistant
FBS	Fetal bovine serum
FSH	Follicle-stimulating hormone
GCK	Germinal center kinase
GEM	Genetically engineered mouse
GnRH	Gonadotropin-releasing hormone
JNK	c-Jun N-terminal kinase
LH	Luteinizing hormone
NCAM1	Neural cell adhesion marker 1
NE	Neuroendocrine
NEPC	Neuroendocrine prostate cancer
PAP	Prostatic acid phosphatase
PCa	Prostate cancer
PCR	Polymerase chain reaction
PDX	Patient derived xenograft
PSA	Prostate specific antigen
qPCR	Quantitative real-time PCR
RNA-seq	RNA sequencing
RT-PCR	Reverse transcription polymerase chain reaction
Ste20	Sterile20
TCF4	T-cell factor-4
TCGA	The Cancer Genome Atlas
TGF-β1	Transforming growth factor beta 1
TNFR	Tumor necrosis factor receptor
TNIK	Traf2- and Nck-interacting kinase

Acknowledgements

First, I would like to express my greatest appreciation and thanks to my supervisor, Dr. Amina Zoubeidi, for providing me with the biggest support and guidance throughout my MSc program. Dr. Zoubeidi is not just my supervisor, she is also an important mentor in my life and career. She provided the biggest opportunity for me to develop my personal and research skills. Without her constant support and encouragement, my MSc study and research career would not be successful.

Second, I would like to thank my thesis committee, Dr. Vincent Duronio and Dr. Christopher Ong, for generously offering their time, support, and guidance throughout my MSc degree. I really appreciated them for spending their time in providing all the valuable comments and feedbacks in the preparation and review of this thesis. I would also like to thank Dr. Caigan Du and Dr. Emma Guns for their time and support to be the external examiner and chair for my thesis defense.

Third, I would like to thank all my lab mates, especially Alastair, Sepideh, Daksh, Jenna, Kirsi for all the helpful comments, support, and suggestion. I would also like to thank Eliana, Fraser, and Soojin for their friendship supports in the lab. Without their supports and advices, I would not be able to overcome the challenges throughout my MSc degree.

Finally, I would like to thank my parents and my brother for all the support in helping me get through the difficult moments throughout my life. Without them consistently cheering me up when I felt challenged, I would not be able to keep myself moving forward in my MSc study.

To my family, for their endless love and support

Chapter 1: Introduction

1.1 Traf2- and Nck-interacting kinase (TNIK)

1.1.1 Overview

Traf2- and Nck-interacting kinase (TNIK) was first discovered as an interaction partner for adaptor proteins Traf2 and Nck in a yeast two-hybrid screening in 1999 [1]. TNIK is a serine/threonine kinase that belongs to the sterile 20 (Ste20) kinase family [1]. Members of the Ste20 kinase family share homology to Ste20p, a kinase that is required in the mating pathway in budding yeast *Saccharomyces cerevisiae* [2, 3]. The Ste20 kinase family is divided into two groups based on the location of the kinase domain: p21-activated protein kinases (PAKs) and germinal center kinases (GCKs) [4].

The structure of PAKs consists of a C-terminal kinase domain and an N-terminal GTPase binding domain [4]. In general, PAKs can be activated by the binding of small GTPases Rac1 and Cdc42 [5]. PAKs play a key role in regulating cellular events such as cell cycle progression, cytoskeletal dynamics, cell proliferation, and apoptosis [6]. Upregulation or hyperactivation of PAKs has been observed in various types of cancer such as breast, ovarian, and pancreatic cancers [7]. Aberrant activation of PAK signaling promoted cancer cell growth, inhibited apoptosis, activated invasion and metastasis, which contribute to the hallmarks of cancer and drug resistance [8-10]. Therefore, PAKs are attractive therapeutic targets for cancer.

On the other hand, the structure of kinases in the GCK family consists of an N-terminal kinase domain and a C-terminal regulatory domain [4]. Kinases in the GCK family are known to regulate cellular processes such as ion transport, apoptosis, and cytoskeletal reorganization [11]. Recent studies have shown that some kinases in the GCK family are also involved in immune regulation [12]. Since there is variation in the protein structure, kinases in the GCK family are

further divided into eight subfamilies. TNIK belongs to the GCK-IV subfamily, which includes Mitogen-activated protein kinase kinase kinase kinase 4 (MAP4K4), Misshapen-like kinase 1 (MINK1), and NIK-related kinase (NRK) [3]. Among the GCK IV subfamily kinases, TNIK is closely related to MAP4K4 and MINK1. TNIK has highest homology to MAP4K4 sharing 90% of amino acid identity at the kinase domain and 88% at the GCKH domain [1].

Structurally, each of the GCK-IV subfamily kinases is comprised of an N-terminal kinase domain, an intermediate domain, and a GCK homology (GCKH) regulatory domain [3]. The GCKH domain is also found in GCK-I subfamily kinases, but the homology of GCKH domain between GCK-I and GCK-IV subfamily kinases is only 20% [4]. The specific function of GCKH domain is not known, but it has been shown to play a role in protein-protein interaction. For example, MINK1 and TNIK have been shown to bind to Ras GTPase Rap2 via their GCKH domains and induce phosphorylation of postsynaptic scaffold protein TANC1 [13-15]. The interaction of GCKH domain of MAP4K4 with MEKK1 protein is required for inducing c-Jun N-terminal kinase (JNK) activation [16]. The GCKH domain is also found in human Vam6p protein and is required for lysosome clustering and fusion [17].

1.1.2 Structure of TNIK

The TNIK gene is located on human chromosome 3 at the locus 3q26.2-q26.31 [3]. It encodes a protein that consists of 1360 amino acids with a molecular weight of 155 kDa [14]. The structure of TNIK protein has an N-terminal kinase domain (amino acids 25-288), an intermediate domain (amino acids 289-1041), and a C-terminal GCKH domain (amino acids 1042-1340) [14]. The intermediate domain of TNIK has three known alternative splicing sites at amino acids 447-475, 537-591, and 795-802, which results in eight possible transcript variants

(**Figure 1.1**) [1]. Specific biological function of each TNIK protein isoforms has not been reported.

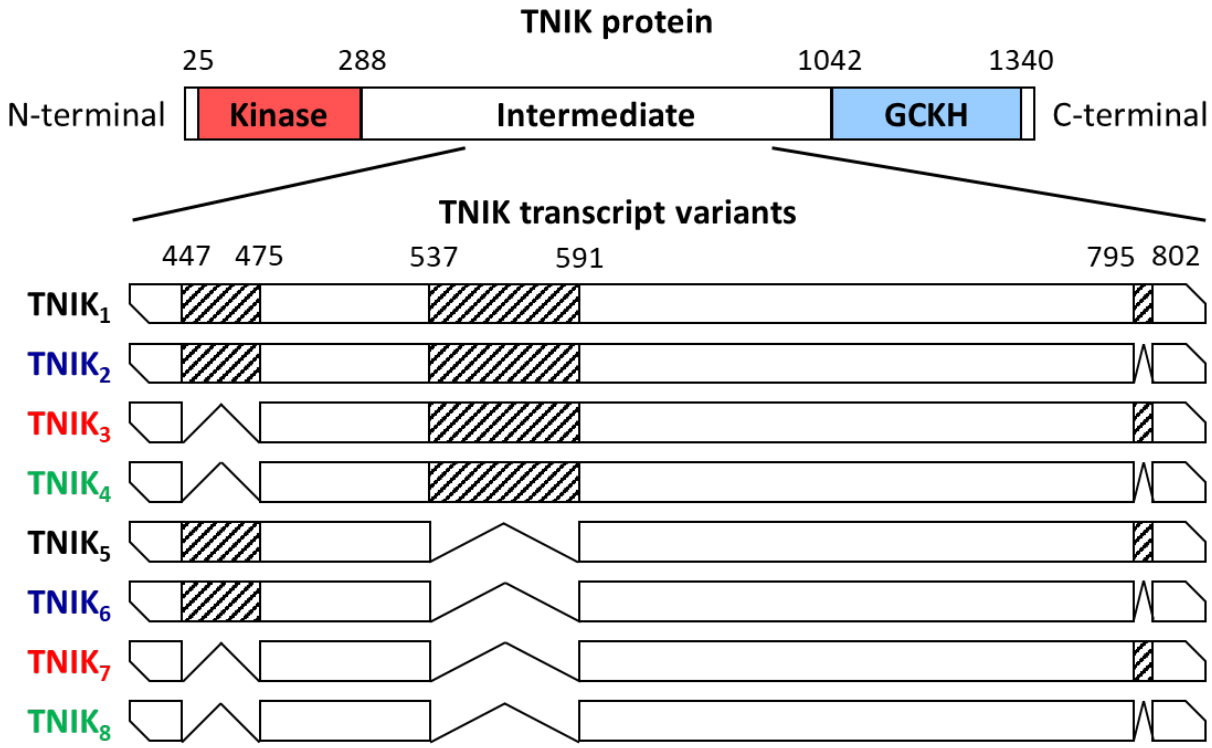

Figure 1.1 Structure of TNIK protein and transcript variants

The structure of TNIK protein consists of an N-terminal kinase domain, an intermediate domain, and a C-terminal GCKH domain. The intermediate domain of TNIK has three alternative splicing sites generated eight different transcript variants (Adapted from Fu et al., 1999 [1]).

1.1.3 Function of TNIK

When TNIK protein was first discovered, it was shown that TNIK interacted with Traf2 and Nck via its intermediate domain [1]. However, the role of these protein-protein interactions is not known yet. A study suggests that the signaling of a member of the tumor necrosis factor receptor (TNFR) family, CD27, is linked to activation of Wnt signaling through interaction of Traf2 and TNIK in leukaemia stem cells [18]. Traf2, TNFR-associated factor 2, is a member of

Traf family, which mediates TNFR signaling [19]. Nck is an adaptor protein containing Src-homology 2 and 3 domains and it plays a role in signal transduction from cell surface receptors to the actin cytoskeleton [20]. However, the precise downstream effect of TNIK and Nck interaction has not yet been reported. In the African clawed frog *Xenopus laevis*, Xenopus TNIK (XTNIK) was shown to be essential in axis formation in embryonic development via Wnt signaling [21]. Knockdown of XTNIK resulted in malformation in Xenopus embryos with loss of head and axis structures. In humans, TNIK is highly expressed in the heart, brain, and skeletal muscle [1]. TNIK has been reported to function in actin cytoskeleton and inhibiting cell spreading [1, 14]. In particular, the kinase domain of TNIK is required for cytoskeleton regulation, activation of Wnt signaling, and regulation of neurite growth [1, 22, 23]. The intermediate domain of TNIK interacts with other proteins such as Traf2, Nck, β-catenin, and Nedd4-1 [1, 22, 23]. The GCKH domain of TNIK mediates activation of JNK and interacts with Rap2 [1, 14].

Several proteomic studies found that TNIK is enriched at the postsynaptic density of neurons [24-26], but the functional role of TNIK in the brain is not well established yet. A loss of function mutation in *TNIK* resulted in truncated formation of TNIK protein is reported to be associated with intellectual disability in human [27]. In an *in vivo* study conducted by Coba et al., TNIK knockout mice exhibited hyperlocomotor behavior compared to wild type mice [28]. This finding suggests that TNIK regulates cognitive function in mice and potentially humans. In the same study, the authors also demonstrated that activation of glutamate receptors could modify TNIK phosphorylation at serine 735 (S735) in TNIK wildtype mice [28]. They showed that activation of metabotropic glutamate receptor 1 could increase TNIK S735 phosphorylation. This suggests that TNIK phosphorylation at the postsynaptic density may play a role in the

regulation of synaptic signal transduction. Moreover, phosphorylation of TNIK at serine 735 (S735) in mouse is homologous to serine 764 (S764) in human. The S764 residue was identified as a phosphorylation site of TNIK by liquid chromatography–tandem mass spectrometry and it had been proposed to be an autophosphorylation site of TNIK [29, 30]. This S764 phosphorylated form of TNIK has also been shown to translocate into the nucleus that interacts with the components of transcriptional complex in activated Wnt signaling [30].

TNIK has been reported to be amplified or upregulated in gastric and pancreatic cancer [31, 32]. In particular, TNIK is a biomarker in pancreatic cancer associated with poor prognosis [32]. Its functional role has been studied more intensively in colorectal cancer. In the majority of colorectal cancers carrying mutation in at least one gene in the Wnt signaling pathway, about 80% of colorectal cancers carry a loss-of-function mutation in adenomatous polyposis coli (APC) and 5% carry activating mutations in β-catenin [33]. Although the activating mutations in β-catenin and the loss-of-function mutation of APC were often found to be mutually exclusive, these genetic events both converge to yield constitutive activation of Wnt signaling [33, 34]. Notably, TNIK was identified to be required for activating Wnt signaling in colorectal cancer [22, 30]. In particular, it has been reported that TNIK-mediated phosphorylation of T-cell factor-4 (TCF4) at serine 154 in the nucleus leads to activated transcription of Wnt target genes through the TCF4/β-catenin transcriptional complex. In support, the TCF4/β-catenin transcription could be abrogated by inactive mutant of TNIK (K54R) with substitution at lysine 54 in the kinase domain [22, 30]. Knockdown of TNIK also decreased transcription of Wnt target genes and inhibited colorectal cancer cell proliferation *in vitro* and tumor growth *in vivo* [30].

1.1.4 TNIK as a therapeutic target for cancer

Since TNIK is a potential therapeutic target for human Wnt-activated colorectal cancer, development of TNIK inhibitors are currently focused on targeting the Wnt signaling pathway [35-37]. TNIK inhibitors are currently under preclinical development. Among these inhibitors, NCB-0846 is a small-molecule TNIK inhibitor that has been reported to have anti-Wnt activity and anti-cancer stem cell activity in colorectal cancer [38]. NCB-0846 was designed to bind to TNIK in its inactive conformation.

Another small-molecule TNIK inhibitor, KY-05009, was also shown to inhibit epithelial-mesenchymal transition (EMT) in human lung cancer cells that was mediated by transforming growth factor beta 1 (TGF-β1) [39]. TGF-β1 is a cytokine that has been shown to induce EMT and promoted cancer progression [40]. EMT is an important process in embryonic development of tissues and organs, but cancer cells often hijack this process to acquire migratory and invasive properties [41].

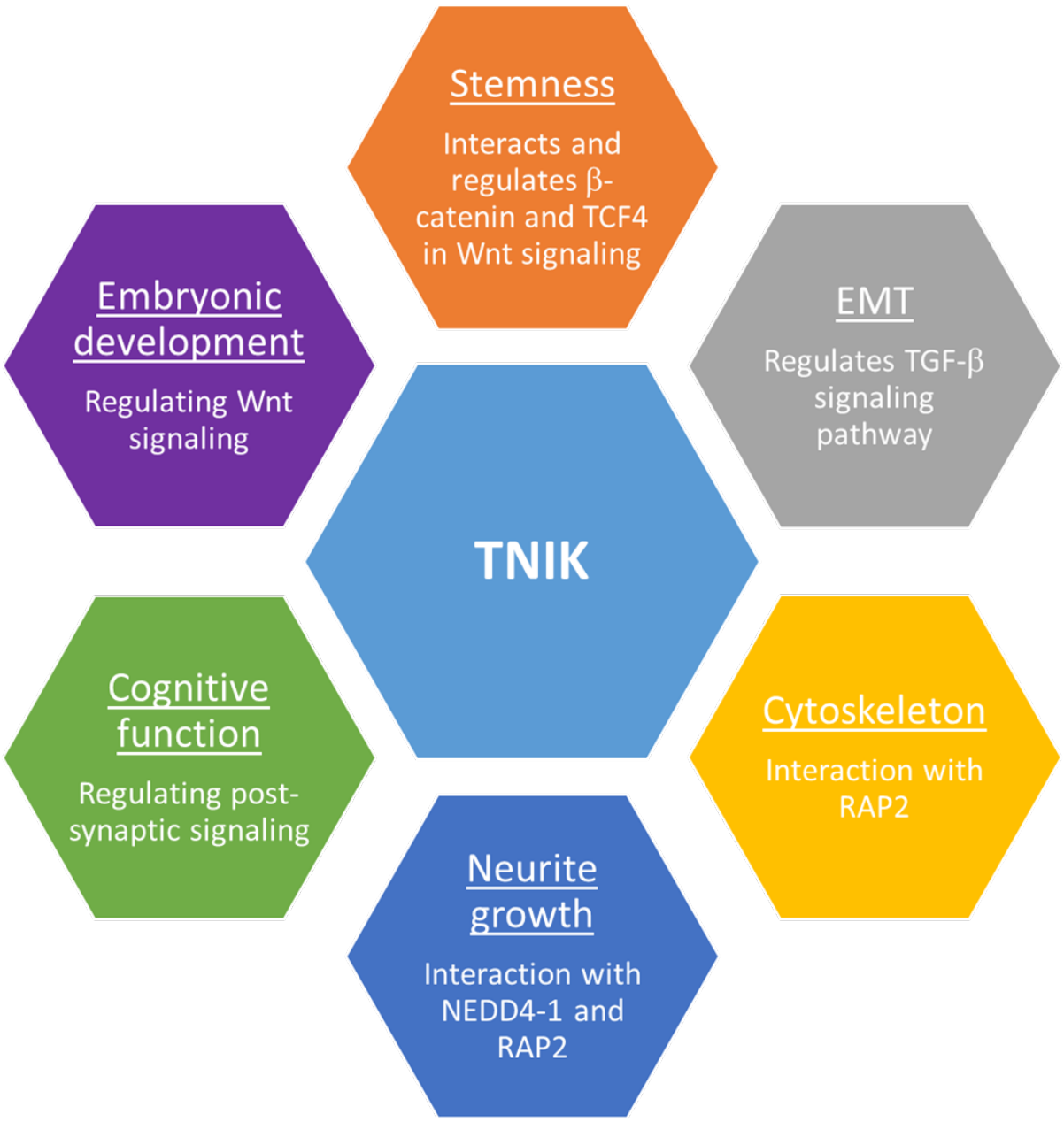

Figure 1.2 Schematic summary on the functions of TNIK

A schematic summary on the functions of TNIK. TNIK has been reported to be involved in Wnt signaling, cytoskeleton regulation, cognitive function, neurite growth, and EMT [14, 21-23, 28, 30, 38, 39].

1.2 Prostate cancer (PCa)

1.2.1 Overview

Based on Canadian Cancer Statistics, an estimate of 21,300 cases of prostate cancer (PCa) would be diagnosed in Canadian men and it would expect to have 4,100 deaths from the disease in the year of 2017 [42]. PCa is the most common cancer and the third leading cause of cancer-related death in Canadian men [42]. An estimate of 1 in 7 Canadian men is expected to develop PCa in their lifetime and 1 in 29 men will die from the disease [42]. Until now, multiple systemic therapies could prolong the survival of patients with metastatic PCa, but the disease could still develop treatment resistance and eventually lead to death.

1.2.2 The prostate

The prostate gland is only found in men and it surrounds the urethra and is located below the bladder and in front of the rectum in the pelvic cavity [43]. As an exocrine gland of the male reproductive system, the prostate produces prostatic fluid enriched in zinc ion, citrate, and kallikreins [44]. The prostatic fluid makes up about 20 to 30% of the seminal fluid and it contributes in bringing the necessary condition to aid in the biological processes for sperms to fertilize eggs [44]. In embryonic development, the prostate develops during the third fetal month, and results from epithelial invaginations of the posterior urogenital sinus [45]. The urogenital sinus is an embryonic structure that develops into reproductive and urinary organs. During this process, circulating fetal testosterone is required for stimulating androgen receptor (AR) in the urogenital sinus mesenchyme, which induces prostatic budding, proliferation, and differentiation to form the ductal structures [45]. The prostate gland in childhood is small with a weight around two grams and grows to the size of a walnut with an average weight of 20 grams at puberty [45].

The prostate gland consists of glandular epithelium embedded in a fibromuscular stroma [44]. The fibromuscular stroma is mainly composed of smooth muscle cells, endothelial cells, fibroblasts, nerve cells, and immune cells [46]. The glandular epithelium of the prostate consists of three types of epithelial cells: secretory luminal cells, basal epithelial cells, and neuroendocrine (NE) cells (**Figure 1.3**). Secretory luminal cells locate along the glandular lumen and form the inner layer of the prostate epithelium [47]. Secretory luminal cells are columnar and express AR, as well as cytokeratins 8 and 18 [48]. These cells are responsible of producing enzymes, such as prostate specific antigen (PSA) and prostatic acid phosphatase (PAP), that are secreted into the glandular lumina [48]. Being both androgen-independent and non-secretory, basal epithelial cells separate secretory luminal cells from the basement membrane and form the outer layer of the prostate epithelium [47]. Basal epithelial cells are cuboidal and express p63, and cytokeratins 5 and 14 [48]. NE cells are a small population of epithelial cells irregularly distributed within the two layers of basal epithelial and secretory luminal cells. NE cells are terminally differentiated, non-proliferative, and androgen-independent [48]. They do not express AR and PSA. Prostatic NE cells secrete neuropeptides such as bombesin, calcitonin, and serotonin that are proposed to maintain homeostasis of surrounding epithelial cells [49].

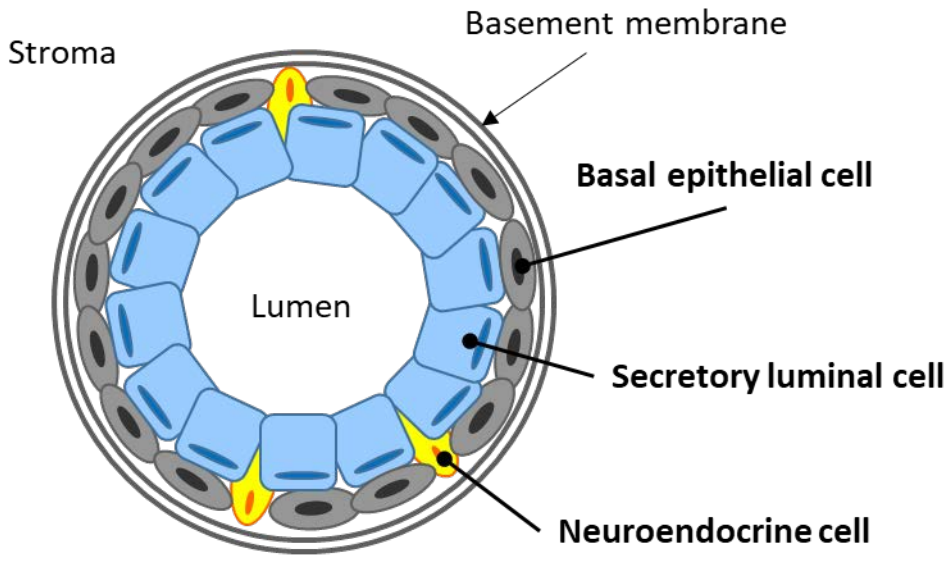

Figure 1.3 Microscopic structure of the prostate epithelium

Basal epithelial, secretory luminal, and neuroendocrine cells in the prostatic epithelium (Adapted from Barron and Rowley, 2012 [46]).

1.2.3 Androgen and androgen receptor (AR) signaling

Androgens are male sex hormones that are essential in the development of male phenotypes during embryogenesis [50]. In adulthood, androgens are responsible for maintenance of male reproductive function and behavior [50]. Testosterone is the predominate androgen that is produced by the testes in men. Small amount of androgens such as androstenedione and dehydroepiandrosterone (DHEA) are produced by the adrenal glands. Free testosterone enters the prostate cells and is converted to a more potent androgen, dihydrotestosterone (DHT), by the enzyme 5-alpha-reductase [51]. DHT has 5-fold higher affinity for AR than testosterone [52]. DHT is the primary ligand for AR.

In men, androgen biosynthesis and spermogenesis are regulated by the hypothalamic-pituitary-gonadal axis. Hypothalamus releases gonadotropin-releasing hormone (GnRH), which

stimulates the secretion of follicle-stimulating hormone (FSH) and luteinizing hormone (LH) from the anterior pituitary gland [53, 54] (**Figure 1.4**). LH and FSH travel through the bloodstream to the testes. LH stimulates the Leydig cells in the testes for testosterone synthesis and secretion. FSH acts on the Sertoli cells and stimulates sperm production [54]. Gonadal peptide hormone, inhibin, is also produced by the Sertoli cells from stimulation of FSH. High levels of testosterone in turn reduce the release of GnRH and LH from hypothalamus and anterior pituitary gland in a negative feedback mechanism [53]. Inhibin also exerts a negative feedback control on FSH secretion from the anterior pituitary gland.

Androgen receptor (AR), also known as NR3C4 (nuclear receptor subfamily 3, group C, gene 4), is a member of the steroid hormone nuclear receptor family with the estrogen receptor, glucocorticoid receptor, progesterone receptor, and mineralocorticoid receptor [55]. The AR gene is located on the X chromosome at locus Xq11-Xq12 and it encodes a protein that consists of 919 amino acids with a molecular weight of 110 kDa [56]. The structure of AR protein consists of a ligand-independent N-terminal transactivation domain, a DNA-binding domain, a hinge region, and a ligand binding domain [55]. AR is a ligand-regulated transcription factor, which is activated by the binding of its ligand androgen.

Androgen receptor (AR) signaling is initiated when androgen binds to the ligand binding domain of AR in the cytoplasm [57]. When not bound to androgen, AR is bound by a complex of heat shock protein 90 (Hsp90) and other co-chaperones to maintain a conformation that enables ligand binding. Binding of ligand to AR induces conformational change and dissociation of AR from the heat shock protein complex. Ligand-bound AR translocates to the nucleus where it dimerizes and binds to the androgen response element (ARE) of target genes, such as *PSA*, *TMPRSS2*, *FKBP5*, and *NKX3.1*, initiating transcription. The ARE is comprised of two 6-base

pair (bp) half-site repeats 5'-TGTTCT-3' separated by 3 nucleotides and is typically located in the promoter or enhancer of target genes [56].

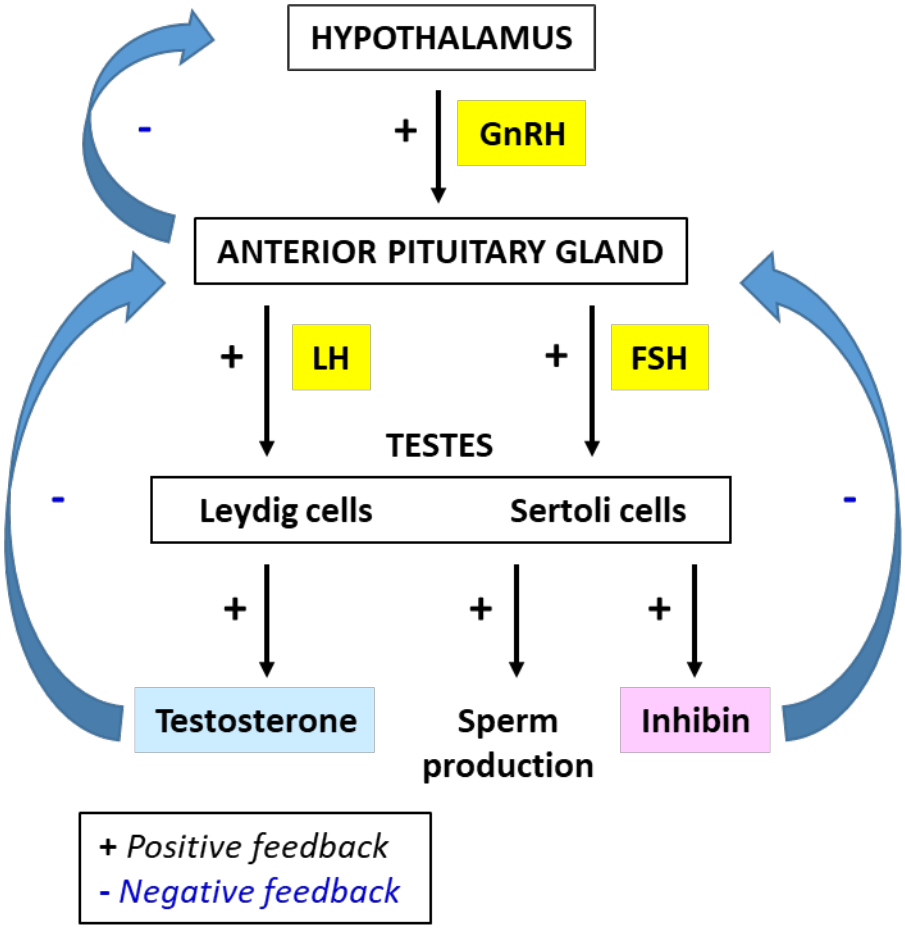

Figure 1.4 Hypothalamus-pituitary-gonadal axis

Secretion of luteinizing hormone (LH) and follicle-stimulating hormone (FSH) from the anterior pituitary gland is stimulated by gonadotropin releasing hormone (GnRH) produced from the hypothalamus. LH and FSH induce testosterone synthesis, sperm production, and inhibin secretion in the testes. Testosterone and inhibin exert negative feedback control on hormones release from the hypothalamus and anterior pituitary gland.

1.2.4 Castration resistant prostate cancer (CRPC)

Current detection methods for PCa include abnormal digital rectum examination and testing for elevated serum PSA level (greater than 4 ng/mL), followed by transrectal ultrasound guided biopsy of the prostate gland [58]. Surgery, radiotherapy, and active surveillance are treatment options for early stage of localized PCa [59]. Advanced PCa may spread to nearby tissues and metastasize to the bones, lymph nodes, or other parts of the body. Since Huggins and Hodge first demonstrated that PCa cells were dependent on the presence of androgens for growth in 1944, androgen deprivation therapy (ADT) has been the first-line hormone therapy for locally advanced or metastatic PCa [60]. ADT impedes the growth of PCa cells by reducing the level of male hormone androgen in the body. To lower male androgen production, ADT can be performed by surgical castration using bilateral orchiectomy or by chemical castration using GnRH agonists or antagonists [61].

PCa initially would respond to ADT, but it would relapse after a median of 18 to 24 months and progress to a more aggressive stage of the disease termed castration resistant prostate cancer (CRPC) [62]. PCa progress to CRPC from an androgen-dependent state to an androgen-independent state. CRPC is still considered to be dependent on AR signaling. Therefore, second generation anti-androgens such as abiraterone acetate and enzalutamide (ENZ) are used to target AR signaling [63-66]. These agents function to blunt AR signaling through inhibition of androgen synthesis or competitively binding to AR, respectively. Although these treatment prolonged the survival of metastatic CRPC patients to some extent, patients eventually develop resistance and progress to more aggressive form of the disease. Several molecular mechanisms have been proposed to explain how CRPC develops resistance to first-line or second-line therapies: overexpression or amplification of AR, constitutively activation of AR by splice

variants (namely AR-V7), intratumoral androgen production, and bypass pathway mediated by glucocorticoid receptor [61, 67]. Treatment resistance remains the biggest challenge in treating PCa and there is no effective therapy at the late stage of this disease besides platinum-based chemotherapy [68].

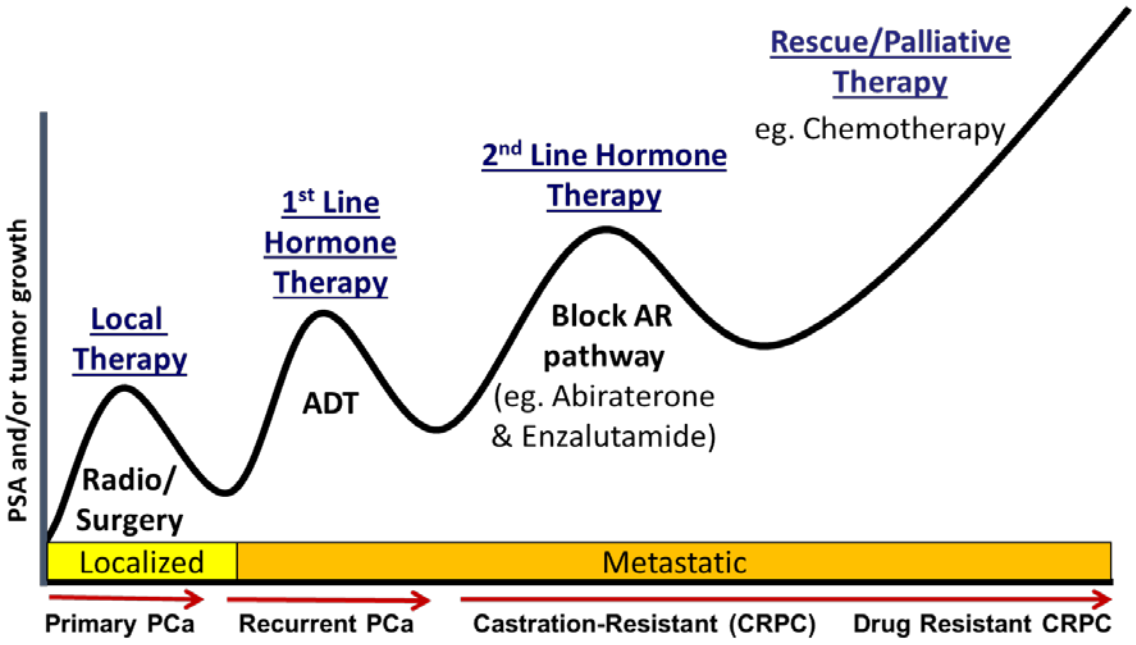

Figure 1.5 Current state of hormonal therapy

For localized PCa, it can be treated by surgery or radiotherapy. ADT is the first-line hormonal therapy for advanced or metastatic PCa. Second generation anti-androgens, abiraterone acetate and enzalutamide, are used to target AR signaling in metastatic CRPC.

1.3 Neuroendocrine prostate cancer (NEPC)

1.3.1 Overview

Neuroendocrine prostate cancer (NEPC) is one of the most aggressive forms of PCa with a median survival rate of 7 months from the time of diagnosis [69]. NEPC rarely arises *de novo* in less than 2% of all primary PCa; however, treatment-induced NEPC is found in about 10 to 15%

of metastatic CRPC [70-73]. Recent findings suggested that development of treatment-induced NEPC is a consequence of the selective pressure from AR pathway inhibition on prostatic adenocarcinoma (Adeno) [74-77]. Transformation from Adeno to NEPC is promoted by ADT and is postulated to be one of the mechanism of treatment resistance and disease progression [68]. With the introduction of highly potent AR-targeted agents into the clinic, the incidence rate of treatment-induced NEPC is escalating [78, 79]. Currently, platinum-based chemotherapy is the only treatment given to NEPC patients for palliative care [80]. There is no effective or standard treatment for patients with NEPC. Aurora kinase A (AURKA) has been identified as a potential therapeutic target for NEPC [81]. AURKA inhibitor MLN8237 is currently in phase II clinical trial (NCT01799278) for treating patients with metastatic CRPC and NEPC.

1.3.2 Clinical features and challenges

Physicians often use PSA as a biomarker for diagnosing and monitoring progression of PCa [82]. Therefore, PCa patients relapse with CRPC from ADT can be detected with elevation in serum PSA level [82]. NEPC is a subtype of AR-independent CPRC, which is unresponsive to hormonal therapy and frequently metastasizes to visceral organs with poor prognosis [69]. Because NEPC does not express AR and PSA, the diagnosis of NEPC is difficult with low to undetectable serum level of PSA. NEPC is primarily diagnosed by immunohistochemistry with the expression of NE markers such as neural cell adhesion marker 1 (NCAM1), neuron-specific enolase (NSE), synaptophysin (SYP), and chromogranin A (CHGA) [83, 84]. Unfortunately, development of treatment-induced NEPC is often under-recognized due to lack of post-treatment biopsy in CRPC patients with rapid progression and metastasis [68]. Serum NE biomarkers can be used for diagnosis of NEPC, but they are not reliable. For example, serum NSE biomarker has

high sensitivity but low specificity [85]. The serum level of CHGA in patients may be increased by other factors or treatments such as impaired kidney function, inflammatory bowel disease, and the use of proton pump inhibitors [86], which could lead to false positive results in the diagnosis of NEPC. Noninvasive methods such as circulating tumor cells and cell-free DNA are under development to provide genomic profile of patients for monitoring advanced PCa progression and treatment [87, 88].

1.3.3 Molecular mechanism of NEPC development

The emergence of NEPC has been controversial. There are two prevalent theories for how NEPC arise. It is first proposed that NE tumors in the prostate can arise *de novo* and NE-like PCa cells share the same cell of origin with normal prostatic NE cells due to similarities in their features [89, 90]. Unlike CRPC patients experiencing bone and lymph node metastasis with rising serum PSA level, NEPC patients have metastasis to visceral organs with low or undetectable serum PSA [91]. NE-like PCa cells and prostatic NE cells both express NE markers but lack of AR and PSA. Secretion of neuropeptides from NE cells could also influence androgen-independent growth of surrounding PCa cells in autocrine and paracrine manners [89]. These features give rise to the theory that NE-like PCa cells emerge from oncogenic mutation of normal NE cells in the prostate.

However, recent studies favor to support another theory that tumor cells acquire resistance by a phenotypic change into a different cell type that no longer dependent on the drug target via a mechanism called lineage plasticity [90]. It is postulated that Adeno cells acquire NE phenotype via lineage plasticity as a mechanism driving resistance to evade AR-targeted therapies. Clinically, the *TMPRSS2-ERG* gene fusion was thought to be specific to Adeno, but this fusion

was also detected in 50% of NEPC patients [92, 93]. This indicates that Adeno and NEPC tumors share common genomic alteration, which further suggests that NEPC is clonally derived from Adeno.

Lin et al. have established a unique patient-derived xenograft (PDX) model of complete transdifferentiation into lethal NEPC from Adeno under prolong exposure to androgen withdrawal following castration [75]. They have reported that the placental gene *PEG10* is negatively regulated by AR and drives the proliferation and invasion of NEPC [94]. A neural transcription factor, *BRN2*, and an RNA splicing factor, *SRRM4*, have also been reported to drive NE transdifferentiation of Adeno under the pressure of AR pathway inhibition [76, 77]. These findings further support that Adeno transform into NEPC to evade AR pathway inhibition.

To study the molecular mechanisms driving transdifferentation of treatment-induced NEPC, multiple approaches were used including *in vitro* studies, genetically engineered mouse (GEM) models, and patients data comparing alterations between CRPC and NEPC. Mutations in tumor suppressor genes such as retinoblastoma (*RB1*), *TP53*, and *PTEN* had been associated with PCa development [95]. Loss of *RB1* by deletion had been found to be a characteristic of NEPC tumors [96]. Moreover, loss of the retinoblastoma tumor suppressor gene *RB1* (in 70% NEPC versus 32% Adeno) and mutation or deletion of tumor suppressor gene *TP53* (in 66.7% NEPC versus 31.4% Adeno) had been observed to be more frequent in NEPC compared to Adeno patients [74].

In *in vivo* models, it was first observed that tumors developed NE phenotype in the prostate epithelium in transgenic adenocarcinoma mouse prostate (TRAMP) models when tumor suppressors *RB1* and *TP53* were inhibited by the expression of simian virus 40 (SV40) large T antigen [97]. In an *in vivo* study conducted by Ku et al., loss of *RB1* induced lineage plasticity

and metastasis in PCa cells initiated by *PTEN* mutation and caused resistance to antiandrogen therapy in combination with loss of *TP53* [98]. Gene expression profiling of tumors from these mice indicated increased expression of epigenetic regulator *EZH2* and reprogramming transcription factor *SOX2*. The authors showed that EZH2 inhibition could also restore sensitivity to ENZ treatment of the PCa cells isolated from these mice.

To determine if loss of *RB1* and *TP53* were required for ENZ resistance, Mu et al. knocked down *TP53* and *RB1* with sh-RNA in PCa cells [99]. They observed that loss of *TP53* function alone was not sufficient to confer ENZ resistance in PCa cells and xenografts. Conversely, combined knockdown of *TP53* and *RB1* in PCa cells had nearly complete ENZ resistance in both of their *in vitro* and *in vivo* models. In their study, cells lacking *RB1* and *TP53* had decreased expression of AR-dependent luminal epithelial cell markers and increased expression of AR-independent basal epithelial and NE cell markers. In agreement with the findings from Ku et al., the authors also showed that ENZ resistance was resulted from lineage plasticity through upregulation of *SOX2* by loss of *TP53* and *RB1*. This phenomenon could be reversed when they knocked down *SOX2*. Taken together, these results suggested that *SOX2* promoted ENZ resistance in PCa cells through lineage plasticity in the loss of *RB1* and *TP53*.

In an *in vivo* study conducted by Zou et al. using GEM model with *PTEN* and *TP53* knockout, tumors failed to respond to antiandrogen abiraterone and had progression from Adeno to treatment-induced NEPC by transdifferentiation that was suggested to be mediated by neural differentiation factor *SOX11* [100]. Their lineage tracing *in vivo* study also indicated that NEPC cells were arise from luminal adenocarcinoma cells. In agreement with the findings from Mu et al., these results suggested that PCa cells lose luminal epithelial lineage and acquire NE lineage

to become less dependent on AR signaling as an adaptive mechanism for resistance to AR-targeted therapies.

Moreover, a master repressor of neuronal differentiation, *REST*, was found to be downregulated in 50% of NEPC tumors and silencing *REST* with siRNA in Adeno LNCaP cells resulted in increased expression of NE markers *in vitro* [101]. Clinically, overexpression or gene amplification of *AURKA* and *MYCN* were also found in 40% of NEPC and only 5% of Adeno tumors [81]. *MYCN* is an oncogene in human neuroblastoma that is a highly aggressive NE tumor. Overexpression of *MYCN* had been shown to be an oncogenic driver of NEPC [102, 103]. Overexpression of *MYCN* resulted in increased *EZH2* expression and chromatin remodelling. Likewise, *EZH2* expression was observed to be two times higher in NEPC than Adeno patients and EZH2-repressed target genes were downregulated in NEPC patients [74]. Overall, these findings suggested that NEPC development was also associated with downregulation of *REST*, overexpression or amplification of *AURKA* and *MYCN*, as well as epigenetic changes by *EZH2*.

In addition, microenvironment changes could induce NE differentiation in PCa cells. LNCaP cells are androgen sensitive human Adeno cells derived from lymph node metastasis from a male PCa patient [104]. Previous *in vitro* studies have shown that NE differentiation of LNCaP cells can be induced through exposure to treatments or stimuli such as androgen depletion, interleukin-6, cAMP, hypoxia, and ionizing radiation [105-108]. Moreover, Nouri et al. had also shown that PCa cells cultured in a neural crest stem transition medium undergo lineage plasticity to acquire a neural crest stem-like phenotype and become resistance to AR pathway inhibition [109]. These cells with neural crest stem-like phenotype could re-differentiate into neuronal-like, oligodendrocyte-like, osteoblast-like, and glia-like lineages with further stimuli. These findings further suggest that lineage plasticity enable PCa cells to adapt changes

in the microenvironment. Further understanding of the molecular underpinnings of NEPC could provide insights for new therapeutic strategies.

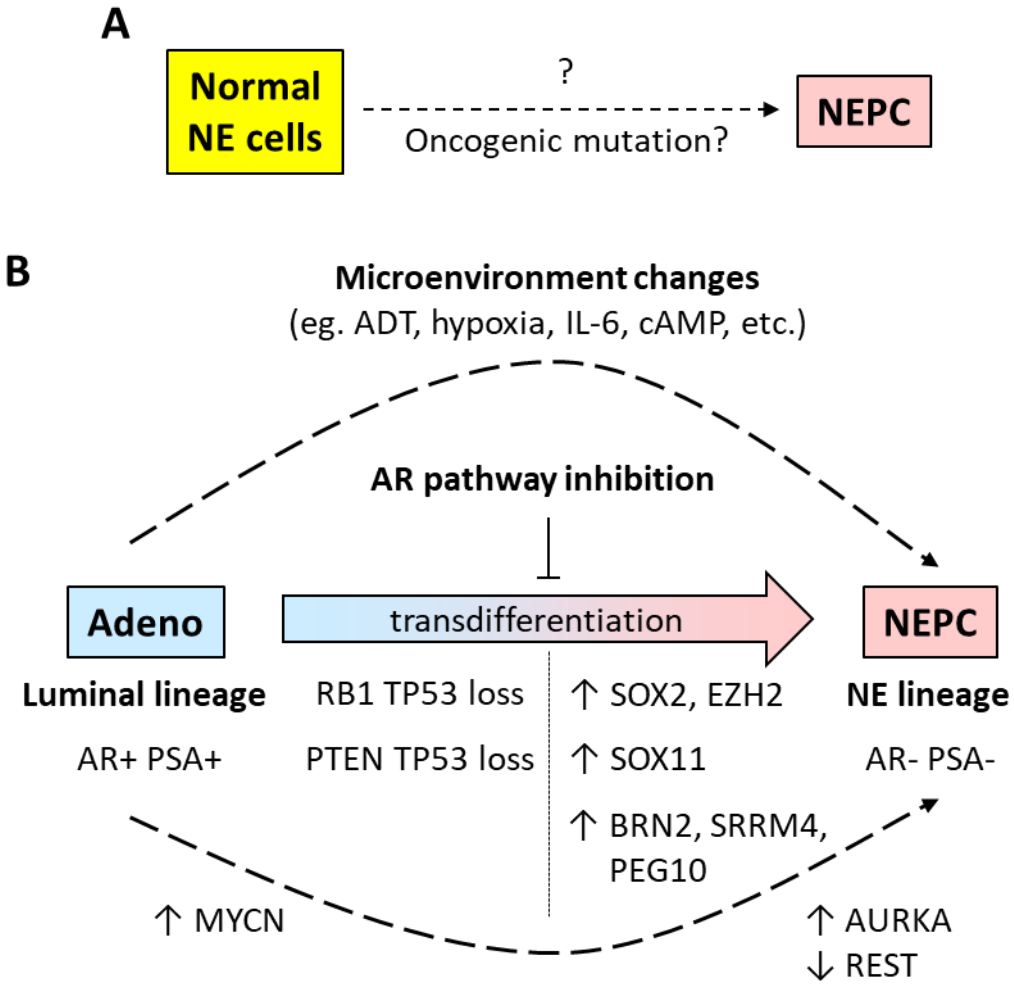

Figure 1.6 Proposed models for NEPC development

(A) NE tumors in the prostate share the same origin as normal prostatic NE cells. (B) Adeno cells undergo lineage transformation into NEPC cells.

1.4 Rationale

1.4.1 Prostate cancer patient cohort analysis

With more highly aggressive and lethal forms of PCa resulting from acquired resistance to current therapies, understanding the molecular mechanism of treatment resistance and disease progression of PCa is needed for identifying alternative targets for effective treatments. TNIK has been studied in several types of cancers and has been identified as a potential therapeutic target for colorectal cancer, but the role of TNIK in PCa has not yet been described. To investigate the clinical relevance of TNIK in PCa, we interrogated public human PCa patient data to correlate TNIK expression with different features of PCa. We assessed TNIK expression in RNA sequencing (RNA-seq) data from 37 Adeno, 34 CRPC, and 15 NEPC patient samples in Beltran H et al., 2016 cohort [74] and from 30 Adeno and 6 NEPC samples in Beltran H et al., 2011 cohort [81]. In both independent cohorts, TNIK mRNA expression was significantly increased in NEPC patients compared to Adeno patients (**Figure 1.7**).

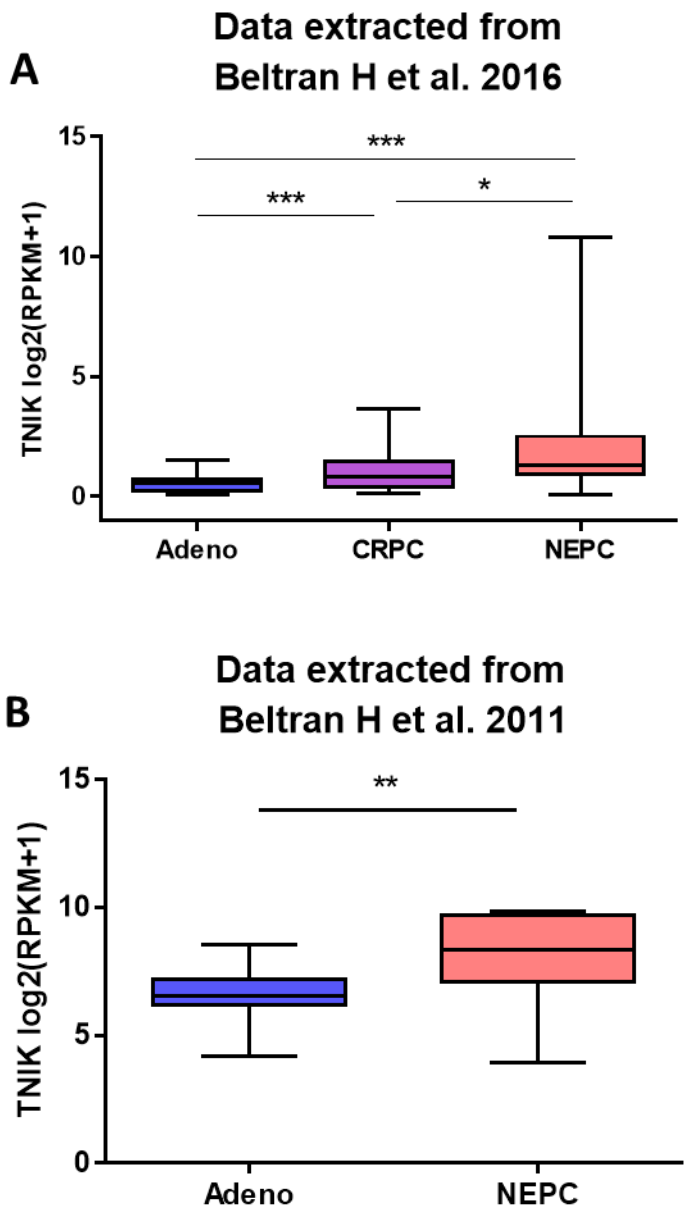

Figure 1.7 Expression of TNIK in human PCa patient

TNIK mRNA expression was assessed in (A) human Adeno, CRPC, and NEPC patients from Beltran H et al 2016 cohort and (B) human Adeno and NEPC patients from Beltran H et al 2011 cohort based on RNA-seq.

1.4.2 Hypothesis

TNIK expression was highly correlated with human NEPC, thus suggesting a possible link between TNIK and NEPC. Based on this finding, we **hypothesized** that TNIK is a potential marker, driver, or therapeutic target in NEPC.

Chapter 2: Materials and Methods

2.1 Public data mining

The University of California Santa Cruz (UCSC) developed and hosted a web-based software called the UCSC Xena Genome Browser (http://xena.ucsc.edu) [110]. It allows researchers to interpret, visualize, and analyze public and shared functional genomics data sets. Analyzing genomics data from 550 patient samples in The Cancer Genome Atlas (TCGA) prostate cancer dataset, the UCSC Xena software was used to visualize the clinical correlation of mRNA expression of *TNIK* with NE markers and androgen regulated genes. The NE markers were *NCAM1*, *ENO2*, *CHGB*, and *MYCN*. The androgen regulated genes were *KLK3*, *TMPRSS2*, *FKBP5*, and *NKX3.1*. Expression of NE markers and androgen regulated genes in each sample was stratified by the expression of TNIK in the gene expression heat maps.

2.2 Cell culture and reagents

PC3, DU145, NCI-H660, and HEK293T cells were purchased from American Type Culture Collection (ATCC; Manassas, VA, USA). LNCaP cells were kindly provided by Dr. Leland W.K. Chung (1992, MDACC, Houston, TX, USA) and authenticated by whole-genome and whole-transcriptome sequencing on Illumina Genome Analyzer IIx platform in 2013. CRPC (16D) and ENZ-resistant (49C, 49F, 42D, and 42F) cell lines were derived through serial xenograft passages of LNCaP as previously described [76]. PC3 and DU145 cells were cultured in DMEM media (Hyclone) with 10% fetal bovine serum (FBS; Life Technologies). HEK293T cells were maintained in DMEM media with 5% FBS. LNCaP cells were cultured in RPMI-1640 media (Hyclone) with 10% FBS. Similarly, ENZ-resistant (ENZR) cell lines were maintained in RPMI-1640 media with 10% FBS and supplemented with 10 μM ENZ (Haoyuan Chemexpress

Co.). NCI-H660 cells were cultured in HITES media (RPMI-1640 medium containing 0.005 mg/mL insulin, 0.01 mg/mL transferrin, 30 nM sodium selenite, 10 nM Hydrocortisone, 10 nM beta-estradiol, and 2 mM L-glutamine) with 5% FBS. The information on species, tissue origin, and characteristic of each cell line being used is listed in **Table 2.1**. For experiments with androgen deprivation, cells were cultured in RPMI-1640 phenol red-free media (Invitrogen) with 10% charcoal stripped serum (CSS; Hyclone). Synthetic androgen R1881 were purchased from Perkin Elmer. TNIK small-molecule inhibitor KY-05009 was purchased from Sigma-Aldrich.

Table 2.1 Cell line information

Information on species, tissue origin, and characteristic of each cell line being used.

Name	**Species and tissue origin**	**Characteristics**
LNCaP	Human prostate from lymph node metastasis	Adeno (AR+, PSA+)
$16D^{CRPC}$	LNCaP-derived xenograft	CRPC (AR+, PSA+)
$49C^{ENZR}$	LNCaP-derived xenograft	ENZR with Adeno phenotype
$49F^{ENZR}$	LNCaP-derived xenograft	ENZR with Adeno phenotype (AR+, PSA+)
$42D^{ENZR}$	LNCaP-derived xenograft	ENZR with NE-like phenotype (AR+, PSA-)
$42F^{ENZR}$	LNCaP-derived xenograft	ENZR with NE-like phenotype (AR+, PSA-)
DU145	Human prostate from brain metastasis	Lack of AR (AR-)
PC3	Human prostate from bone metastasis	Lack of AR (AR-)
NCI-H660	Human prostate	NEPC
HEK293T	Human kidney	Embryonic

2.3 Plasmid constructs

The pRK5-HA-TNIK plasmid was kindly provided by Dr. Arnd Kieser and it contained the sequence of human wild-type TNIK cDNA tagged with HA epitope at the N-terminus (HA-

TNIK) [111]. The HA-TNIK sequence was cloned from pRK5-HA-TNIK into a lentiviral expression vector pLVX-IRES-Puro (Clontech) by PCR to generate pLVX-HA-TNIK-IRES-Puro (see **Section 2.13** for more details on the construction of the HA-TNIK lentiviral plasmid). The HA-TNIK lentiviral plasmid was used along with lentiviral packaging vector pCMV delta R8.2 and lentiviral envelope vector pCMV-VSV-G (Addgene plasmid #12263 and #8454) for lentivirus production.

2.4 siRNA and plasmid transfections

$42D^{ENZR}$ cells were transfected with 20 nM of Silencer Select siRNA for TNIK (siTNIK) or control (siCtr; Ambion) using Lipofectamine RNAiMAX transfection reagent (Life Technologies) according to manufacturer's procedure. For transient overexpression of TNIK, $16D^{CRPC}$ cells were transfected with pLVX-IRES-Puro encoding HA-TNIK or the empty vector using TransIT-2020 transfection reagent (Mirus Bio) according to manufacturer's procedure. For stable overexpression of TNIK, pLVX-IRES-Puro encoding HA-TNIK or its empty vector was co-transfected with pCMV delta R8.2 and pCMV-VSV-G into HEK293T cells using Calcium Phosphate transfection method (Promega) according to manufacturer's procedure for lentivirus production. $16D^{CRPC}$ cells were infected with lentivirus expressing HA-TNIK or empty vector and maintained under puromycin (Life Technologies) selection.

2.5 Cell proliferation and viability assay

For cell proliferation assay, cells transfected with siCtr or siTNIK were seeded at 4000 cells per well in triplicates on 96-well plate. One plate was prepared for each time point. Similarly, for cell viability assay, cells were seeded at 4000 cells per well in triplicates on 96-

well plate and treated with KY-05009 on the following day at indicated doses for 72 hours. At the indicated time points, cells were fixed in 1% glutaraldehyde and stained with 0.5% crystal violet. Cells were washed with water and air dried. Bound crystal violet was eluted using Sorensen's solution (30 mM sodium citrate, 50% ethanol, and 0.02 M HCl). The absorbance was measured at 560 nm using a microplate reader (BioTek).

2.6 Western blotting

Total protein was extracted from cultured cells using RIPA lysis buffer (Pierce) containing protease and phosphatase inhibitors (Roche). Approximately 30 µg of each protein samples was separated by sodium dodecyl sulfate-polyacrylamide gel electrophoresis and transferred onto polyvinylidene difluoride membrane (Millipore). The following primary antibodies were used for western blotting: TNIK (BD Biosciences), p-TNIK (S764) (Santa Cruz), PSA (Cell Signaling Technology), HA (Santa Cruz) and Vinculin (Millipore). Blots were incubated at 4 ˚C overnight with designated primary antibodies at 1:1000 dilution, unless noted otherwise. Proteins were visualized using the Odyssey system (LI-COR Biosciences).

2.7 Quantitative real-time PCR (qPCR) and reverse transcription PCR (RT-PCR)

Total RNA was isolated from cultured cells using TRIzol® reagent (Life Technologies) according to the manufacturer's protocol. Reverse transcription PCR (RT-PCR) was performed to make cDNA from the RNA samples using MMLV reverse transcriptase and random hexamers (Life Technologies) as previously reported [76]. Each cDNA sample was amplified using FastStart Universal SYBR Green master (Rox) mix (Roche) on ABI ViiA7 Real-time PCR

System (Applied Biosystems). Target gene expression was normalized to GAPDH levels in three replicates per sample. The qPCR primer sequences are listed in **Appendix A.1**.

2.8 Chromatin immunoprecipitation (ChIP) assay

$16D^{CRPC}$ and $42D^{ENZR}$ cells were seeded at 3 x 10^6 cells on each of 15-cm plate and cultured in RPMI-1640 phenol red-free media with 10% CSS for 48 hours. Cells were then stimulated with 1 nM R1881 for 24 hours. ChIP assay was performed using EZ ChIP™ kit according to the manufacturer's protocol (Millipore). Briefly, cells were cross-linked with 1% formaldehyde (Sigma-Aldrich) and quenched with 0.125 M Glycine. Cells were then lysed and sonicated to shear DNA in SDS lysis buffer (Millipore). Lysates were immunoprecipitated with either 5 μg of AR antibody (PG-21, Millipore) or normal rabbit IgG antibody at 4 ˚C overnight. DNA was purified using the spin column provided in the EZ ChIP™ kit. The extracted DNA fragments were subjected to qPCR. TNIK primers were designed within the predicted AR binding site between the regions approximately 231997 bp and 232096 bp downstream of TNIK transcription initiation site using Primer3. The sequences of TNIK primers for ChIP assay are listed in **Appendix A.2**.

2.9 ChIP-sequencing (ChIP-seq)

$16D^{CRPC}$ cells were seeded at 3 x 10^6 cells on a 15-cm plate and cultured in RPMI-1640 phenol red-free media with 10% CSS for 72 hours. Cells were stimulated with 10 nM DHT for 4 hours prior to fixation. ChIP assay was performed with AR antibody and purified DNA was sent for ChIP-sequencing (ChIP-seq). ChIP-seq data were generated by Illumina Hi-seq platform. Reads were aligned and mapped to the Human Reference Genome (assembly hg19, Genome

Reference Consortium GRCh37, February 2009) using Bowtie 2. Peaks were called using MACS (Model-based Analysis of ChIP-seq) and visualized using Integrative Genomics Viewer.

2.10 Polymerase chain reaction (PCR)

Polymerase chain reaction (PCR) was performed using Q5 Hot Start High-Fidelity DNA polymerase (New England Biolabs) for plasmid cloning of HA-TNIK or detection of TNIK transcript variants. Depending on the application, PCR programs using Tetrad 2 thermal cycler (Bio-Rad) are listed in **Appendices B.1 and B.2**.

2.11 Agarose gel electrophoresis

Plasmid DNA, PCR products, and restriction digested DNA samples were separated on agraose gel. DNA fragments were visualized on the gel stained with Sybr Safe DNA gel stain (Invitrogen). Gels were scanned using GelDoc EZ system (Bio-Rad) for further analysis.

2.12 Cloning methods

2.12.1 Plasmid DNA purification

Purification of plasmid DNA was performed using Plasmid Miniprep purification kit or Plasmid Maxiprep purification kit (Invitrogen) according to the manufacturer's protocol. Plasmid DNA was eluted from the spin column using TE buffer. Plasmid DNA concentration and purity were measured using NanoDrop 2000 spectrophotometer (Thermo Scientific).

2.12.2 Restriction enzyme digestion of DNA and subsequent purification

Restriction enzymes *Xho*I and *Xba*I (New England Biolabs) were used to digest plasmid DNA and PCR products according to the manufacturer's protocol. Each of the restriction digestion was performed at 37 ˚C for 2 hours. The restriction digested DNA samples were separated by agarose gel electrophoresis. DNA fragments were visualized and cut with a clean scalpel from the agraose gel stained with Sybr Safe DNA gel stain (Invitrogen) on a UV transilluminator. Extraction of the DNA fragments from the gel slice was performed using QIAquick gel extraction kit (Qiagen) according to the manufacturer's protocol. DNA fragments were eluted from spin column using Buffer EB.

2.12.3 Ligation of DNA fragment

Ligation of DNA fragments was performed using T4 DNA ligase (New England Biolabs) according to the manufacturer's protocol. The ligation reaction was setup at 3:1 insert to vector molar ratio. The ligation mix was incubated at 16 ˚C overnight.

2.12.4 Plasmid transformation

Transformation of plasmid DNA into DH5α^{TM} Competent cells (Invitrogen) was performed according to the manufacturer's protocol. Briefly, 100 ng of plasmid DNA or 5 µL of ligation mix was added to the cells and incubated on ice for 30 minutes. The cells were then heat shocked for 40 seconds in a 42 ˚C water bath and incubated on ice for another 2 minutes. 250 µL of S.O.C. medium (Invitrogen) was added to the cells and incubated at 37 ˚C for 1 hour at 225 rpm. Each transformation was spread on an agar plate with 100 µg/mL ampicillin. The plates were incubated upside down at 37 ˚C overnight.

2.13 Construction of HA-TNIK lentiviral plasmid

To investigate the biological function of TNIK in PCa, we needed a plasmid for overexpressing TNIK for generating stable cell lines in our gain-of-function studies. Dr. Arnd Kieser kindly provided us with the pRK5-HA-TNIK plasmid, which contained the human TNIK full length cDNA with an N-terminal HA epitope tag (HA-TNIK) [111]. We subcloned the HA-TNIK sequence into the *Xho*I/*Xba*I sites of pLVX-IRES-Puro vector (Clontech) by PCR to generate the TNIK lentiviral vector (pLVX-HA-TNIK-IRES-Puro). We used pLVX-IRES-Puro vector because it encoded the puromycin resistant marker, which would allow us to select and maintain stably transfected cells using puromycin.

In order to clone the HA-TNIK sequence from pRK5-HA-TNIK into pLVX-IRES-Puro, we designed PCR primers to add recognition sequences of *Xho*I to 5' end and *Xba*I to 3' end of the HA-TNIK insert (**Appendix A.3**). PCR was performed according to PCR program in **Appendix B.1**. The HA-TNIK PCR product and pLVX-IRES-Puro vector were restriction digested by *Xho*I and *Xba*I overnight, which were separated by agarose gel electrophoresis (**Appendix C.1**). Double digested HA-TNIK insert (4.1kb) and pLVX-IRES-Puro vector (8.1kb) were extracted from agarose gel and ligated together. Ligation mix was transformed into DH5α^{TM} Competent cells. After transformation, 12 colonies were randomly selected for Miniprep plasmid DNA isolation. Uncut plasmid DNA of pLVX-IRES-Puro empty vector and 12 clones of pLVX-HA-TNIK-IRES-Puro vector were ran on an agarose gel for checking the qualities of the plasmids (**Appendix C.2**). Most of the clones of pLVX-HA-TNIK-IRES-Puro vector were in good qualities with at least two clear bands except clone 8 in lane 9. The clones of pLVX-HA-TNIK-IRES-Puro had bigger size compared to pLVX-IRES-Puro on the agarose gel, which indicated that they might contain the HA-TNIK insert. Based on the quality on agarose gel

and absorbance reading from a NanoDrop (data not shown), we picked clone 3 in lane 4 to be the construct of pLVX-HA-TNIK-IRES-Puro for our studies.

To verify the pLVX-HA-TNIK-IRES-Puro vector we constructed, we performed PCR to confirm the orientation of HA-TNIK insert. We used PCR cloning primers to amplify HA-TNIK in pRK5-HA-TNIK and pLVX-HA-TNIK-IRES-Puro. The size of PCR products from both vectors gave bands on agarose gel that matched the predicted size of HA-TNIK insert at 4.1kb (**Appendix C.3**). This indicated that pLVX-HA-TNIK-IRES-Puro vector contained HA-TNIK insert in the correct orientation.

2.14 Detection of TNIK transcript variants

In this study, we developed a method for detecting each transcript variant of TNIK in three steps: 1) RT-PCR to make cDNA from RNA samples, 2) PCR using the cDNA samples, and 3) agarose gel electrophoresis of the PCR samples [112]. TNIK had 3 alternative splicing sites, which produced 8 transcript variants [1]. **Table 2.2** listed the accession numbers and sizes of each TNIK transcript variant from NCBI database we used for designing PCR primers from cDNA samples.

Figure 2.1 showed our strategy for designing the PCR primers to detect each TNIK transcript variant. All PCR primer sequences for TNIK transcript variants are listed in **Appendix A.4**. We designed two forward and two reverse PCR primer sequences that were specific to a cassette exon or a splice junction at the first and third splice sites of TNIK mRNA using Primer-Blast. For the first splicing site, we designed a forward primer A specific to the exon sequence that could be spliced. We designed a reverse primer B at the exon that could be spliced out at the third splicing site. Using primer A and B in a PCR reaction, it would produce DNA fragments

with sizes of 1092bp and 927bp that represented transcript variants 1 and 5. Similarly, we designed a forward primer C at the junction of the sequence where the exon was spliced out at the first splicing site and a reversed primer D at the junction of the sequence where the exon was spliced out at the third splicing site. Using primer C and D in a PCR reaction, it would produce DNA fragments with sizes of 980bp and 815bp that represented transcript variants 4 and 8. If we setup PCR reaction by using primer A and D, it would have DNA fragments at 1061bp and 896bp that would represent transcript variants 2 and 6. If we setup PCR reaction by using primer C and B, it would have DNA fragments at 1011bp and 846bp that would represent transcript variants 3 and 7. The size of each PCR product is listed in **Table 2.3**. Since the PCR product of each transcript variant had different sizes, the DNA fragments could be separated by agarose gel electrophoresis.

Table 2.2 TNIK transcript variants from NCBI database

Accession number and size of each TNIK transcript variant from NCBI database.

TNIK	Transcript variant mRNA	bp
1	NM_015028.3	9906
2	NM_001161560.2	9882
3	NM_001161561.2	9819
4	NM_001161562.2	9795
5	NM_001161563.2	9741
6	NM_001161564.2	9717
7	NM_001161565.2	9654
8	NM_001161566.2	9630

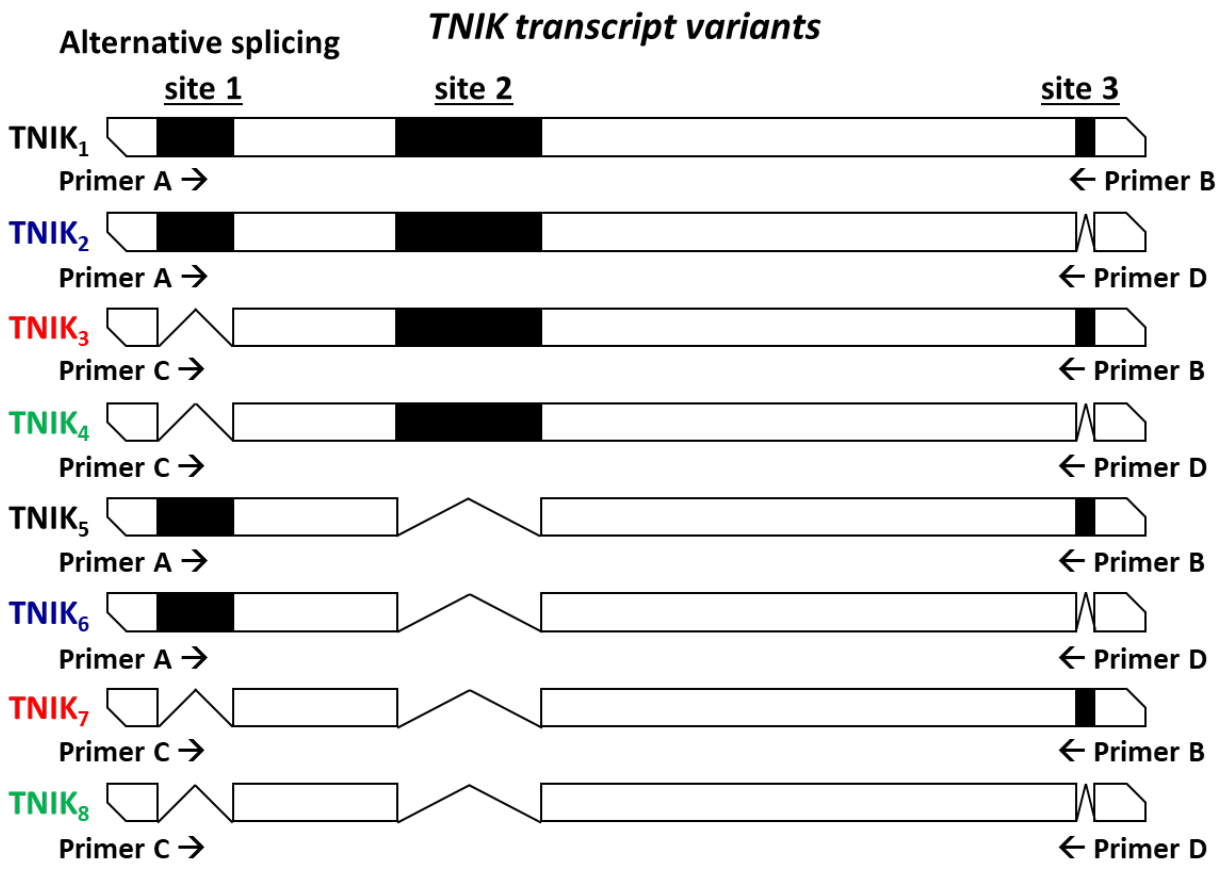

Figure 2.1 Schematic illustration of PCR primer design for TNIK transcript variants

At each alternative splicing site, (■) represents an exon and (/\) represents a splice junction. Forward primers A and C and reverse primers B and D were designed using the sequences at the exons and splice junctions.

Table 2.3 PCR primer combination for detecting TNIK transcript variants

The predicted PCR product size for detecting each transcript variant (v) of TNIK.

PCR reaction	**1**	**2**	**3**	**4**
Primer pair	**Primer A + B**	**Primer A + D**	**Primer C + B**	**Primer C + D**
Transcript variant and product size	v1: 1092 bp	v2: 1061 bp	v3: 1011 bp	v4: 980 bp
	v5: 927 bp	v6: 896 bp	v7: 846 bp	v8: 815 bp

2.15 Immunofluorescence

$16D^{Mock}$ and $16D^{TNIK}$ cells were seeded at 40,000 cells per well in 12-well plates with coverslips. 48 hours later, cells were fixed with 4% paraformaldehyde, permeabilized with 0.2% Triton X-100 in PBS, and blocked with 3% bovine serum albumin. Primary antibodies for total TNIK (BD Biosciences) and HA (Santa Cruz) were used at 1/100 dilution. Green-fluorescent Alexa Flour 488 secondary antibody (Invitrogen) was used at 1/500 dilution. Cells were mounted using Vectashield mounting media with DAPI (Vector Labs). Pictures were taken by 40X objective lens using 780 LSM confocal microscope (Zeiss).

2.16 Statistical analysis

Pearson correlations (95% confidence interval) were performed using Prism 6 software (GraphPad). *P* values were also calculated to evaluate statistical significance using Student's t-test by Prism 6 software. Significance is indicated as follows: *, $P < 0.05$; **, $P < 0.01$; ***, $P < 0.001$.

Chapter 3: Results

3.1 TNIK expression in prostate cancer

3.1.1 Correlation of TNIK expression with neuroendocrine markers

As illustrated in **Figure 1.6**, TNIK expression was elevated in human NEPC compared to Adeno in both Beltran H et al. 2016 and 2011 cohorts. To further validate the link between TNIK and NEPC, we assessed TNIK mRNA expression in a unique NE transdifferentiation patient-derived xenograft (PDX) model from Akamatsu S et al., 2015 cohort [94]. Analysis of RNA-seq data collected from this PDX model, TNIK expression increased by 26-folds after 8 and 12 weeks of castration and it was further upregulated in terminally transdifferentiated NEPC by 50-folds compared to Adeno before castration (**Figure 3.1**). In agreement, TNIK mRNA expression was positively correlated with NE markers (*NCAM1, ENO2, CHGB, MYCN*) in the TCGA PCa cohort (**Figure 3.2**). Together, these data suggest an association between TNIK expression and NE phenotype in PCa.

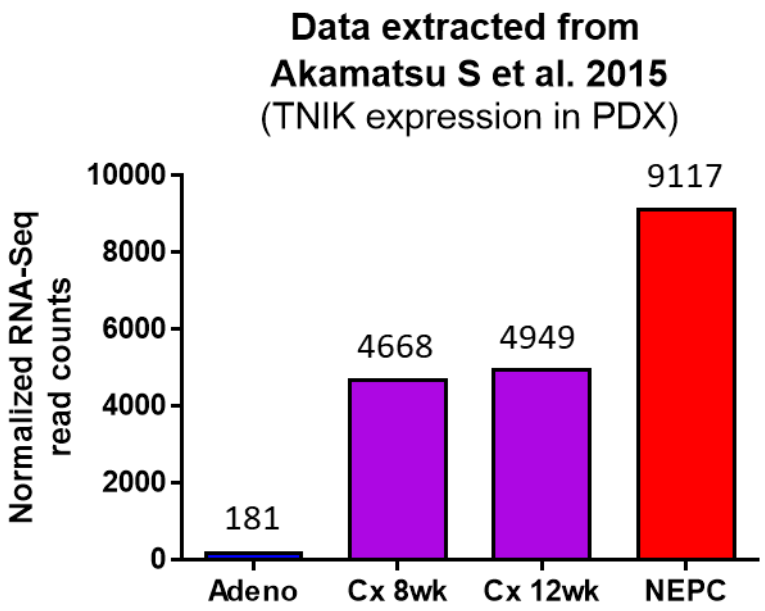

Figure 3.1 Expression of TNIK in human NE transdifferentiation PDX model

TNIK mRNA expression was assessed in patient-derived prostatic adenocarcinoma xenografts (Adeno), castration (Cx) after 8 and 12 weeks (wk), and terminally transdifferentiated NEPC tumor (NEPC) from Akamatsu S et al 2015 cohort based on RNA-seq.

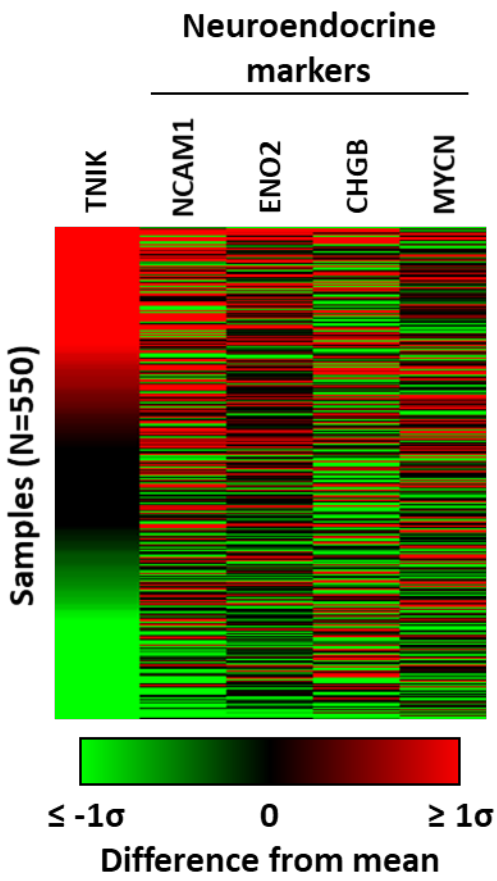

Figure 3.2 TNIK expression positively correlates with NE markers

Heat map of TCGA data showing gene expression of neuroendocrine markers (*NCAM1*, *ENO2*, *CHGB*, *MYCN*) in 550 human PCa patient samples stratified by their TNIK mRNA expression (http://xena.ucsc.edu).

3.1.2 Correlation of TNIK expression with androgen regulated genes

Treatment-induced NEPC had been suspected in rapidly progressing CRPC patients with low levels of serum PSA [79]. Our data analysis of CRPC patient samples from the Grasso CS et al 2012 cohort revealed that TNIK mRNA expression had a significant inverse correlation with serum PSA level (Pearson's correlation coefficient r = -0.563, P<0.0008) (**Figure 3.3**). Furthermore, our RNA-seq analysis of the TCGA PCa cohort showed that the mRNA expression of TNIK was inversely correlated with androgen regulated genes (*KLK3, TMPRSS2, FKBP5, NKX3.1*) (**Figure 3.4**). These results suggested that TNIK expression increased as AR activity decreased.

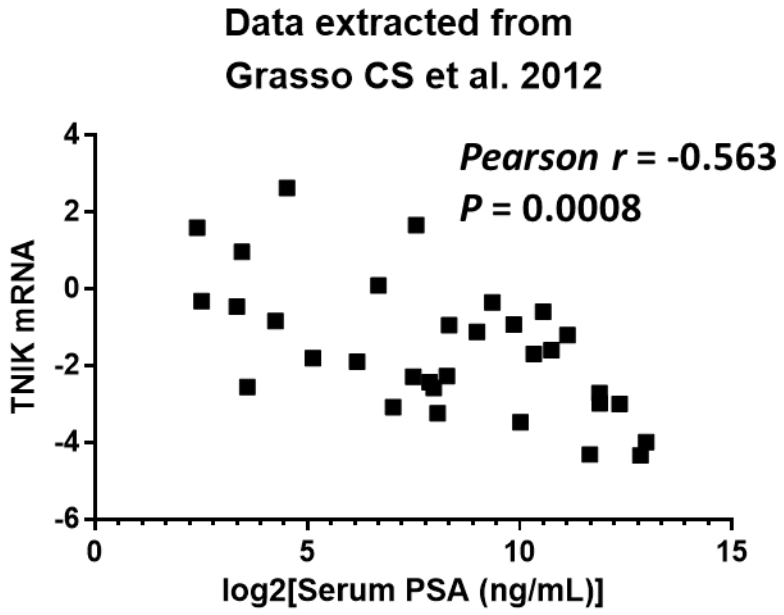

Figure 3.3 TNIK mRNA expression inversely correlated with serum PSA level in CRPC

Correlation of TNIK mRNA expression and serum PSA level were analyzed from CRPC patient samples in Grasso CS et al 2012 cohort.

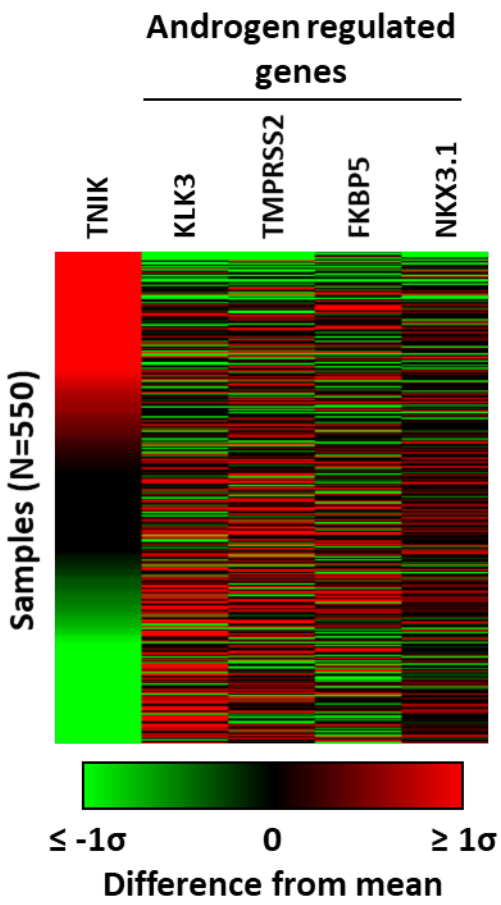

Figure 3.4 TNIK expression inversely correlates with androgen regulated genes

Heat map of TCGA data showing gene expression of androgen regulated genes (*KLK3*, *TMPRSS2*, *FKBP5*, *NKX3.1*) in 550 human PCa samples stratified by their TNIK mRNA expression (http://xena.ucsc.edu).

3.1.3 Expression of TNIK in prostate cancer cell lines

To explore the relationship of TNIK expression with respect to PCa progression, we performed qPCR to evaluate TNIK mRNA expression in different PCa cell lines that recapitulate the disease progression from Adeno to CRPC, ENZR with Adeno and NE-like phenotypes, lack of AR (AR -), and NEPC. $16D^{CRPC}$, $49C^{ENZR}$, $49F^{ENZR}$, $42D^{ENZR}$, and $42F^{ENZR}$ were cell lines previously developed from our lab from LNCaP-CRPC and ENZR LNCaP-CRPC xenograft tumors to model ENZR disease [76]. The ENZR cell lines retained AR expression *in vitro*. $49C^{ENZR}$ and $49F^{ENZR}$ were ENZR cell lines with Adeno phenotype derived from PSA+ tumors. $42D^{ENZR}$ and $42F^{ENZR}$ were ENZR cell lines with NE-like phenotype derived from PSA- tumors. Moreover, we used DU145 and PC3 as AR- cell lines and NCI-H660 as NEPC cell line.

We observed that TNIK mRNA level was upregulated in cell lines $42D^{ENZR}$, $42F^{ENZR}$, DU145, PC3, and NCI-H660 compared to LNCaP (**Figure 3.5A**). AR was inactive in $42D^{ENZR}$ and $42F^{ENZR}$ and absent in DU145, PC3, and NCI-H660. Compared to LNCaP, cell lines lacking AR activity had either lower or undetectable levels of PSA mRNA (**Figure 3.5B**). On the other hand, cell lines $16D^{CRPC}$, $49C^{ENZR}$, and $49F^{ENZR}$ with active AR had detectable levels of PSA mRNA and there were no significant difference in their TNIK mRNA expression compared to LNCaP.

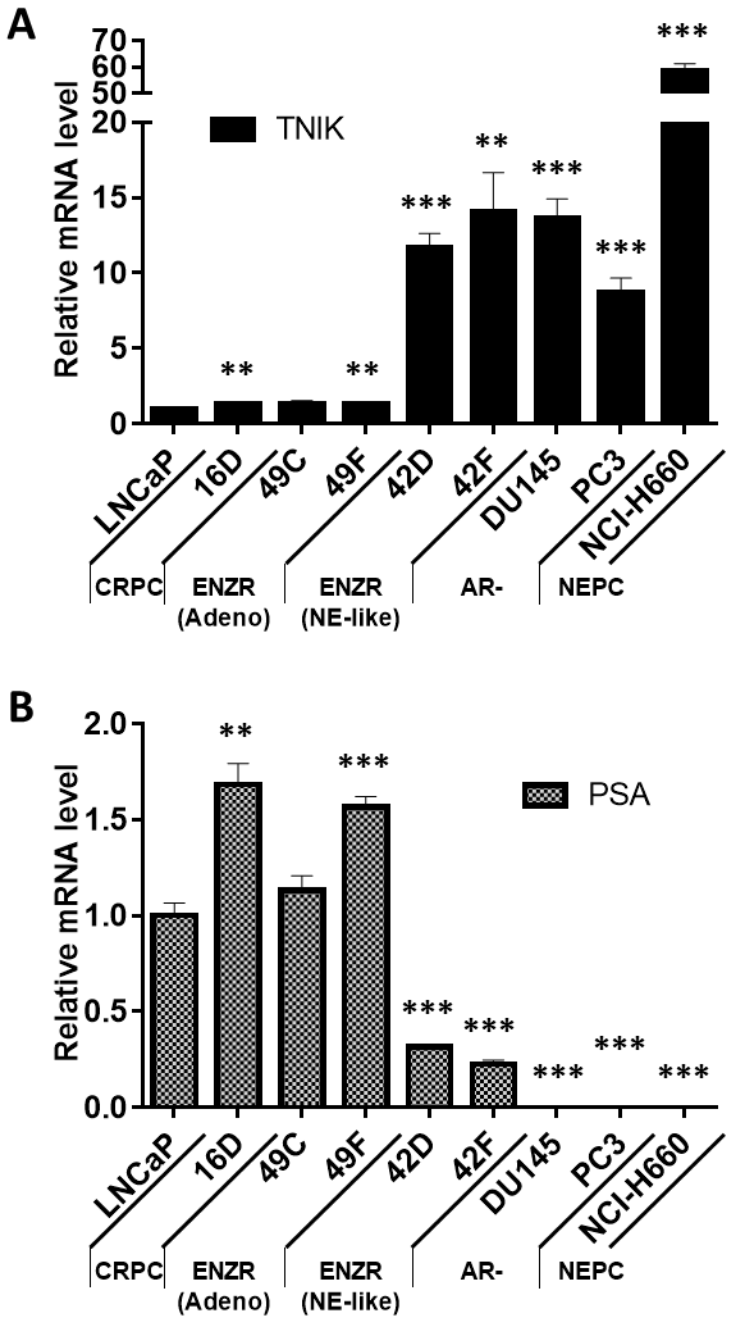

Figure 3.5 mRNA expression of TNIK in PCa cell lines

Relative mRNA expression of (A) TNIK and (B) PSA normalized to GAPDH were assessed in human PCa cell lines $16D^{CRPC}$, $49C^{ENZR}$, $49F^{ENZR}$, $42D^{ENZR}$, $42F^{ENZR}$, DU145, PC3, and NCI-H660 compared to LNCaP by qPCR.

At protein level, we evaluated the expression pattern of TNIK in the same panel of PCa cell lines. We assessed endogenous protein expression of total TNIK, phosphorylated TNIK (p-TNIK (S764)), and PSA in the cell lines by western blot. Since S764 has been proposed to be an autophosphorylation site of TNIK, we used p-TNIK (S764) antibody to assess the level of activated TNIK protein in the cell lines. p-TNIK (S764) level followed the same trend as TNIK mRNA expression in the cell lines. p-TNIK (S764) level was upregulated in cell lines $42D^{ENZR}$, $42F^{ENZR}$, DU145, PC3, and NCI-H660, which had undetectable levels of PSA protein (**Figure 3.6**). However, there was no significant difference in the expression of total TNIK protein in the cell lines. Taken together, these results indicated that transcription and activity of TNIK were increased in absence of classical AR signaling.

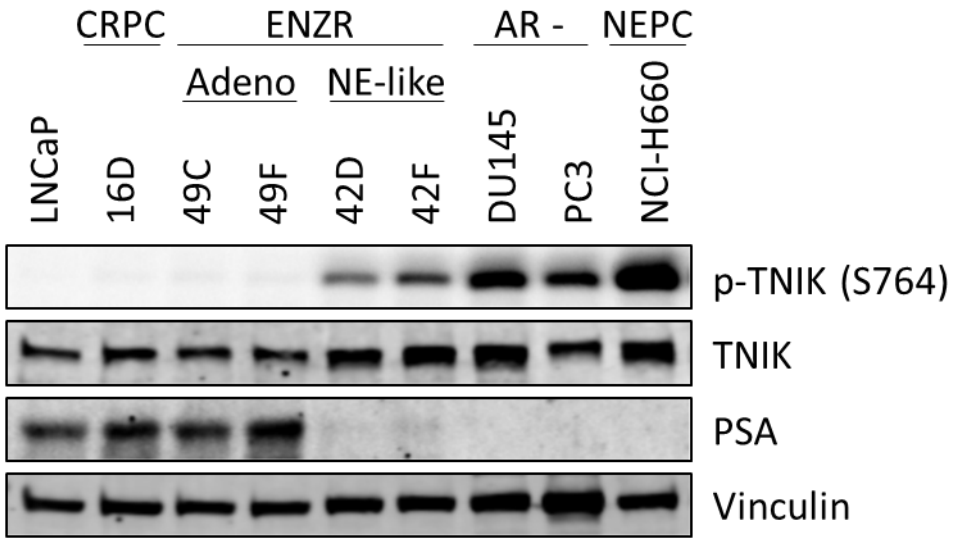

Figure 3.6 Protein expression of TNIK in PCa cell lines

Protein expression of p-TNIK (S764), total TNIK (T-TNIK), and PSA were assessed in human PCa cell lines $16D^{CRPC}$, $49C^{ENZR}$, $49F^{ENZR}$, $42D^{ENZR}$, $42F^{ENZR}$, DU145, PC3, and NCI-H660 compared to LNCaP by western blot. Vinculin was used as a loading control.

3.2 Identification of TNIK as an androgen regulated gene

3.2.1 Effect of AR pathway inhibition on TNIK mRNA expression

Since TNIK mRNA expression was upregulated when AR was inactive or absent in PCa cell lines and had an inverse correlation with androgen regulated genes in PCa patients, we investigated if AR pathway inhibition would induce TNIK expression. To mimic AR pathway inhibition *in vitro*, we took two different approaches using castrated condition or an AR inhibitor. To mimic castrated condition, LNCaP and $16D^{CRPC}$ cells were cultured in media containing normal serum (10% FBS) or in androgen-depleted media (10% CSS) for 7 days. We found that TNIK mRNA levels were increased in both LNCaP and $16D^{CRPC}$ cells by about 4-fold in the absence of androgen (**Figure 3.7**). In a second set of experiments with an AR inhibitor (ENZ), LNCaP and $16D^{CRPC}$ cells were treated with 10 μM ENZ in media containing 10% FBS for 2, 4, and 7 days. Similarly, we observed that TNIK mRNA expression was elevated after ENZ treatment in a time-dependent manner (**Figure 3.8**). The 7-day ENZ treatment yielded a 5-fold increase in TNIK mRNA expression in the LNCaP and $16D^{CRPC}$ cells. These results indicated that TNIK expression was induced when AR signaling was suppressed.

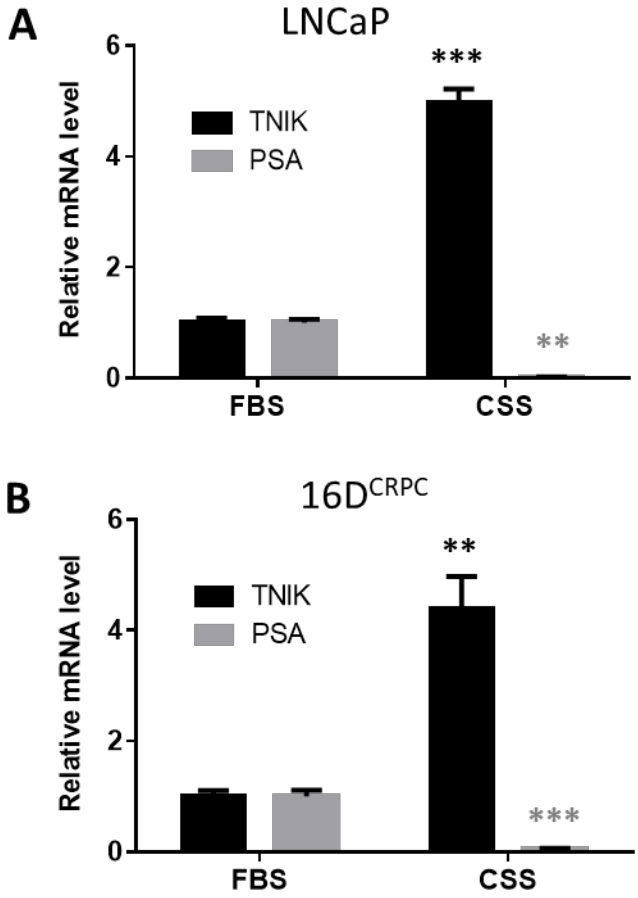

Figure 3.7 Effect of androgen depletion on TNIK expression

Relative mRNA expression of TNIK and PSA normalized to GAPDH were assessed in (A) LNCaP and (B) $16D^{CRPC}$ cells that were cultured in androgen-depleted media (10% CSS) compared to media containing normal serum (10% FBS) for 7 days compared to no treatment (0 day) by qPCR.

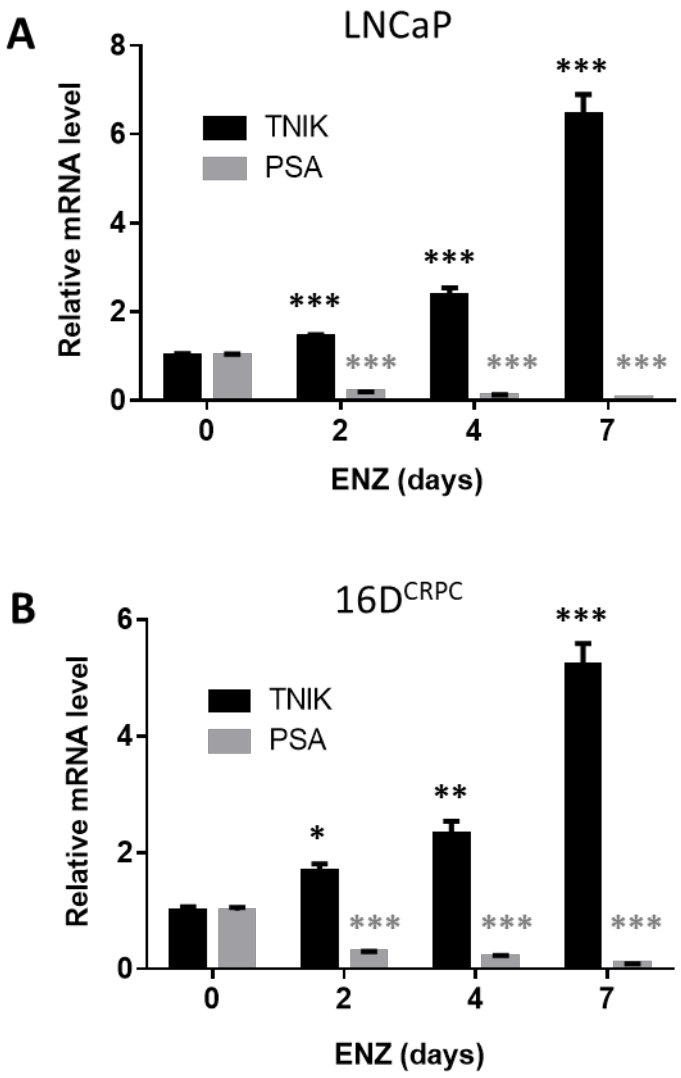

Figure 3.8 Effect of ENZ treatment on TNIK expression

Relative mRNA expression of TNIK and PSA normalized to GAPDH were assessed in (A) LNCaP and (B) $16D^{CRPC}$ cells that were treated with 10 μM ENZ in media containing 10% FBS for 2, 4, and 7 days compared to no treatment (0 day) by qPCR.

3.2.2 Androgen regulated TNIK mRNA expression

Since AR pathway inhibition induced TNIK mRNA expression, we further investigated the relationship of AR activity on TNIK expression by testing the effect of stimulating AR activity with addition of androgen. First, we pre-cultured LNCaP and $16D^{CRPC}$ cells in 10% CSS media for 7 days to induce TNIK expression. LNCaP and $16D^{CRPC}$ cells were then stimulated with synthetic androgen R1881 at 0.1, 1, and 5 nM with or without 10 μM ENZ. We observed that R1881 stimulation reduced TNIK expression in both LNCaP and $16D^{CRPC}$ cells in a dose-dependent manner, which corresponded to AR activity (**Figures 3.9A and 3.10A**). The level of reduction in TNIK expression by R1881 was lowered in presence of ENZ. TNIK expression was lowest when PSA expression was highest in the samples of LNCaP and $16D^{CRPC}$ cells stimulated with 5 nM R1881 (**Figures 3.9B and 3.10B**). These results suggested that TNIK mRNA expression was negatively regulated by AR activity in PCa.

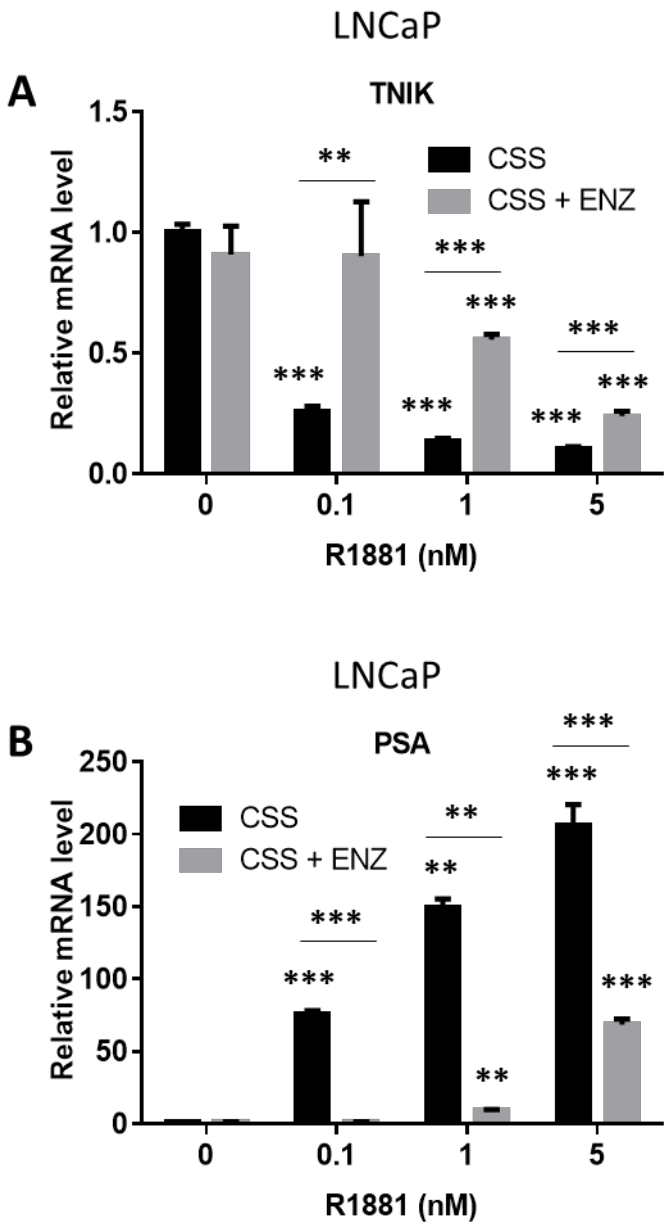

Figure 3.9 Androgen decreased TNIK mRNA expression in LNCaP

Relative mRNA expression of (A) TNIK and (B) PSA mRNA normalized to GAPDH were assessed by qPCR in LNCaP cells pre-cultured in 10% CSS for 7 days followed by addition of synthetic androgen R1881 at a dose-dependent manner in presence or absence of 10 μM ENZ. The mRNA expression of TNIK and PSA in each sample was compared to control untreated cells cultured in CSS.

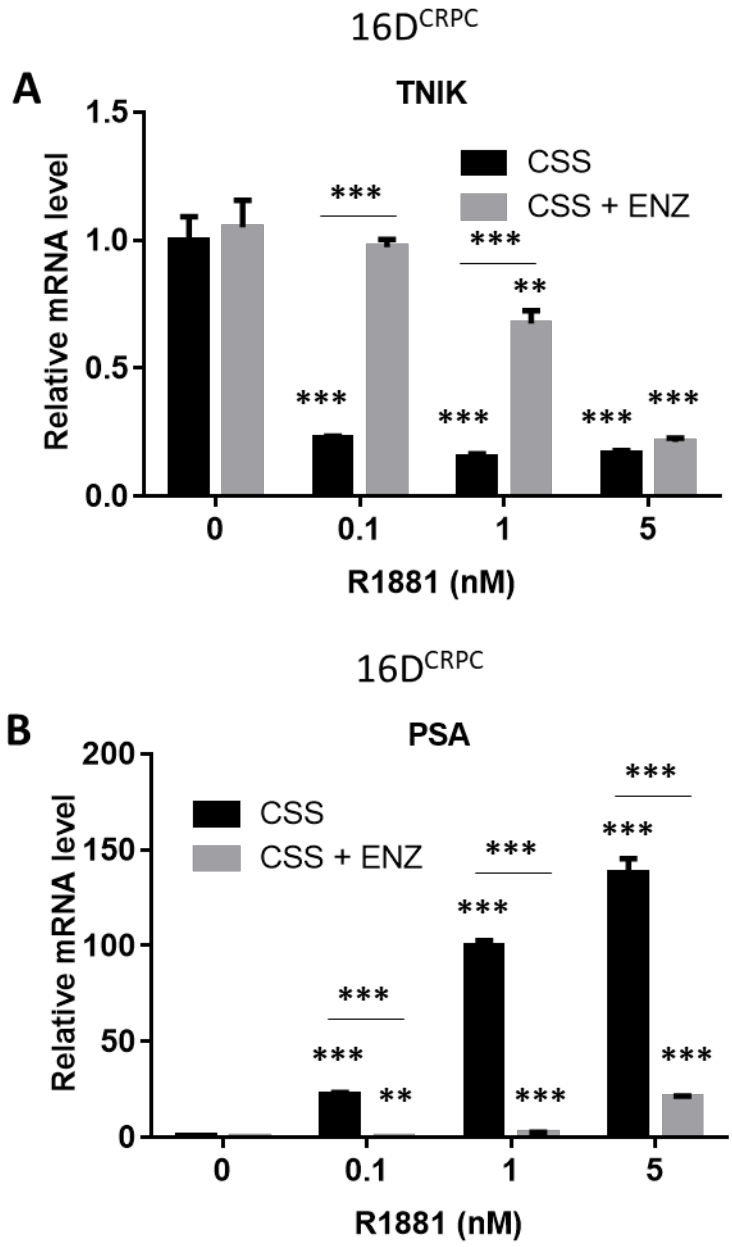

Figure 3.10 Androgen decreased TNIK mRNA expression in 16D^{CRPC}

Relative mRNA expression of (A) TNIK and (B) PSA mRNA normalized to GAPDH were assessed by qPCR in 16D^{CRPC} cells pre-cultured in 10% CSS for 7 days followed by addition of synthetic androgen R1881 at a dose-dependent manner in presence or absence of 10 μM ENZ. The mRNA expression of TNIK and PSA in each sample was compared to control untreated cells cultured in CSS.

3.2.3 AR binding site on TNIK gene

To evaluate whether AR-mediated regulation on TNIK was direct, we examined AR ChIP-seq data from $16D^{CRPC}$ cells stimulated with DHT for potential AR binding sites surrounding the TNIK locus. AR ChIP-seq data analysis identified a putative AR binding site on the TNIK gene (**Figure 3.11A**). The AR binding site was located within 300 bp upstream of exon 3 of the TNIK gene, which was also an enhancer region of TNIK. Interestingly, the AR binding site contained a sequence located between +232045 and +232061 bp of TNIK gene (5'-TGTTTCTGTGTGTGTCT-3') similar to the sequence of an AR consensus binding site (5'-TGTTCTNNNTGTTCT-3') [113] (**Figure 3.11B**). Comparing to the AR consensus binding sequence, each of the AR half-binding site on TNIK contained a base insertion as underlined.

Therefore, we designed primers between +231997 and +232096 bp of TNIK gene to perform ChIP assay with AR antibody for confirming if AR bound to this region of TNIK gene. $16D^{CRPC}$ and $42D^{ENZR}$ cells were cultured in androgen depleted media for 48 hours followed by addition of R1881 1 nM for 24 hours. We observed increased binding of AR to TNIK +231997/+232096 region in presence of R1881 in both $16D^{CRPC}$ and $42D^{ENZR}$ by AR ChIP assay (**Figure 3.12**). These results indicated that AR directly bound to TNIK gene and suppressed transcript expression of TNIK.

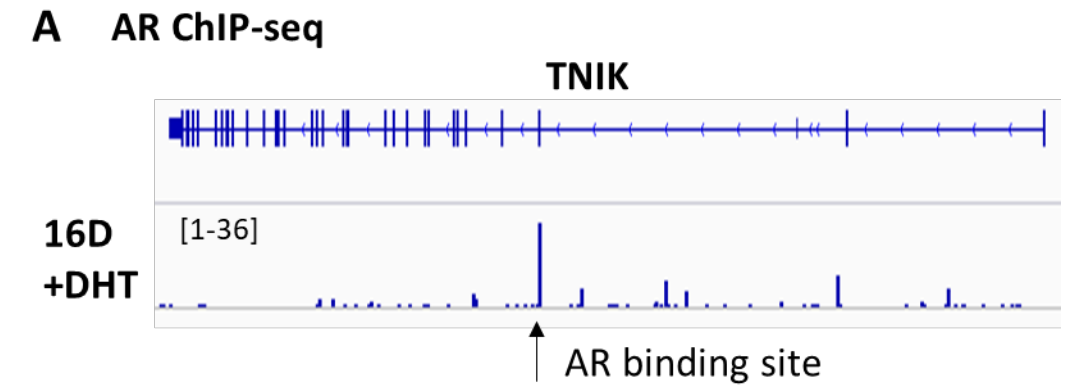

B

AR binding site on TNIK gene (300 bp upstream of TNIK exon 3):

Homo sapiens chromosome 3, GRCh37.p13 Primary Assembly (170946310 - 170946010)

CATAAATCCTCCTCTCATATAAGCTCTTGTCAAATGCCTTGGAGAGGAG
TTAGAACCAAATTGTTCAACATTGCATTTTTTATTTGACTTGACACCCA

+231997

CTGTGAAAATAAACAAAGTGACTGGGGACGTTTTACAAAATAAACACT

+232045 **+232061**

AAGTAGACATGGTGTTTCTGTGTGTGTCTGTCTTTCTCTCTCCCCCAT

+232096

TGACATAGTACAGCACTGATCCAAGCAATTTTTCTTTATTGTTGGAATT
GAATGCTACTATTCATCATCAGAACTAAATCTTTTGTTATTATTTTTTCTT
CACAGG

Consensus AR binding site:

TGTTCTNNNTGTTCT

Figure 3.11 AR ChIP-seq of 16D^{CRPC} in presence of androgen

(A) An AR binding site on TNIK gene was identified in 16D^{CRPC} cells stimulated by androgen (DHT) from AR ChIP-seq data. (B) Potential AR binding sequence of TNIK gene (highlighted in blue). Primers were designed between +231997 and +232096 bp of TNIK gene for AR ChIP assay (highlighted and underlined in red).

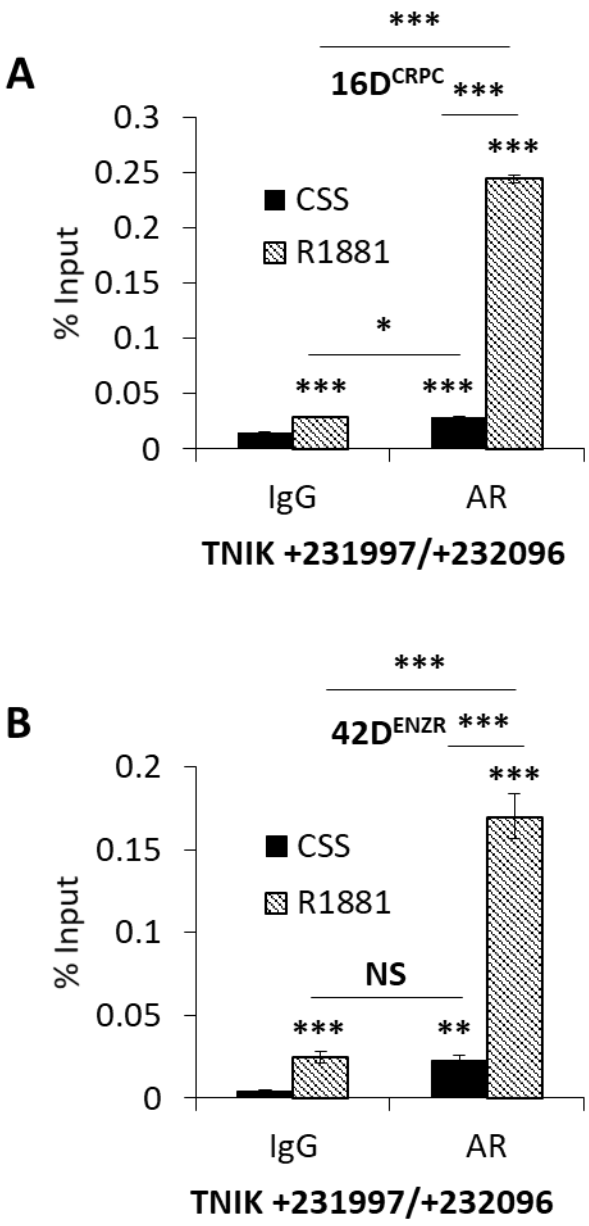

Figure 3.12 AR ChIP assay of 16D^{CRPC} and 42D^{ENZR} in presence of androgen

AR ChIP assay in (A) 16D^{CRPC} and (B) 42D^{ENZR} cells cultured in presence or absence of R1881 between +231997 and +232096 bp region of TNIK gene.

3.2.4 Effect of AR activity on TNIK phosphorylation

Previously, we observed that TNIK was activated in PCa cells when classic AR signaling was absent (**Figure 3.6**). Therefore, we tested if AR pathway inhibition would affect TNIK activity. First, we evaluated the effect of androgen depletion on TNIK phosphorylation. LNCaP and 16D^{CRPC} cells were cultured in media containing either 10% FBS or 10% CSS for 7 days. We observed increase in the levels of p-TNIK (S764) in 10% CSS compared to 10% FBS as the levels of PSA decreased in LNCaP and 16D^{CRPC} cells (**Figure 3.13**). The levels of total TNIK protein remain relatively similar between 10% FBS and 10% CSS in both cell lines. Next, we evaluated the effect of ENZ treatment on TNIK phosphorylation. LNCaP and 16D^{CRPC} cells were treated with 10 μM ENZ in media containing 10% FBS for 2, 4, and 7 days. We observed upregulation of p-TNIK (S764) in LNCaP and 16D^{CRPC} cells in a time-dependent manner (**Figure 3.14**). The levels of total TNIK also remain relatively similar after ENZ treatment in both cell lines. These results suggest that TNIK is activated in absence of classic AR signaling. Therefore, we investigated if TNIK phosphorylation was modulated by AR activity. LNCaP cells were pre-cultured in media with 10% CSS for 7 days and followed by addition of R1881 at 0.1, 1, and 5 nM with or without 10 μM ENZ. Upon R1881 stimulation, we observed that the levels of p-TNIK (S764) in each sample was reduced in a dose-dependent manner in LNCaP as PSA level increased (**Figure 3.15**). Similarly, in the presence of ENZ, the level of p-TNIK (S764) reduced as the doses of R1881 increased. Expression of total TNIK protein remained fairly similar in all condition. Taken together, these results suggested that TNIK phosphorylation was negatively regulated by AR activity.

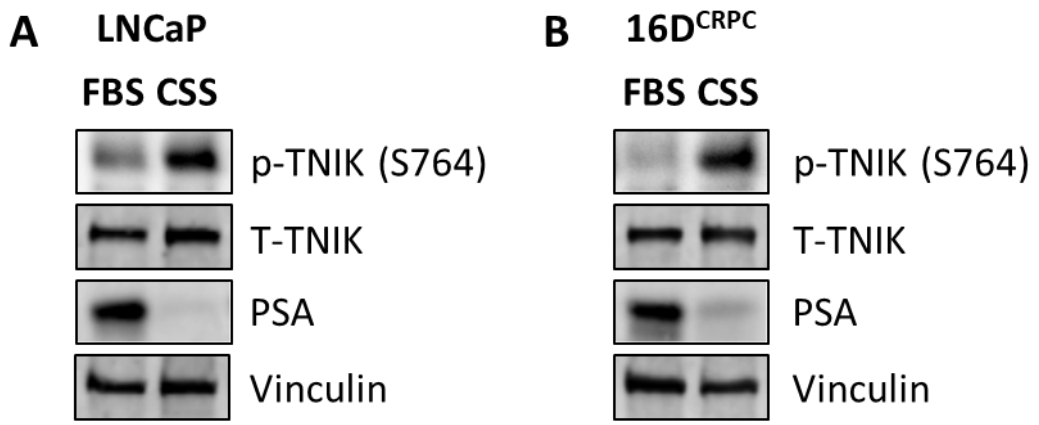

Figure 3.13 Effect of androgen depletion on TNIK phosphorylation

p-TNIK (S764), T-TNIK, and PSA protein expression were assessed in (A) LNCaP and (B) $16D^{CRPC}$ cells that were cultured in media containing 10% FBS or 10% CSS for 7 days by western blot. Vinculin was used as loading control.

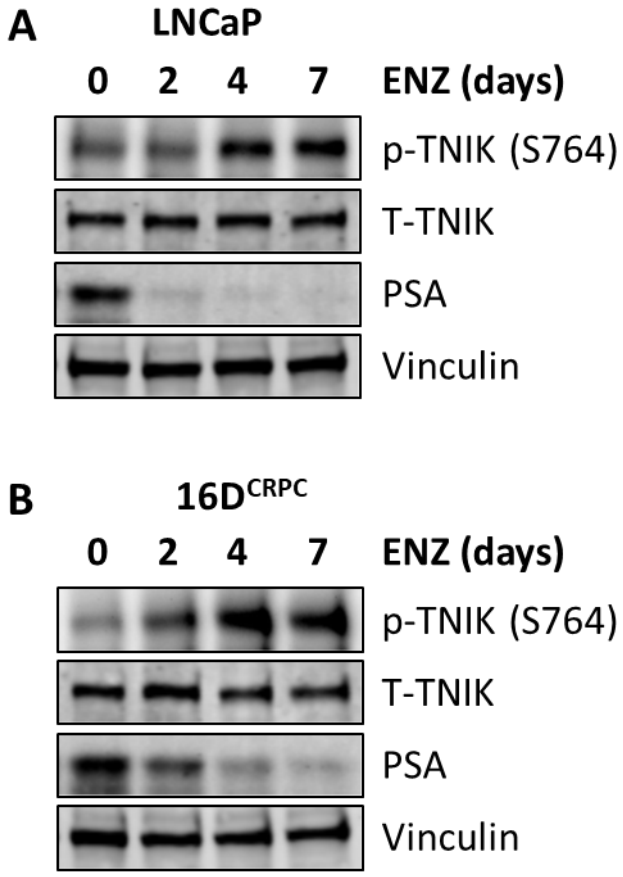

Figure 3.14 TNIK and p-TNIK (S764) protein expression after AR pathway inhibition

p-TNIK (S764), T-TNIK, and PSA protein expression were assessed in (A) LNCaP and 16D^{CRPC} cells that were treated with 10 μM ENZ in media containing 10% FBS for 2, 4, and 7 days by western blot. Vinculin was used as loading control.

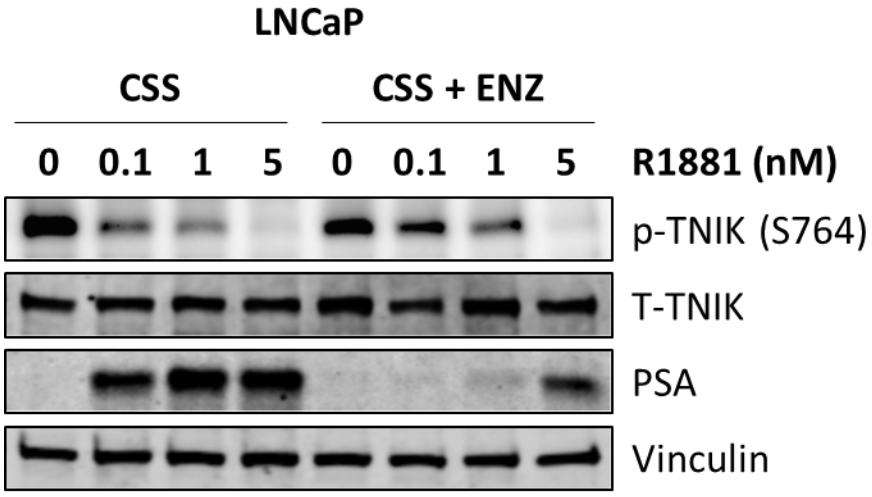

Figure 3.15 Androgen decreased the level of p-TNIK (S764) induced by androgen depletion

p-TNIK (S764), total TNIK, and PSA protein levels were assessed by western blot in LNCaP cells pre-cultured in 10% CSS for 7 days followed by addition of synthetic androgen R1881 at a dose-dependent manner in presence or absence of 10 μM ENZ. Vinculin was used as loading control.

3.2.5 Investigate if TNIK is a driver for NEPC

Since we found that TNIK expression was elevated in human NEPC patients and also after AR pathway inhibition, we sought to determine if TNIK is a driver of NEPC or NE transdifferentiation under AR pathway inhibition. First, we constructed a pLVX-HA-TNIK-IRES-Puro vector for overexpressing TNIK in cell lines. We transiently transfected $16D^{CRPC}$ cells with pLVX-HA-TNIK-IRES-Puro vector (HA-TNIK plasmid) at 1, 1.5, and 2 μg. Protein and RNA were extracted from the cells after 48 hours of transfection. We observed expression of TNIK mRNA, total TNIK, p-TNIK (S764), and HA proteins increased in a dose-dependent manner with the amount of HA-TNIK plasmid transfected (**Figure 3.16**). This suggested that pLVX-HA-TNIK-IRES-Puro could be used for generating stable TNIK overexpressing cell lines.

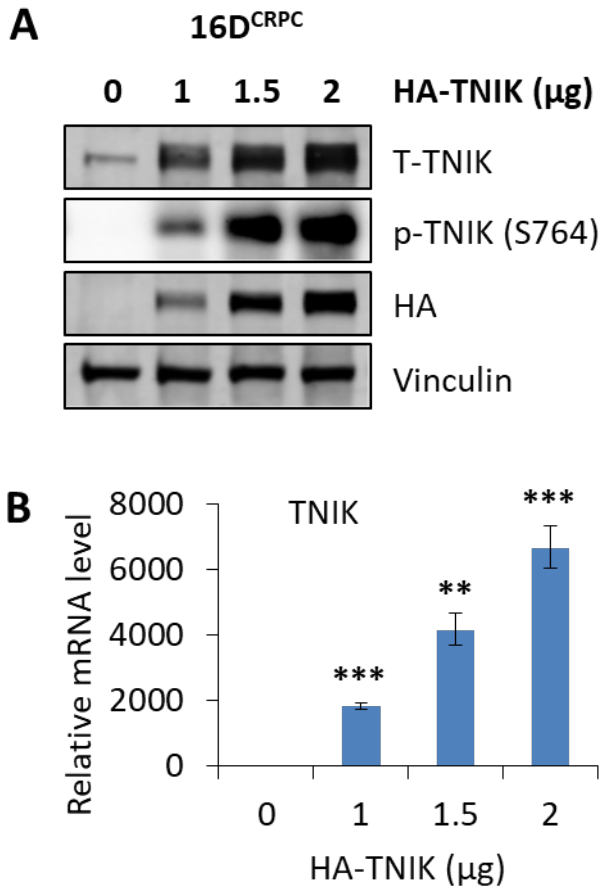

Figure 3.16 Transient overexpression of TNIK in 16D^{CRPC} cells

16D^{CRPC} cells were transiently transfected with pLVX-HA-TNIK-IRES-Puro (HA-TNIK plasmid) at indicated amount. 48 hours post-transfection, (A) total TNIK, p-TNIK, HA, and Vinculin expression were assessed by western blot. (B) Relative mRNA expression of TNIK normalized to GAPDH was assessed by qPCR. TNIK mRNA expression in each sample was compared to control untransfected cells.

$16D^{CRPC}$ cells were stably transfected with empty vector to generate $16D^{Mock}$ cells and with HA-TNIK plasmid to generate $16D^{TNIK}$ cells. Using immunofluorescence, total TNIK and HA proteins were detected in the cytoplasm in $16D^{TNIK}$ cells (**Figures 3.17A and B**). Based on the immunofluorescence result, $16D^{TNIK}$ cells had mixed population of cells with different levels of TNIK protein, so we performed clonal selection in $16D^{TNIK}$ cells and isolated 3 clones. We quantified the amount of TNIK protein and mRNA from these clones with western blot and qPCR and observed that $16D^{TNIK(clone1)}$ had the highest TNIK protein and mRNA expression compared to $16D^{Mock}$ (**Figures 3.18A and B**).

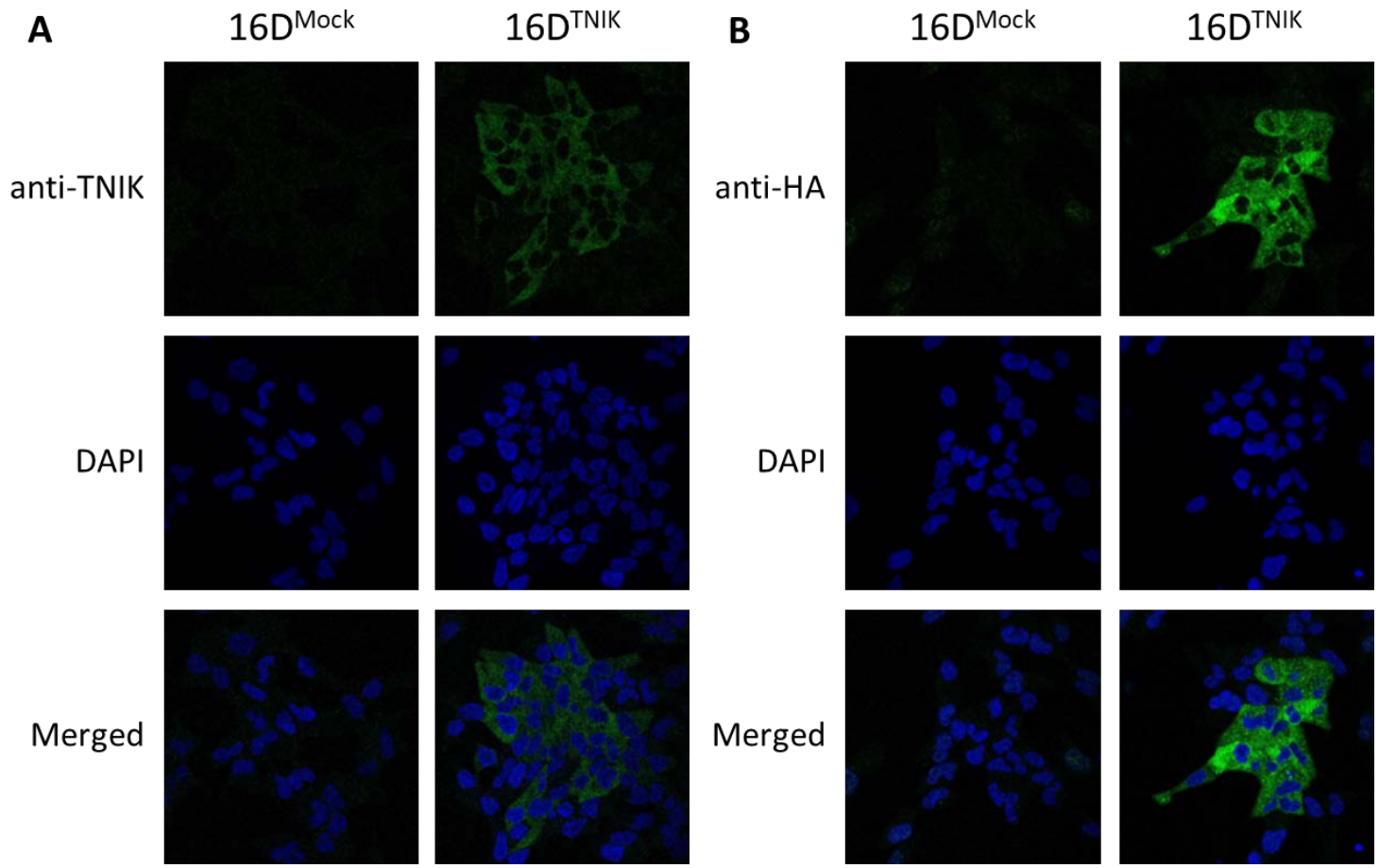

Figure 3.17 TNIK localized in the cytoplasm.

Immunofluorescence was performed in $16D^{Mock}$ and $16D^{TNIK}$ cells using (A) total TNIK antibody (green) and DAPI (nuclei, blue) or (B) HA antibody (green) and DAPI (nuclei, blue).

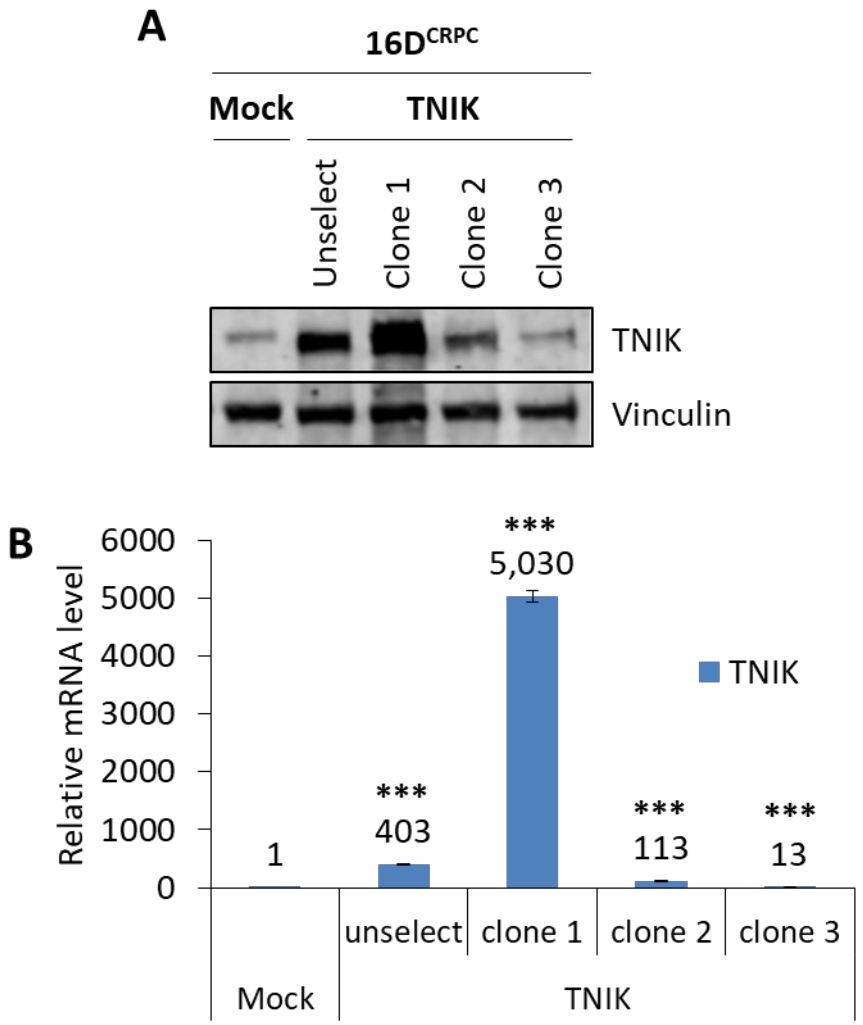

Figure 3.18 TNIK expression in 16D^{Mock} and 16D^{TNIK} stable cell lines

TNIK protein and mRNA expression in 16D TNIK stably overexpressing cells (unselected and clones 1, 2, 3) compared to empty vector transfected control 16D cells (Mock) were assessed by (A) western blot and (B) qPCR.

To determine if TNIK was a driver of NEPC, we assessed the mRNA expression of the terminal NE markers NSE, SYP, and CHGA in $16D^{TNIK(unselected)}$ and $16D^{TNIK(clone1)}$ cells comparing to $16D^{Mock}$ cells by qPCR. However, there were no significant increase in the expression of NE markers in $16D^{TNIK(unselected)}$ and $16D^{TNIK(clone1)}$ compared to $16D^{Mock}$ (**Figure 3.19**). These data indicated that overexpression of TNIK alone was not sufficient to induce NE differentiation.

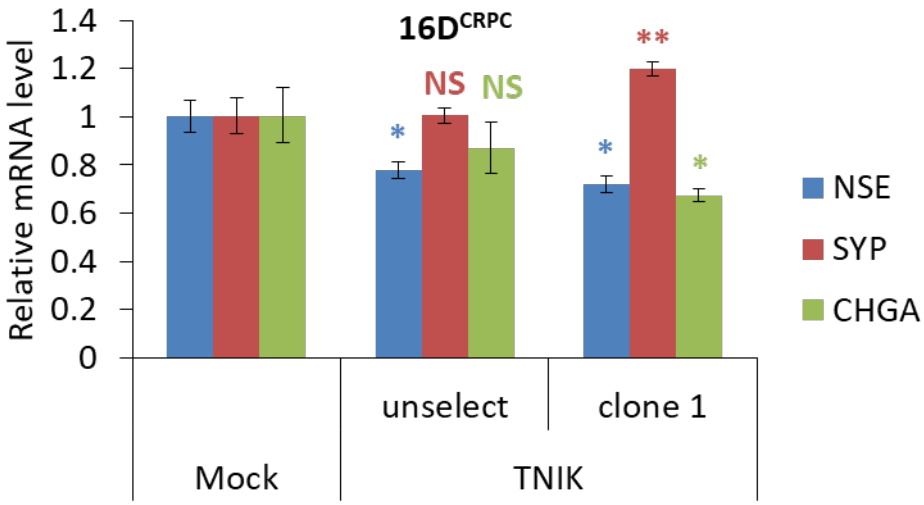

Figure 3.19 Effect of overexpressing TNIK on NE differentiation

Relative mRNA expression of NE markers in 16D TNIK overexpressing cells (unselect and clone 1) compared to 16D Mock were assessed by qPCR.

Next, we tested if overexpression of TNIK could drive the emergence of NE phenotype under AR pathway inhibition. $16D^{CRPC}$ parental, $16D^{Mock}$, and $16D^{TNIK(clone1)}$ cells were treated with ENZ 10 μM for 3 and 14 days. The mRNA expression of TNIK, PSA and NE markers (NSE, SYP, and CHGA) were assessed by qPCR. After 3 days of ENZ treatment while mRNA levels of NE markers had not been increased by ENZ in $16D^{CRPC}$ parental and $16D^{Mock}$ cells yet, there were no significant changes in the expression of NE markers in $16D^{TNIK(clone1)}$ cells compared to $16D^{CRPC}$ parental cells with no treatment control (ENZ 0 day) (**Figures 3.20A and 3.21**). After 14 days of ENZ treatment, the levels of increase in expression of NE markers in $16D^{CRPC}$ parental, $16D^{Mock}$ cells, $16D^{TNIK(clone1)}$ cells were relatively similar compared to $16D^{CRPC}$ parental cells with control (ENZ 0 day). The levels of PSA mRNA were reduced in $16D^{CRPC}$ parental, $16D^{Mock}$, and $16D^{TNIK(clone1)}$ cells after ENZ treatment for 3 and 14 days compared to $16D^{CRPC}$ parental cells with control (ENZ 0 day) (**Figure 3.20B**). These results indicated that overexpression of TNIK did not facilitate the emergence of NE phenotype under AR pathway inhibition.

Since ENZ treatment had increased TNIK expression and activity, we evaluated if overexpression of TNIK conferred resistance of PCa cells to ENZ. $16D^{Mock}$ and $16D^{TNIK(clone1)}$ cells were treated with ENZ in a dose-dependent manner at indicated doses for 72 hours. After ENZ treatment, cell viability was assessed by crystal violet. We observed no significant change in cell viability of $16D^{TNIK(clone1)}$ cells compared to $16D^{Mock}$ cells after ENZ treatment (**Figure 3.22**). This result indicated that overexpression of TNIK did not affect sensitivity of cells to ENZ treatment.

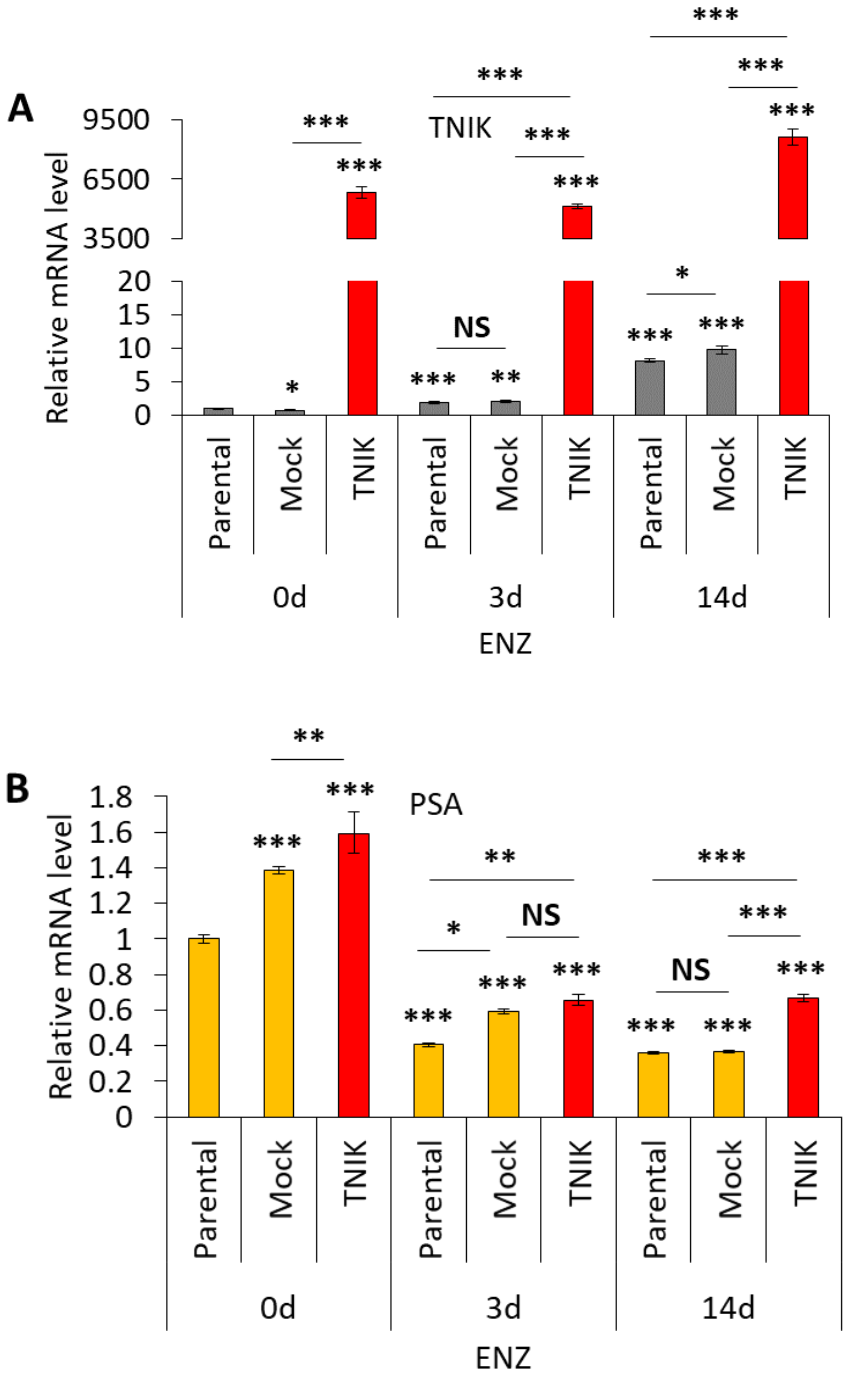

Figure 3.20 Effect of ENZ on TNIK and PSA expression with TNIK overexpression

$16D^{CRPC}$ parental, $16D^{Mock}$, and $16D^{TNIK(clone1)}$ cells were treated with 10 μM ENZ for 3 and 14 days (d). ENZ 0 day represented no treatment control. Relative mRNA expression of TNIK and PSA compared to $16D^{CRPC}$ parental (ENZ 0 day) were assessed by qPCR.

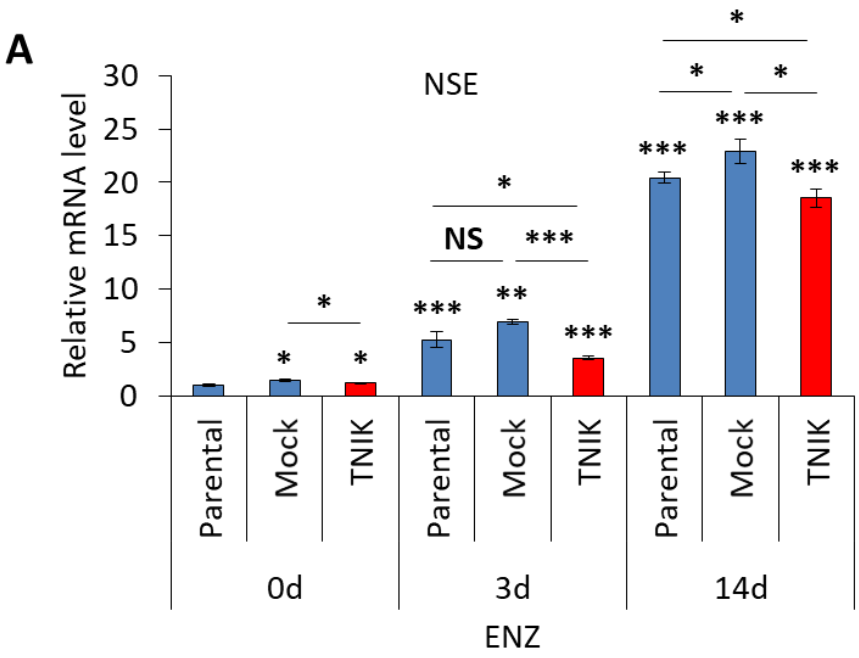
A
NSE
Relative mRNA level
30
25
20
15
10
5
0
Parental
Mock
TNIK
0d
3d
14d
ENZ
NS
*
**
***

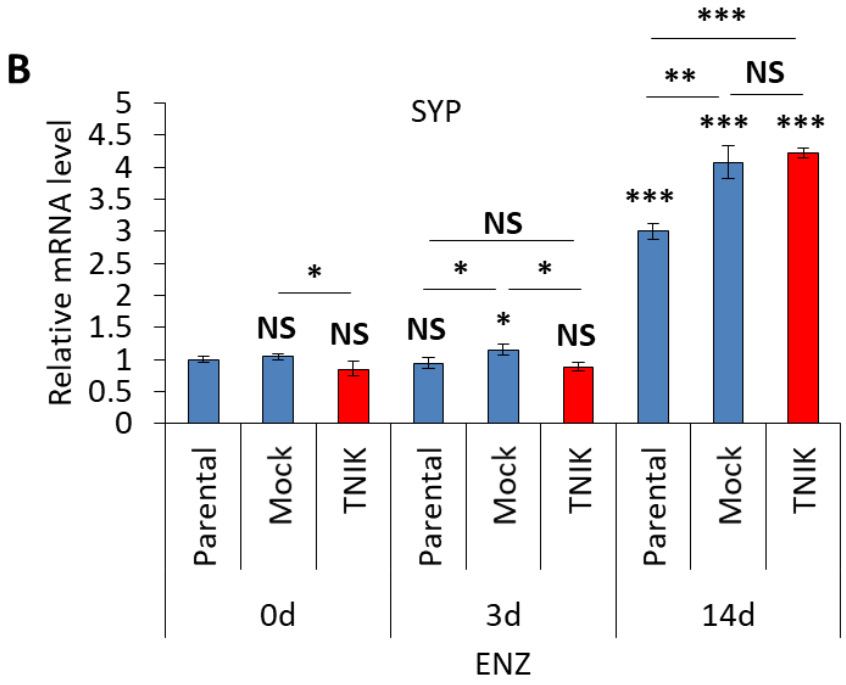
B
SYP
Relative mRNA level
5
4.5
4
3.5
3
2.5
2
1.5
1
0.5
0
Parental
Mock
TNIK
0d
3d
14d
ENZ
NS
*
**
***

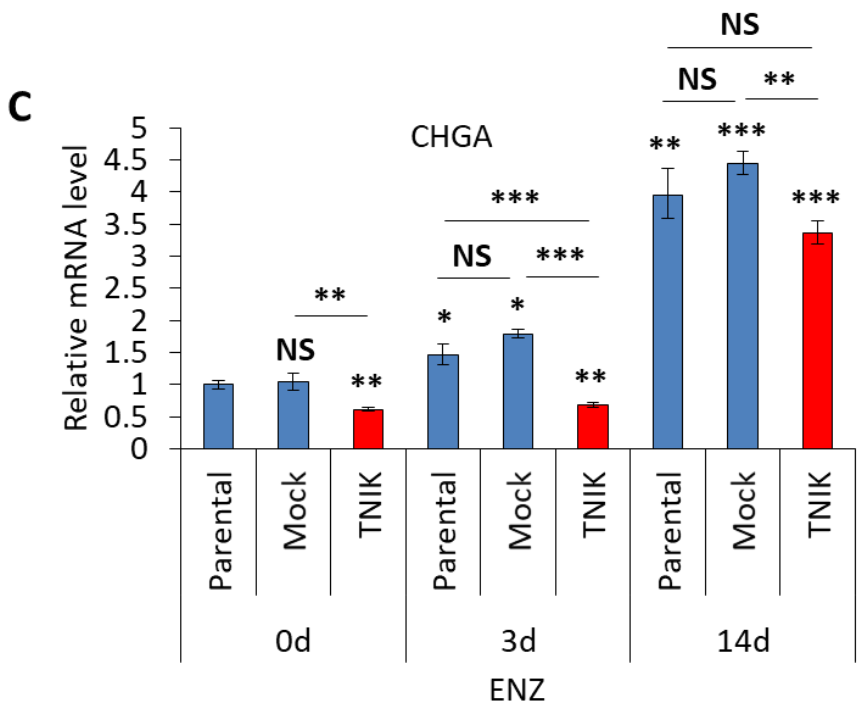

Figure 3.21 Effect of ENZ on NE differentiation with TNIK overexpression

$16D^{CRPC}$ parental, $16D^{Mock}$, and $16D^{TNIK(clone1)}$ cells were treated with 10 μM ENZ for 3 and 14 days (d). Relative mRNA expression of NE markers (A) NSE, (B) SYP, and (C) CHGA compared to $16D^{CRPC}$ parental (ENZ 0 day) were assessed by qPCR.

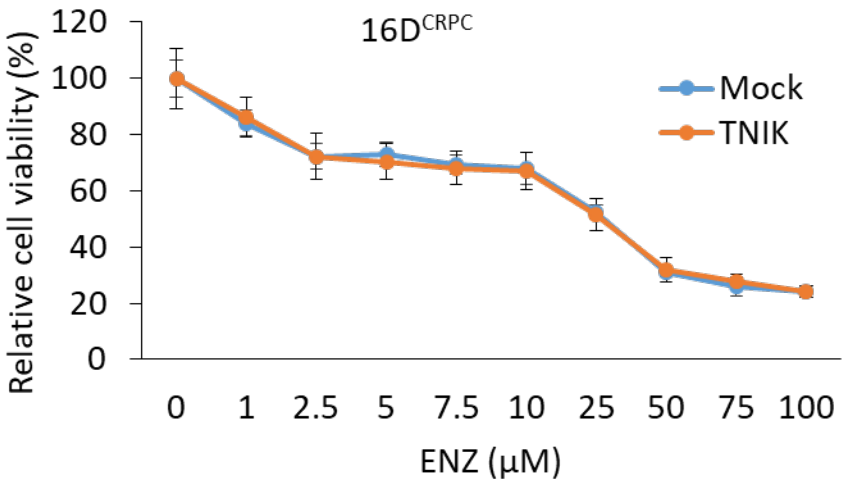

Figure 3.22 Effect of ENZ on cell viability with TNIK overexpression

$16D^{Mock}$ and $16D^{TNIK(clone1)}$ cells were treated with ENZ at indicated doses for 72 hours. After treatment, cells were fixed and cell viability was assessed by crystal violet.

3.2.6 Investigate if TNIK is a therapeutic target for NEPC

In this study, we also investigated if TNIK is a therapeutic target for NEPC. We tested if TNIK is required for cell growth and maintaining NE phenotype in PCa. To assess the effect of TNIK knockdown on cell growth and expression of NE markers, $42D^{ENZR}$ cells were transfected with 20 nM of control siRNA (siCtr) or TNIK siRNA (siTNIK). Cell proliferation was assessed by crystal violet assay from 1 to 5 days after transfection. mRNA expression of TNIK and NE markers were assessed by qPCR. We observed that silencing TNIK with siRNA in $42D^{ENZR}$ had no significant effects on cell proliferation and expression of NE markers compared to control siRNA (**Figure 3.23**).

Using another approach, we tested if inhibiting TNIK activity would affect cell viability. $42D^{ENZR}$ cells were treated with TNIK small molecule inhibitor KY-05009 in a dose-dependent manner for 72 hours. Due to the insolubility of KY-05009 in the media, the cells could only be

treated with this inhibitor at a dose up to 5 μM. After 72 hours of treatment, 5 μM of KY-05009 reduced $42D^{ENZR}$ cell viability by nearly 30% (**Figure 3.24A**). We assessed TNIK activity in $42D^{ENZR}$ cells after KY-05009 treatment at a dose of 0.5, 2.5, and 5 μM for 72 hours by western blot. p-TNIK (S764) level was greatly reduced in $42D^{ENZR}$ cells at 2.5 and 5 μM of KY-05009 treatment (**Figure 3.24B**). To determine if the reduction in cell viability of $42D^{ENZR}$ by KY-05009 treatment was specific to cell lines with upregulation of p-TNIK (S764), we treated LNCaP, $16D^{CRPC}$, $42D^{ENZR}$, and $42F^{ENZR}$ cells with 5 μM of KY-05009 for 72 hours. However, the reduction in cell viability by KY-05009 treatment in cell lines with low level of p-TNIK (S764) (LNCaP and $16D^{CRPC}$) was similar to cell lines with high level of p-TNIK (S764) ($42D^{ENZR}$ and $42F^{ENZR}$) (**Figure 3.25**).

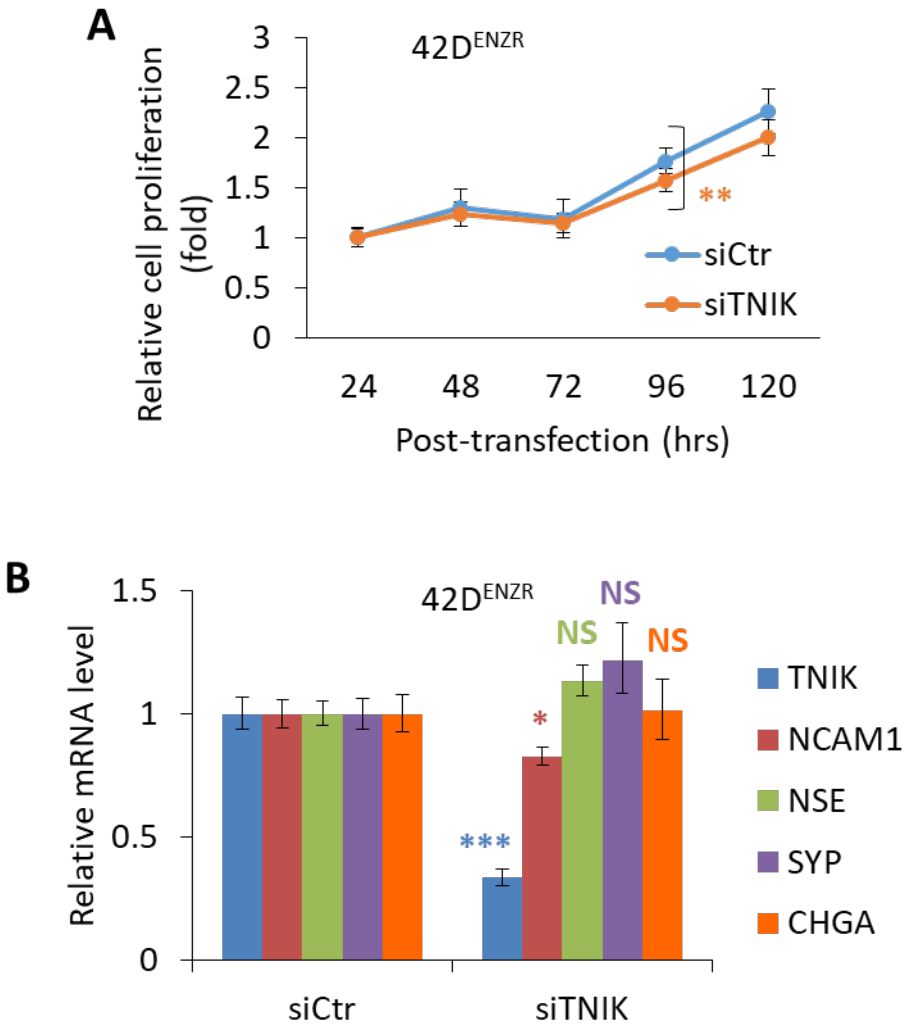

Figure 3.23 Effect of silencing TNIK with siRNA on cell growth *in vitro*

$42D^{ENZR}$ cells were transfected with 20 nM control or TNIK siRNA. (A) Cell proliferation was assessed by crystal violet assay from 1 to 5 days after transfection. (B) Relative mRNA expression of TNIK and NE markers normalized to GAPDH in $42D^{ENZR}$ transfected with siTNIK compared to siCtr were assessed by qPCR.

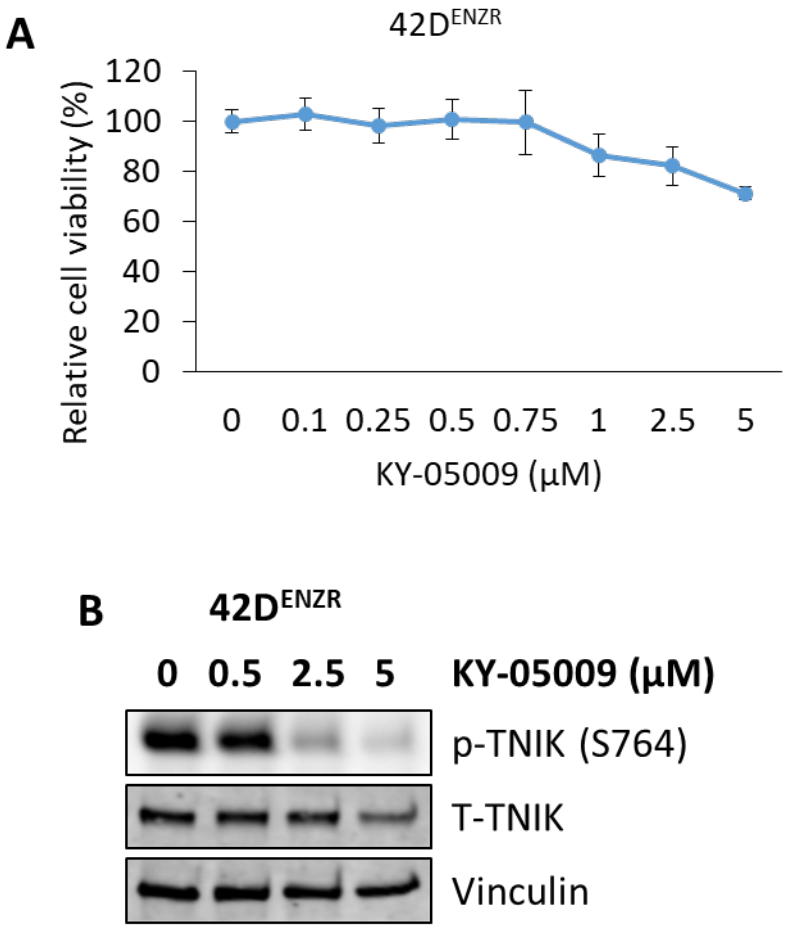

Figure 3.24 Effect of TNIK inhibitor on cell viability in dose-dependent manner *in vitro*

$42D^{ENZR}$ cells were treated with TNIK small molecule inhibitor KY-05009 at indicated doses for 72 hours. (A) Cell viability was assessed by crystal violet assay. (B) p-TNIK (S764), total TNIK, and Vinculin protein expression were assessed by western blot.

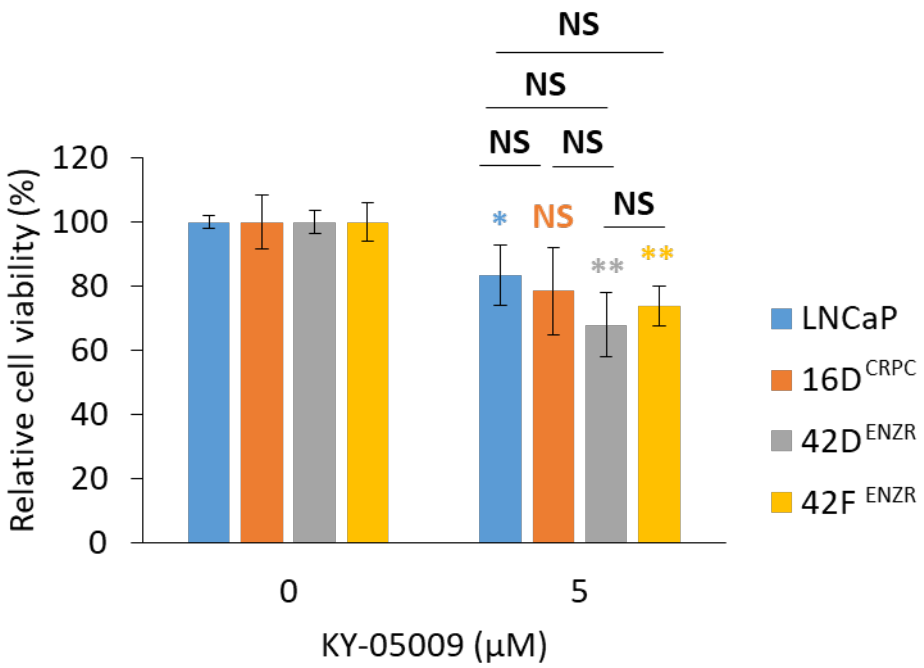

Figure 3.25 Effect of TNIK inhibitor on cell viability in different cell lines *in vitro*

LNCaP, $16D^{CRPC}$, $42D^{ENZR}$, and $42F^{ENZR}$ cells were treated with 5 μM of KY-05009 for 72 hours. Cell viability of cells after treatment was compared to their untreated control and was assessed by crystal violet assay.

3.3 Detection of TNIK transcript variants in PCa

Previously, we observed that TNIK expression was elevated in NEPC patients and TNIK had been reported to have 8 splice variants. A gene could produce multiple isoforms through alternative splicing and the expression of each isoform could change in different stages of cancer progression [114]. Therefore, we investigated if a specific TNIK splice variant was expressed or upregulated in NEPC that could be served as a novel biomarker for NEPC. To determine which TNIK transcript variants were expressed in PCa, we designed primers and setup four PCR reactions on cDNA samples from LNCaP and NCI-H660 according to **Table 2.3** and ran the PCR products on agarose gel. Based on the sizes of the DNA fragments, we observed that TNIK

transcript variants 1, 2, 3, 4, 7, and 8 were detected in both LNCaP and NCI-H660 (**Figure 3.26**).

TNIK transcript variants 5 and 6 were not detectable in LNCaP and NCI-H660.

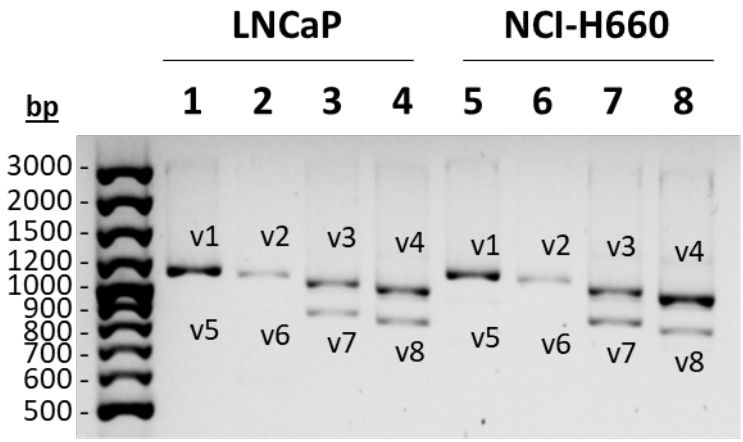

Figure 3.26 Transcript variants of TNIK in LNCaP and NCI-H660 cells

PCR was performed from cDNA of LNCaP and NCI-H660 using TNIK primers specific to each transcript variants. PCR products were separated by agarose gel electrophoresis. PCR samples of LNCaP were loaded in lanes 1-4 and NCI-H660 were loaded in lanes 5-8.

Chapter 4: Discussion

In this study, we found that TNIK expression was highly upregulated in human NEPC patients and human NE transdifferentiation PDX model (**Figures 1.6 and 3.1**). We also observed that expression of TNIK was negatively correlated with androgen regulated genes and positively correlated with NE markers in patient data from prostate cancer TCGA cohort (**Figures 3.2 and 3.4**). NEPC is often associated with low or non-rising PSA in aggressive metastatic CRPC [68]. Interestingly, we found that the expression of TNIK was significantly inverse correlated with serum PSA level in CRPC patient samples (**Figure 3.3**). Taken together, these results showed that TNIK expression was strongly associated with features of aggressive form of PCa, which included NEPC.

First, we assessed TNIK expression in PCa cell lines with different features. We found that expression of TNIK mRNA was increased in PCa cell lines when classic AR signaling was absent (**Figure 3.5**). Under androgen depletion and ENZ treatment, we observed increase of TNIK mRNA expression in both LNCaP and $16D^{CRPC}$ cells (**Figures 3.7 and 3.8**). These conditions had been previously established and shown to increase expression of NE markers [76, 105]. Addition of R1881 could reduce TNIK mRNA expression after androgen depletion or ENZ treatment in LNCaP and $16D^{CRPC}$ cells (**Figures 3.9 and 3.10**). These results suggested that suppression of classic AR signaling led to increase of TNIK expression, which was accompanied with induction of NE differentiation.

Next, we investigated the molecular mechanism of AR regulation on TNIK expression. Our AR ChIP-seq data analysis revealed that AR could bind to a region of TNIK gene in $16D^{CRPC}$ in presence of androgen and that could be a potential AR binding site on TNIK gene (**Figure 3.11**). Comparing with publicly available AR ChIP-seq data sets GSM2122804 and

GSM2122804, the potential AR binding site also presented in LNCaP cells cultured in media with normal serum (FBS) (**Appendix C.4A**). Interestingly, in AR ChIP-seq data sets GSM1691153 and GSM1691147, the peak at this AR binding site on TNIK gene was higher upon R1881 stimulation in LNCaP cells, which indicated increased binding of AR on TNIK gene when AR was activated (**Appendix C.4B**). Therefore, we further confirmed by AR ChIP assay that stimulation with R1881 increased AR occupancy to this region of TNIK gene in $16D^{CRPC}$ and $42D^{ENZR}$ cells (**Figure 3.12**). These results suggested that TNIK was a direct target of transcription repression by AR in PCa.

In the predicted AR binding site in TNIK gene, we identified a sequence that contained two single nucleotide insertions (5'-TGTTTCTGTGTGTGTCT-3') compared to the known consensus DNA-binding site of AR (5'-TGTTCTNNNTGTTCT-3'). The known consensus DNA-binding site of AR was ARE in genes for activating transcription upon binding of AR. Conversely, our results showed that AR activity negatively regulated TNIK mRNA expression. Moreover, these single nucleotide insertions were located in each of the two 6-bp half-sites of AR. These findings suggested that the mutation in the ARE could potentially modified the function of AR into a repressor of TNIK.

Since AR activity negatively regulated TNIK expression transcriptionally, we also assessed if TNIK activity could be modulated by AR activity. We observed that level of p-TNIK (S764) was increased in PCa cell lines with absence of classic AR signaling (**Figure 3.6**). Interestingly, p-TNIK (S764) level was increased under AR pathway inhibition in LNCaP and $16D^{CRPC}$ cells (**Figures 3.13 and 3.14**). This phenomenon could be reversed by androgen supplementation via R1881, which decreased p-TNIK (S764) level (**Figure 3.15**). Taken together, these results

suggested that TNIK could be activated through inhibition of AR pathway and might have a role in PCa progression in an AR-independent manner.

To study the role of TNIK in PCa, we investigated if TNIK could be a driver or a therapeutic target for NEPC. In our gain-of-function studies on TNIK, overexpressing TNIK in $16D^{CRPC}$ cells did not induce NE differentiation (**Figure 3.19**). Overexpression of TNIK also did not induce NE differentiation under ENZ treatment or affect sensitivity to ENZ in $16D^{CRPC}$ cells (**Figures 3.20-3.22**). In our loss-of function studies on TNIK, we silenced TNIK with siRNA in $42D^{ENZR}$ cells, but we observed no significant effects on cell proliferation *in vitro* and the expression of NE markers (**Figure 3.23**). We also treated LNCaP, $16D^{CRPC}$, $42D^{ENZR}$, and $42F^{ENZR}$ cells with TNIK small-molecule inhibitor KY-05009 and we observed no significant effect on cell viability *in vitro* (**Figures 3.24-3.25**). These results indicated that TNIK may not be a driver or therapeutic target for NEPC; however, more experiments are needed to further confirm with these findings.

Since previous studies showed that TNIK was required in Wnt signaling in colorectal cancer [22, 30], we further examined if TNIK played a role in Wnt signaling in PCa. We used luciferase assay to assess the effect of TNIK expression on TCF transcriptional activity. However, overexpression of TNIK in $16D^{TNIK}$ cells did not enhance TCF transcriptional activity compared to $16D^{Mock}$ cells (**Appendix C.5**). Silencing TNIK with siRNA (siTNIK) in $42D^{ENZR}$ cells also did not reduced TCF transcriptional activity compared to control siRNA (siCtr). These results suggested that TNIK did not play a role in activating Wnt signaling in PCa. Comparing to 80% of colorectal cancer that carried APC gene mutation in aberrantly activation of Wnt signaling, only 3-10% of PCa were reported to carry mutation in APC [33, 115]. These data

suggested that TNIK might not be as important for activation of Wnt signaling in PCa as it was in APC-mutated tumors.

Moreover, phosphorylated TNIK (p-TNIK S764) had been previously shown to be translocated into the nucleus and co-localized with TCF4 in Wnt-activated colorectal cancer cells [30]. In our study, overexpression of TNIK increased the level of p-TNIK (S764) in $16D^{CRPC}$ cells (**Figures 3.16**). Using TNIK stably overexpressing ($16D^{TNIK}$) cells, immunofluorescence showed no nuclear translocation of TNIK (**Figures 3.17**). TNIK was localized in the cytoplasm of $16D^{TNIK}$ cells. These results suggested that TNIK could possibly interact with proteins in the cytoplasm and involve in other signaling pathways in PCa. Previous study showed that TNIK co-localized with RAP2 in the cytoplasm and acted as a downstream effector of RAP2 in regulating actin cytoskeleton in mouse embryo fibroblast cells [14]. TNIK forms a complex with Nedd4-1 and Rap2, which is essential for regulating neurite development in mouse neurons [23]. This protein complex is also required in glioma cells in regulation of migration and invasion [116]. In addition, previous studies had reported that TNIK inhibitors reduced EMT in human non-small cell lung cancer and cancer stem cell (CSC) phenotypes in colorectal cancer [38, 39]. Although long term ADT is associated with NE differentiation, ADT can also induce EMT and CSC phenotypes in PCa [117]. There may be a relationship between NEPC and CSC because both cells do not express AR and PSA [118]. Altogether, for future experiments of this study, it would be interesting to investigate if TNIK plays a role in migration, invasion, EMT, or CSC phenotypes, which may possibly be linked to Nedd4-1 and Rap2 in PCa.

Alternative splicing from one gene could generate multiple protein isoforms with different biological properties such as intracellular localization, protein-protein interaction, and functions [119, 120]. For example, alternative splicing of the Bcl-x gene produced two isoforms that had

opposite functions with a long anti-apoptotic isoform and a short pro-apoptotic isoform [121]. Previous study had reported that alternative splicing produced eight TNIK protein isoforms [1]. Currently, the biological function of each protein isoform of TNIK had not been reported. Since TNIK expression was highly increased in NEPC compared to Adeno, it could be a biomarker for NEPC. We sought to investigate if the expression of TNIK splice variants or protein isoforms varied between Adeno and NEPC. Currently, no method has been reported for detecting the TNIK transcript variants or protein isoforms yet. There was also limitation in studying TNIK protein isoforms; for example, there are no antibodies available for detecting each of TNIK protein isoforms specifically.

In this study, we developed a simple method for detecting each transcript variant of TNIK using PCR amplification on cDNA samples. Unfortunately, PCR was a qualitative method, it could only be used to detect the presence or absence of a specific DNA product [122]. We evaluated the presence of each TNIK splice variant in LNCaP and NCI-H660 cells based on the PCR products separated on agarose gel by size. We found that LNCaP and NCI-H660 cells expressed TNIK transcript variants 1, 2, 3, 4, 7, and 8 (**Figure 3.26**). This result could help explain why TNIK mRNA levels were not correlated with total TNIK protein expression in some of our experiments.

At mRNA level, we observed that TNIK was about 60-fold higher in NCI-H660 than LNCaP cells (**Figure 3.5**). The proposed autophosphorylation of TNIK at S764 residue were highly upregulated in NCI-H660 compared to LNCaP, but the total TNIK protein expression was similar between the cell lines (**Figure 3.6**). Under androgen deprivation and ENZ treatment, we also observed no significant changes in total TNIK protein expression when TNIK mRNA and p-TNIK (S764) were upregulated (**Figures 3.7, 3.8, 3.13 and 3.14**). However, when we transiently

overexpressed TNIK in $16D^{CRPC}$ cells with different amount of TNIK wild type plasmid encoding transcript variant 1, the cells had increased levels of TNIK mRNA, total TNIK, p-TNIK (S764), and HA proteins in a dose-dependent manner (**Figure 3.16**). According to the structure of each TNIK isoform, the total TNIK antibody used in this study recognized TNIK protein at amino acids 522 to 644, which located at one of the alternative splicing sites (**Figure 1.1**). Therefore, this indicated that the total TNIK antibody used in this study could be detecting isoforms 1 to 4 with similar total TNIK protein expression. Thus, the TNIK isoforms upregulated in cell lines or conditions with inactive AR signaling could be 5, 6, 7, or 8. Moreover, LNCaP and NCI-H660 cells did not express TNIK transcript variants 5 and 6 from the PCR result. Therefore, our results together suggested that TNIK transcript variants 7 and 8 might be predominantly upregulated in the absence of AR signaling and NEPC.

Chapter 5: Conclusion

5.1 Summary of findings

In summary, our study revealed that TNIK was associated with aggressive form of PCa. In clinical data, we found that TNIK was most highly expressed in patients with NEPC compared to Adeno. We also found that TNIK expression was positively correlated with NE markers and negatively correlated with androgen regulated genes in PCa patient data. Our results showed that inhibition of AR signaling induced TNIK expression and activity, which were negatively regulated by AR activity in PCa. Although our results showed that TNIK might not be a driver or therapeutic target for NEPC, we identified TNIK as a novel AR-repressed gene in PCa. We further discovered that an ARE on TNIK gene could possibly switch the function of AR from a transcriptional activator to a repressor upon DNA binding. Based on our findings, TNIK could be a biomarker for NEPC.

5.2 Limitations and future directions

In this study, we identified a potential ARE on TNIK gene. For future work to study the functional role of this potential ARE on TNIK gene, we could design a 20-bp DNA aptamer that could prevent AR from binding to this region of TNIK as previously described [76]. The DNA aptamer is a single-stranded oligonucleotides that could block other molecules from binding to its complementary sequence [123]. We could transfect the aptamer into $42D^{ENZR}$ cells and assess if the aptamer could prevent AR from inhibiting transcription of TNIK in presence of R1881.

To further address the role of TNIK in NE differentiation in future experiments, we could evaluate the effect of silencing or inhibiting TNIK on cell growth and NE phenotype in more cell lines such as NEPC NCI-H660 cells, as well as the effects following AR pathway inhibition in

Adeno cell lines such as LNCaP and 16D^{CRPC}. Furthermore, there were limitations in the experiments using TNIK inhibitor KY-05009 because of its insolubility in the media. We could not perform our experiments with doses higher than 5 μM. Since the experiments in this study were only performed with one TNIK siRNA and TNIK inhibitor, we could also test with other TNIK siRNAs and TNIK inhibitors such as NCB-0846 to further support our findings.

TNIK has been reported to be involved in EMT and CSC. Thus, we could determine if overexpressing, silencing, or inhibiting TNIK have any effects on cell migration, invasion, and the expression of EMT and CSC markers in PCa. To study these effects, we could perform experiments such as wound healing assay, invasion assay, and spheroid assay. Moreover, S764 phosphorylation of TNIK was upregulated under androgen deprivation and ENZ treatment. We could also generate constitutively active and inactive kinase mutants of TNIK to explore the roles of TNIK in PCa along with wild type overexpression of TNIK. Based on our results, TNIK transcripts 7 and 8 could be the predominant forms being upregulated in NEPC. We could overexpress TNIK transcript variants 7 and 8 to determine if they induce NE differentiation, migration, invasion or stemness in PCa.

In addition, there were limitations for us to study the expression of TNIK transcript variants or isoforms in this study. We did not have a total TNIK antibody that could detect all TNIK isoforms, which might have affected our results in evaluating total TNIK protein levels by western blotting. There was also no antibodies commercially available that could detect each TNIK isoforms specifically. If another total TNIK antibody is available that could recognize amino acid residues shared by all TNIK isoforms, we could use it to evaluate the total TNIK protein expression in our experiments. Moreover, we were not able to assess the expression of each TNIK splice variant in LNCaP and NCI-H660 cells quantitatively using PCR. It was also

difficult to design primers for qPCR for quantitative analysis because each of TNIK splice variants did not have a unique sequence to distinguish between them. In the future, if other quantitative method such as RNA-seq available for assessing the expression of each TNIK splice variant in different samples, it could identify the splice variant that could serve as a biomarker for NEPC or other diseases.

Bibliography

1. Fu, C.A., M. Shen, B.C. Huang, J. Lasaga, D.G. Payan, and Y. Luo, *TNIK, a novel member of the germinal center kinase family that activates the c-Jun N-terminal kinase pathway and regulates the cytoskeleton.* J Biol Chem, 1999. **274**(43): p. 30729-37.
2. Wu, C., M. Whiteway, D.Y. Thomas, and E. Leberer, *Molecular characterization of Ste20p, a potential mitogen-activated protein or extracellular signal-regulated kinase kinase (MEK) kinase kinase from Saccharomyces cerevisiae.* J Biol Chem, 1995. **270**(27): p. 15984-92.
3. Delpire, E., *The mammalian family of sterile 20p-like protein kinases.* Pflugers Arch, 2009. **458**(5): p. 953-67.
4. Dan, I., N.M. Watanabe, and A. Kusumi, *The Ste20 group kinases as regulators of MAP kinase cascades.* Trends Cell Biol, 2001. **11**(5): p. 220-30.
5. Sells, M.A. and J. Chernoff, *Emerging from the Pak: the p21-activated protein kinase family.* Trends Cell Biol, 1997. **7**(4): p. 162-7.
6. Molli, P.R., D.Q. Li, B.W. Murray, S.K. Rayala, and R. Kumar, *PAK signaling in oncogenesis.* Oncogene, 2009. **28**(28): p. 2545-55.
7. Ye, D.Z. and J. Field, *PAK signaling in cancer.* Cell Logist, 2012. **2**(2): p. 105-116.
8. Radu, M., G. Semenova, R. Kosoff, and J. Chernoff, *PAK signalling during the development and progression of cancer.* Nat Rev Cancer, 2014. **14**(1): p. 13-25.
9. Lu, H., S. Liu, G. Zhang, W. Bin, Y. Zhu, D.T. Frederick, Y. Hu, W. Zhong, S. Randell, N. Sadek, W. Zhang, G. Chen, C. Cheng, J. Zeng, L.W. Wu, J. Zhang, X. Liu, W. Xu, C. Krepler, K. Sproesser, M. Xiao, B. Miao, J. Liu, C.D. Song, J.Y. Liu, G.C. Karakousis, L.M. Schuchter, Y. Lu, G. Mills, Y. Cong, J. Chernoff, J. Guo, G.M. Boland, R.J. Sullivan, Z. Wei, J. Field, R.K. Amaravadi, K.T. Flaherty, M. Herlyn, X. Xu, and W. Guo, *PAK signalling drives acquired drug resistance to MAPK inhibitors in BRAF-mutant melanomas.* Nature, 2017. **550**(7674): p. 133-136.
10. Huynh, N. and H. He, *p21-activated kinase family: promising new drug targets.* Dove Press, 2015. **5**: p. 119-128.
11. Gagnon, K.B. and E. Delpire, *Molecular physiology of SPAK and OSR1: two Ste20-related protein kinases regulating ion transport.* Physiol Rev, 2012. **92**(4): p. 1577-617.
12. Yin, H., Z. Shi, S. Jiao, C. Chen, W. Wang, M.I. Greene, and Z. Zhou, *Germinal center kinases in immune regulation.* Cell Mol Immunol, 2012. **9**(6): p. 439-45.
13. Nonaka, H., K. Takei, M. Umikawa, M. Oshiro, K. Kuninaka, M. Bayarjargal, T. Asato, Y. Yamashiro, Y. Uechi, S. Endo, T. Suzuki, and K.I. Kariya, *MINK is a Rap2 effector for phosphorylation of the postsynaptic scaffold protein TANC1.* Biochem Biophys Res Commun, 2008. **377**(2): p. 573-578.
14. Taira, K., M. Umikawa, K. Takei, B.E. Myagmar, M. Shinzato, N. Machida, H. Uezato, S. Nonaka, and K. Kariya, *The Traf2- and Nck-interacting kinase as a putative effector of Rap2 to regulate actin cytoskeleton.* J Biol Chem, 2004. **279**(47): p. 49488-96.
15. Hussain, N.K., H. Hsin, R.L. Huganir, and M. Sheng, *MINK and TNIK differentially act on Rap2-mediated signal transduction to regulate neuronal structure and AMPA receptor function.* J Neurosci, 2010. **30**(44): p. 14786-94.

16. Su, Y.C., J. Han, S. Xu, M. Cobb, and E.Y. Skolnik, *NIK is a new Ste20-related kinase that binds NCK and MEKK1 and activates the SAPK/JNK cascade via a conserved regulatory domain.* EMBO J, 1997. **16**(6): p. 1279-90.
17. Caplan, S., L.M. Hartnell, R.C. Aguilar, N. Naslavsky, and J.S. Bonifacino, *Human Vam6p promotes lysosome clustering and fusion in vivo.* J Cell Biol, 2001. **154**(1): p. 109-22.
18. Schurch, C., C. Riether, M.S. Matter, A. Tzankov, and A.F. Ochsenbein, *CD27 signaling on chronic myelogenous leukemia stem cells activates Wnt target genes and promotes disease progression.* J Clin Invest, 2012. **122**(2): p. 624-38.
19. Wajant, H. and P. Scheurich, *Tumor necrosis factor receptor-associated factor (TRAF) 2 and its role in TNF signaling.* Int J Biochem Cell Biol, 2001. **33**(1): p. 19-32.
20. Buday, L., L. Wunderlich, and P. Tamas, *The Nck family of adapter proteins: regulators of actin cytoskeleton.* Cell Signal, 2002. **14**(9): p. 723-31.
21. Satow, R., M. Shitashige, T. Jigami, K. Honda, M. Ono, S. Hirohashi, and T. Yamada, *Traf2- and Nck-interacting kinase is essential for canonical Wnt signaling in Xenopus axis formation.* J Biol Chem, 2010. **285**(34): p. 26289-94.
22. Mahmoudi, T., V.S. Li, S.S. Ng, N. Taouatas, R.G. Vries, S. Mohammed, A.J. Heck, and H. Clevers, *The kinase TNIK is an essential activator of Wnt target genes.* EMBO J, 2009. **28**(21): p. 3329-40.
23. Kawabe, H., A. Neeb, K. Dimova, S.M. Young, Jr., M. Takeda, S. Katsurabayashi, M. Mitkovski, O.A. Malakhova, D.E. Zhang, M. Umikawa, K. Kariya, S. Goebbels, K.A. Nave, C. Rosenmund, O. Jahn, J. Rhee, and N. Brose, *Regulation of Rap2A by the ubiquitin ligase Nedd4-1 controls neurite development.* Neuron, 2010. **65**(3): p. 358-72.
24. Jordan, B.A., B.D. Fernholz, M. Boussac, C. Xu, G. Grigorean, E.B. Ziff, and T.A. Neubert, *Identification and verification of novel rodent postsynaptic density proteins.* Mol Cell Proteomics, 2004. **3**(9): p. 857-71.
25. Peng, J., M.J. Kim, D. Cheng, D.M. Duong, S.P. Gygi, and M. Sheng, *Semiquantitative proteomic analysis of rat forebrain postsynaptic density fractions by mass spectrometry.* J Biol Chem, 2004. **279**(20): p. 21003-11.
26. Collins, M.O., L. Yu, M.P. Coba, H. Husi, I. Campuzano, W.P. Blackstock, J.S. Choudhary, and S.G. Grant, *Proteomic analysis of in vivo phosphorylated synaptic proteins.* J Biol Chem, 2005. **280**(7): p. 5972-82.
27. Anazi, S., H.E. Shamseldin, D. AlNaqeb, M. Abouelhoda, D. Monies, M.A. Salih, K. Al-Rubeaan, and F.S. Alkuraya, *A null mutation in TNIK defines a novel locus for intellectual disability.* Hum Genet, 2016. **135**(7): p. 773-8.
28. Coba, M.P., N.H. Komiyama, J. Nithianantharajah, M.V. Kopanitsa, T. Indersmitten, N.G. Skene, E.J. Tuck, D.G. Fricker, K.A. Elsegood, L.E. Stanford, N.O. Afinowi, L.M. Saksida, T.J. Bussey, T.J. O'Dell, and S.G. Grant, *TNiK is required for postsynaptic and nuclear signaling pathways and cognitive function.* J Neurosci, 2012. **32**(40): p. 13987-99.
29. Wissing, J., L. Jansch, M. Nimtz, G. Dieterich, R. Hornberger, G. Keri, J. Wehland, and H. Daub, *Proteomics analysis of protein kinases by target class-selective prefractionation and tandem mass spectrometry.* Mol Cell Proteomics, 2007. **6**(3): p. 537-47.

30. Shitashige, M., R. Satow, T. Jigami, K. Aoki, K. Honda, T. Shibata, M. Ono, S. Hirohashi, and T. Yamada, *Traf2- and Nck-interacting kinase is essential for Wnt signaling and colorectal cancer growth.* Cancer Res, 2010. **70**(12): p. 5024-33.
31. Yu, D.H., X. Zhang, H. Wang, L. Zhang, H. Chen, M. Hu, Z. Dong, G. Zhu, Z. Qian, J. Fan, X. Su, Y. Xu, L. Zheng, H. Dong, X. Yin, Q. Ji, and J. Ji, *The essential role of TNIK gene amplification in gastric cancer growth.* Oncogenesis, 2014. **3**: p. e93.
32. Zhang, Y., H. Jiang, M. Qin, X. Su, Z. Cao, and J. Wang, *TNIK serves as a novel biomarker associated with poor prognosis in patients with pancreatic cancer.* Tumour Biol, 2016. **37**(1): p. 1035-40.
33. Kwong, L.N. and W.F. Dove, *APC and its modifiers in colon cancer.* Adv Exp Med Biol, 2009. **656**: p. 85-106.
34. Morin, P.J., K.W. Kinzler, and A.B. Sparks, *beta-Catenin Mutations: Insights into the APC Pathway and the Power of Genetics.* Cancer Res, 2016. **76**(19): p. 5587-5589.
35. Masuda, M. and T. Yamada, *The emergence of TNIK as a therapeutic target for colorectal cancer.* Expert Opin Ther Targets, 2017. **21**(4): p. 353-355.
36. Yamada, T. and M. Masuda, *Emergence of TNIK inhibitors in cancer therapeutics.* Cancer Sci, 2017. **108**(5): p. 818-823.
37. Ho, K.K., K.M. Parnell, Y. Yuan, Y. Xu, S.G. Kultgen, S. Hamblin, T.F. Hendrickson, B. Luo, J.M. Foulks, M.V. McCullar, and S.B. Kanner, *Discovery of 4-phenyl-2-phenylaminopyridine based TNIK inhibitors.* Bioorg Med Chem Lett, 2013. **23**(2): p. 569-73.
38. Masuda, M., Y. Uno, N. Ohbayashi, H. Ohata, A. Mimata, M. Kukimoto-Niino, H. Moriyama, S. Kashimoto, T. Inoue, N. Goto, K. Okamoto, M. Shirouzu, M. Sawa, and T. Yamada, *TNIK inhibition abrogates colorectal cancer stemness.* Nat Commun, 2016. **7**: p. 12586.
39. Kim, J., S.H. Moon, B.T. Kim, C.H. Chae, J.Y. Lee, and S.H. Kim, *A novel aminothiazole KY-05009 with potential to inhibit Traf2- and Nck-interacting kinase (TNIK) attenuates TGF-beta1-mediated epithelial-to-mesenchymal transition in human lung adenocarcinoma A549 cells.* PLoS One, 2014. **9**(10): p. e110180.
40. Heldin, C.H., M. Vanlandewijck, and A. Moustakas, *Regulation of EMT by TGFbeta in cancer.* FEBS Lett, 2012. **586**(14): p. 1959-70.
41. Thiery, J.P., H. Acloque, R.Y. Huang, and M.A. Nieto, *Epithelial-mesenchymal transitions in development and disease.* Cell, 2009. **139**(5): p. 871-90.
42. Canadian Cancer Society's Advisory Committee on Cancer Statistics, *Canadian Cancer Statistics 2017.* Canadian Cancer Society, 2017.
43. Lee, C.H., O. Akin-Olugbade, and A. Kirschenbaum, *Overview of prostate anatomy, histology, and pathology.* Endocrinol Metab Clin North Am, 2011. **40**(3): p. 565-75, viii-ix.
44. Verze, P., T. Cai, and S. Lorenzetti, *The role of the prostate in male fertility, health and disease.* Nat Rev Urol, 2016. **13**(7): p. 379-86.
45. Hayward, S.W. and G.R. Cunha, *The prostate: development and physiology.* Radiol Clin North Am, 2000. **38**(1): p. 1-14.
46. Barron, D.A. and D.R. Rowley, *The reactive stroma microenvironment and prostate cancer progression.* Endocr Relat Cancer, 2012. **19**(6): p. R187-204.

47. Vashchenko, N. and P.A. Abrahamsson, *Neuroendocrine differentiation in prostate cancer: implications for new treatment modalities.* Eur Urol, 2005. **47**(2): p. 147-55.
48. Long, R.M., C. Morrissey, J.M. Fitzpatrick, and R.W. Watson, *Prostate epithelial cell differentiation and its relevance to the understanding of prostate cancer therapies.* Clin Sci (Lond), 2005. **108**(1): p. 1-11.
49. Terry, S. and H. Beltran, *The many faces of neuroendocrine differentiation in prostate cancer progression.* Front Oncol, 2014. **4**: p. 60.
50. Heemers, H.V. and D.J. Tindall, *Androgen receptor (AR) coregulators: a diversity of functions converging on and regulating the AR transcriptional complex.* Endocr Rev, 2007. **28**(7): p. 778-808.
51. Liang, T. and S. Liao, *Inhibition of steroid 5 alpha-reductase by specific aliphatic unsaturated fatty acids.* Biochem J, 1992. **285 (Pt 2)**: p. 557-62.
52. Chuu, C.P., J.M. Kokontis, R.A. Hiipakka, J. Fukuchi, H.P. Lin, C.Y. Lin, C. Huo, and L.C. Su, *Androgens as therapy for androgen receptor-positive castration-resistant prostate cancer.* J Biomed Sci, 2011. **18**: p. 63.
53. Corradi, P.F., R.B. Corradi, and L.W. Greene, *Physiology of the Hypothalamic Pituitary Gonadal Axis in the Male.* Urol Clin North Am, 2016. **43**(2): p. 151-62.
54. Kathrins, M. and C. Niederberger, *Diagnosis and treatment of infertility-related male hormonal dysfunction.* Nat Rev Urol, 2016. **13**(6): p. 309-23.
55. Tan, M.H., J. Li, H.E. Xu, K. Melcher, and E.L. Yong, *Androgen receptor: structure, role in prostate cancer and drug discovery.* Acta Pharmacol Sin, 2015. **36**(1): p. 3-23.
56. Gao, W., C.E. Bohl, and J.T. Dalton, *Chemistry and structural biology of androgen receptor.* Chem Rev, 2005. **105**(9): p. 3352-70.
57. Chen, Y., N.J. Clegg, and H.I. Scher, *Anti-androgens and androgen-depleting therapies in prostate cancer: new agents for an established target.* Lancet Oncol, 2009. **10**(10): p. 981-91.
58. Kash, D.P., M. Lal, A.H. Hashmi, and M. Mubarak, *Utility of digital rectal examination, serum prostate specific antigen, and transrectal ultrasound in the detection of prostate cancer: a developing country perspective.* Asian Pac J Cancer Prev, 2014. **15**(7): p. 3087-91.
59. Keyes, M., J. Crook, G. Morton, E. Vigneault, N. Usmani, and W.J. Morris, *Treatment options for localized prostate cancer.* Can Fam Physician, 2013. **59**(12): p. 1269-74.
60. Huggins, C. and C.V. Hodges, *Studies on prostatic cancer: I. The effect of castration, of estrogen and of androgen injection on serum phosphatases in metastatic carcinoma of the prostate. 1941.* J Urol, 2002. **168**(1): p. 9-12.
61. Chandrasekar, T., J.C. Yang, A.C. Gao, and C.P. Evans, *Mechanisms of resistance in castration-resistant prostate cancer (CRPC).* Transl Androl Urol, 2015. **4**(3): p. 365-80.
62. Climent, M.A., L. Leon-Mateos, A. Gonzalez Del Alba, B. Perez-Valderrama, M.J. Mendez-Vidal, B. Mellado, J.A. Arranz, A. Sanchez-Hernandez, J. Cassinello, D. Olmos, and J. Carles, *Updated recommendations from the Spanish Oncology Genitourinary Group for the treatment of patients with metastatic castration-resistant prostate cancer.* Crit Rev Oncol Hematol, 2015. **96**(2): p. 308-18.
63. Scher, H.I., K. Fizazi, F. Saad, M.E. Taplin, C.N. Sternberg, K. Miller, R. de Wit, P. Mulders, K.N. Chi, N.D. Shore, A.J. Armstrong, T.W. Flaig, A. Flechon, P. Mainwaring, M. Fleming, J.D. Hainsworth, M. Hirmand, B. Selby, L. Seely, J.S. de Bono, and A.

Investigators, *Increased survival with enzalutamide in prostate cancer after chemotherapy.* N Engl J Med, 2012. **367**(13): p. 1187-97.
64. de Bono, J.S., C.J. Logothetis, A. Molina, K. Fizazi, S. North, L. Chu, K.N. Chi, R.J. Jones, O.B. Goodman, Jr., F. Saad, J.N. Staffurth, P. Mainwaring, S. Harland, T.W. Flaig, T.E. Hutson, T. Cheng, H. Patterson, J.D. Hainsworth, C.J. Ryan, C.N. Sternberg, S.L. Ellard, A. Flechon, M. Saleh, M. Scholz, E. Efstathiou, A. Zivi, D. Bianchini, Y. Loriot, N. Chieffo, T. Kheoh, C.M. Haqq, H.I. Scher, and C.-A.-. Investigators, *Abiraterone and increased survival in metastatic prostate cancer.* N Engl J Med, 2011. **364**(21): p. 1995-2005.
65. Scher, H.I., T.M. Beer, C.S. Higano, A. Anand, M.E. Taplin, E. Efstathiou, D. Rathkopf, J. Shelkey, E.Y. Yu, J. Alumkal, D. Hung, M. Hirmand, L. Seely, M.J. Morris, D.C. Danila, J. Humm, S. Larson, M. Fleisher, C.L. Sawyers, and C. Prostate Cancer Foundation/Department of Defense Prostate Cancer Clinical Trials, *Antitumour activity of MDV3100 in castration-resistant prostate cancer: a phase 1-2 study.* Lancet, 2010. **375**(9724): p. 1437-46.
66. Ryan, C.J., M.R. Smith, J.S. de Bono, A. Molina, C.J. Logothetis, P. de Souza, K. Fizazi, P. Mainwaring, J.M. Piulats, S. Ng, J. Carles, P.F. Mulders, E. Basch, E.J. Small, F. Saad, D. Schrijvers, H. Van Poppel, S.D. Mukherjee, H. Suttmann, W.R. Gerritsen, T.W. Flaig, D.J. George, E.Y. Yu, E. Efstathiou, A. Pantuck, E. Winquist, C.S. Higano, M.E. Taplin, Y. Park, T. Kheoh, T. Griffin, H.I. Scher, D.E. Rathkopf, and C.-A.-. Investigators, *Abiraterone in metastatic prostate cancer without previous chemotherapy.* N Engl J Med, 2013. **368**(2): p. 138-48.
67. Tilki, D., E.M. Schaeffer, and C.P. Evans, *Understanding Mechanisms of Resistance in Metastatic Castration-resistant Prostate Cancer: The Role of the Androgen Receptor.* Eur Urol Focus, 2016. **2**(5): p. 499-505.
68. Beltran, H., S. Tomlins, A. Aparicio, V. Arora, D. Rickman, G. Ayala, J. Huang, L. True, M.E. Gleave, H. Soule, C. Logothetis, and M.A. Rubin, *Aggressive variants of castration-resistant prostate cancer.* Clin Cancer Res, 2014. **20**(11): p. 2846-50.
69. Wang, H.T., Y.H. Yao, B.G. Li, Y. Tang, J.W. Chang, and J. Zhang, *Neuroendocrine Prostate Cancer (NEPC) progressing from conventional prostatic adenocarcinoma: factors associated with time to development of NEPC and survival from NEPC diagnosis-a systematic review and pooled analysis.* J Clin Oncol, 2014. **32**(30): p. 3383-90.
70. Helpap, B., J. Kollermann, and U. Oehler, *Neuroendocrine differentiation in prostatic carcinomas: histogenesis, biology, clinical relevance, and future therapeutical perspectives.* Urol Int, 1999. **62**(3): p. 133-8.
71. Aparicio, A., C.J. Logothetis, and S.N. Maity, *Understanding the lethal variant of prostate cancer: power of examining extremes.* Cancer Discov, 2011. **1**(6): p. 466-8.
72. Small, E.J., J. Huang, J. Youngren, A. Sokolov, R.R. Aggarwal, G. Thomas, L. True, L. Zhang, A. Foye, J. Alumkal, C.J. Ryan, M. Rettig, C.P. Evans, M. Gleave, R. Baertsch, J. Stuart, R.E. Reiter, P. Lara, K. Chi, and T.M. Beer, *Characterization of neuroendocrine prostate cancer (NEPC) in patients with metastatic castration resistant prostate cancer (mCRPC) resistant to abiraterone (Abi) or enzalutamide (Enz): Preliminary results from the SU2C/PCF/AACR West Coast Prostate Cancer Dream Team (WCDT).* Journal of Clinical Oncology, 2015. **33**(no. 15_suppl (May 2015)): p. 5003-5003.

73. Bluemn, E.G., I.M. Coleman, J.M. Lucas, R.T. Coleman, S. Hernandez-Lopez, R. Tharakan, D. Bianchi-Frias, R.F. Dumpit, A. Kaipainen, A.N. Corella, Y.C. Yang, M.D. Nyquist, E. Mostaghel, A.C. Hsieh, X. Zhang, E. Corey, L.G. Brown, H.M. Nguyen, K. Pienta, M. Ittmann, M. Schweizer, L.D. True, D. Wise, P.S. Rennie, R.L. Vessella, C. Morrissey, and P.S. Nelson, *Androgen Receptor Pathway-Independent Prostate Cancer Is Sustained through FGF Signaling.* Cancer Cell, 2017. **32**(4): p. 474-489 e6.
74. Beltran, H., D. Prandi, J.M. Mosquera, M. Benelli, L. Puca, J. Cyrta, C. Marotz, E. Giannopoulou, B.V. Chakravarthi, S. Varambally, S.A. Tomlins, D.M. Nanus, S.T. Tagawa, E.M. Van Allen, O. Elemento, A. Sboner, L.A. Garraway, M.A. Rubin, and F. Demichelis, *Divergent clonal evolution of castration-resistant neuroendocrine prostate cancer.* Nat Med, 2016. **22**(3): p. 298-305.
75. Lin, D., A.W. Wyatt, H. Xue, Y. Wang, X. Dong, A. Haegert, R. Wu, S. Brahmbhatt, F. Mo, L. Jong, R.H. Bell, S. Anderson, A. Hurtado-Coll, L. Fazli, M. Sharma, H. Beltran, M. Rubin, M. Cox, P.W. Gout, J. Morris, L. Goldenberg, S.V. Volik, M.E. Gleave, C.C. Collins, and Y. Wang, *High fidelity patient-derived xenografts for accelerating prostate cancer discovery and drug development.* Cancer Res, 2014. **74**(4): p. 1272-83.
76. Bishop, J.L., D. Thaper, S. Vahid, A. Davies, K. Ketola, H. Kuruma, R. Jama, K.M. Nip, A. Angeles, F. Johnson, A.W. Wyatt, L. Fazli, M.E. Gleave, D. Lin, M.A. Rubin, C.C. Collins, Y. Wang, H. Beltran, and A. Zoubeidi, *The Master Neural Transcription Factor BRN2 Is an Androgen Receptor-Suppressed Driver of Neuroendocrine Differentiation in Prostate Cancer.* Cancer Discov, 2017. **7**(1): p. 54-71.
77. Li, Y., N. Donmez, C. Sahinalp, N. Xie, Y. Wang, H. Xue, F. Mo, H. Beltran, M. Gleave, Y. Wang, C. Collins, and X. Dong, *SRRM4 Drives Neuroendocrine Transdifferentiation of Prostate Adenocarcinoma Under Androgen Receptor Pathway Inhibition.* Eur Urol, 2017. **71**(1): p. 68-78.
78. Alanee, S., A. Moore, M. Nutt, B. Holland, D. Dynda, A. El-Zawahry, and K.T. McVary, *Contemporary Incidence and Mortality Rates of Neuroendocrine Prostate Cancer.* Anticancer Res, 2015. **35**(7): p. 4145-50.
79. Beltran, H., S.T. Tagawa, K. Park, T. MacDonald, M.I. Milowsky, J.M. Mosquera, M.A. Rubin, and D.M. Nanus, *Challenges in recognizing treatment-related neuroendocrine prostate cancer.* J Clin Oncol, 2012. **30**(36): p. e386-9.
80. Vlachostergios, P.J. and C.N. Papandreou, *Targeting neuroendocrine prostate cancer: molecular and clinical perspectives.* Front Oncol, 2015. **5**: p. 6.
81. Beltran, H., D.S. Rickman, K. Park, S.S. Chae, A. Sboner, T.Y. MacDonald, Y. Wang, K.L. Sheikh, S. Terry, S.T. Tagawa, R. Dhir, J.B. Nelson, A. de la Taille, Y. Allory, M.B. Gerstein, S. Perner, K.J. Pienta, A.M. Chinnaiyan, Y. Wang, C.C. Collins, M.E. Gleave, F. Demichelis, D.M. Nanus, and M.A. Rubin, *Molecular characterization of neuroendocrine prostate cancer and identification of new drug targets.* Cancer Discov, 2011. **1**(6): p. 487-95.
82. Mizokami, A., K. Izumi, H. Konaka, Y. Kitagawa, Y. Kadono, K. Narimoto, T. Nohara, A.K. Bahl, and M. Namiki, *Understanding prostate-specific antigen dynamics in monitoring metastatic castration-resistant prostate cancer: implications for clinical practice.* Asian J Androl, 2017. **19**(2): p. 143-148.
83. Palmgren, J.S., S.S. Karavadia, and M.R. Wakefield, *Unusual and underappreciated: small cell carcinoma of the prostate.* Semin Oncol, 2007. **34**(1): p. 22-9.

84. Epstein, J.I., M.B. Amin, H. Beltran, T.L. Lotan, J.M. Mosquera, V.E. Reuter, B.D. Robinson, P. Troncoso, and M.A. Rubin, *Proposed morphologic classification of prostate cancer with neuroendocrine differentiation.* Am J Surg Pathol, 2014. **38**(6): p. 756-67.
85. Rescigno, P., D.N. Rodrigues, and J.S. de Bono, *Circulating biomarkers of neuroendocrine prostate cancer: an unmet challenge.* BJU Int, 2017. **119**(1): p. 3-4.
86. Gut, P., A. Czarnywojtek, J. Fischbach, M. Baczyk, K. Ziemnicka, E. Wrotkowska, M. Gryczynska, and M. Ruchala, *Chromogranin A - unspecific neuroendocrine marker. Clinical utility and potential diagnostic pitfalls.* Arch Med Sci, 2016. **12**(1): p. 1-9.
87. Beltran, H., A. Jendrisak, M. Landers, J.M. Mosquera, M. Kossai, J. Louw, R. Krupa, R.P. Graf, N.A. Schreiber, D.M. Nanus, S.T. Tagawa, D. Marrinucci, R. Dittamore, and H.I. Scher, *The Initial Detection and Partial Characterization of Circulating Tumor Cells in Neuroendocrine Prostate Cancer.* Clin Cancer Res, 2016. **22**(6): p. 1510-9.
88. Lack, J., M. Gillard, M. Cam, G.P. Paner, and D.J. VanderWeele, *Circulating tumor cells capture disease evolution in advanced prostate cancer.* J Transl Med, 2017. **15**(1): p. 44.
89. Yuan, T.C., S. Veeramani, and M.F. Lin, *Neuroendocrine-like prostate cancer cells: neuroendocrine transdifferentiation of prostate adenocarcinoma cells.* Endocr Relat Cancer, 2007. **14**(3): p. 531-47.
90. Rickman, D.S., H. Beltran, F. Demichelis, and M.A. Rubin, *Biology and evolution of poorly differentiated neuroendocrine tumors.* Nat Med, 2017. **23**(6): p. 1-10.
91. Nadal, R., M. Schweizer, O.N. Kryvenko, J.I. Epstein, and M.A. Eisenberger, *Small cell carcinoma of the prostate.* Nat Rev Urol, 2014. **11**(4): p. 213-9.
92. Tomlins, S.A., D.R. Rhodes, S. Perner, S.M. Dhanasekaran, R. Mehra, X.W. Sun, S. Varambally, X. Cao, J. Tchinda, R. Kuefer, C. Lee, J.E. Montie, R.B. Shah, K.J. Pienta, M.A. Rubin, and A.M. Chinnaiyan, *Recurrent fusion of TMPRSS2 and ETS transcription factor genes in prostate cancer.* Science, 2005. **310**(5748): p. 644-8.
93. Lotan, T.L., N.S. Gupta, W. Wang, A. Toubaji, M.C. Haffner, A. Chaux, J.L. Hicks, A.K. Meeker, C.J. Bieberich, A.M. De Marzo, J.I. Epstein, and G.J. Netto, *ERG gene rearrangements are common in prostatic small cell carcinomas.* Mod Pathol, 2011. **24**(6): p. 820-8.
94. Akamatsu, S., A.W. Wyatt, D. Lin, S. Lysakowski, F. Zhang, S. Kim, C. Tse, K. Wang, F. Mo, A. Haegert, S. Brahmbhatt, R. Bell, H. Adomat, Y. Kawai, H. Xue, X. Dong, L. Fazli, H. Tsai, T.L. Lotan, M. Kossai, J.M. Mosquera, M.A. Rubin, H. Beltran, A. Zoubeidi, Y. Wang, M.E. Gleave, and C.C. Collins, *The Placental Gene PEG10 Promotes Progression of Neuroendocrine Prostate Cancer.* Cell Rep, 2015. **12**(6): p. 922-36.
95. Maddison, L.A., B.W. Sutherland, R.J. Barrios, and N.M. Greenberg, *Conditional deletion of Rb causes early stage prostate cancer.* Cancer Res, 2004. **64**(17): p. 6018-25.
96. Tan, H.L., A. Sood, H.A. Rahimi, W. Wang, N. Gupta, J. Hicks, S. Mosier, C.D. Gocke, J.I. Epstein, G.J. Netto, W. Liu, W.B. Isaacs, A.M. De Marzo, and T.L. Lotan, *Rb loss is characteristic of prostatic small cell neuroendocrine carcinoma.* Clin Cancer Res, 2014. **20**(4): p. 890-903.
97. Chiaverotti, T., S.S. Couto, A. Donjacour, J.H. Mao, H. Nagase, R.D. Cardiff, G.R. Cunha, and A. Balmain, *Dissociation of epithelial and neuroendocrine carcinoma lineages in the transgenic adenocarcinoma of mouse prostate model of prostate cancer.* Am J Pathol, 2008. **172**(1): p. 236-46.

98. Ku, S.Y., S. Rosario, Y. Wang, P. Mu, M. Seshadri, Z.W. Goodrich, M.M. Goodrich, D.P. Labbe, E.C. Gomez, J. Wang, H.W. Long, B. Xu, M. Brown, M. Loda, C.L. Sawyers, L. Ellis, and D.W. Goodrich, *Rb1 and Trp53 cooperate to suppress prostate cancer lineage plasticity, metastasis, and antiandrogen resistance.* Science, 2017. **355**(6320): p. 78-83.
99. Mu, P., Z. Zhang, M. Benelli, W.R. Karthaus, E. Hoover, C.C. Chen, J. Wongvipat, S.Y. Ku, D. Gao, Z. Cao, N. Shah, E.J. Adams, W. Abida, P.A. Watson, D. Prandi, C.H. Huang, E. de Stanchina, S.W. Lowe, L. Ellis, H. Beltran, M.A. Rubin, D.W. Goodrich, F. Demichelis, and C.L. Sawyers, *SOX2 promotes lineage plasticity and antiandrogen resistance in TP53- and RB1-deficient prostate cancer.* Science, 2017. **355**(6320): p. 84-88.
100. Zou, M., R. Toivanen, A. Mitrofanova, N. Floch, S. Hayati, Y. Sun, C. Le Magnen, D. Chester, E.A. Mostaghel, A. Califano, M.A. Rubin, M.M. Shen, and C. Abate-Shen, *Transdifferentiation as a Mechanism of Treatment Resistance in a Mouse Model of Castration-Resistant Prostate Cancer.* Cancer Discov, 2017. **7**(7): p. 736-749.
101. Lapuk, A.V., C. Wu, A.W. Wyatt, A. McPherson, B.J. McConeghy, S. Brahmbhatt, F. Mo, A. Zoubeidi, S. Anderson, R.H. Bell, A. Haegert, R. Shukin, Y. Wang, L. Fazli, A. Hurtado-Coll, E.C. Jones, F. Hach, F. Hormozdiari, I. Hajirasouliha, P.C. Boutros, R.G. Bristow, Y. Zhao, M.A. Marra, A. Fanjul, C.A. Maher, A.M. Chinnaiyan, M.A. Rubin, H. Beltran, S.C. Sahinalp, M.E. Gleave, S.V. Volik, and C.C. Collins, *From sequence to molecular pathology, and a mechanism driving the neuroendocrine phenotype in prostate cancer.* J Pathol, 2012. **227**(3): p. 286-97.
102. Lee, J.K., J.W. Phillips, B.A. Smith, J.W. Park, T. Stoyanova, E.F. McCaffrey, R. Baertsch, A. Sokolov, J.G. Meyerowitz, C. Mathis, D. Cheng, J.M. Stuart, K.M. Shokat, W.C. Gustafson, J. Huang, and O.N. Witte, *N-Myc Drives Neuroendocrine Prostate Cancer Initiated from Human Prostate Epithelial Cells.* Cancer Cell, 2016. **29**(4): p. 536-547.
103. Dardenne, E., H. Beltran, M. Benelli, K. Gayvert, A. Berger, L. Puca, J. Cyrta, A. Sboner, Z. Noorzad, T. MacDonald, C. Cheung, K.S. Yuen, D. Gao, Y. Chen, M. Eilers, J.M. Mosquera, B.D. Robinson, O. Elemento, M.A. Rubin, F. Demichelis, and D.S. Rickman, *N-Myc Induces an EZH2-Mediated Transcriptional Program Driving Neuroendocrine Prostate Cancer.* Cancer Cell, 2016. **30**(4): p. 563-577.
104. Horoszewicz, J.S., S.S. Leong, E. Kawinski, J.P. Karr, H. Rosenthal, T.M. Chu, E.A. Mirand, and G.P. Murphy, *LNCaP model of human prostatic carcinoma.* Cancer Res, 1983. **43**(4): p. 1809-18.
105. Shen, R., T. Dorai, M. Szaboles, A.E. Katz, C.A. Olsson, and R. Buttyan, *Transdifferentiation of cultured human prostate cancer cells to a neuroendocrine cell phenotype in a hormone-depleted medium.* Urol Oncol, 1997. **3**(2): p. 67-75.
106. Deeble, P.D., D.J. Murphy, S.J. Parsons, and M.E. Cox, *Interleukin-6- and cyclic AMP-mediated signaling potentiates neuroendocrine differentiation of LNCaP prostate tumor cells.* Mol Cell Biol, 2001. **21**(24): p. 8471-82.
107. Danza, G., C. Di Serio, F. Rosati, G. Lonetto, N. Sturli, D. Kacer, A. Pennella, G. Ventimiglia, R. Barucci, A. Piscazzi, I. Prudovsky, M. Landriscina, N. Marchionni, and F. Tarantini, *Notch signaling modulates hypoxia-induced neuroendocrine differentiation of human prostate cancer cells.* Mol Cancer Res, 2012. **10**(2): p. 230-8.

108. Deng, X., B.D. Elzey, J.M. Poulson, W.B. Morrison, S.C. Ko, N.M. Hahn, T.L. Ratliff, and C.D. Hu, *Ionizing radiation induces neuroendocrine differentiation of prostate cancer cells in vitro, in vivo and in prostate cancer patients.* Am J Cancer Res, 2011. **1**(7): p. 834-44.
109. Nouri, M., J. Caradec, A.A. Lubik, N. Li, B.G. Hollier, M. Takhar, M. Altimirano-Dimas, M. Chen, M. Roshan-Moniri, M. Butler, M. Lehman, J. Bishop, S. Truong, S.C. Huang, D. Cochrane, M. Cox, C. Collins, M. Gleave, N. Erho, M. Alshalafa, E. Davicioni, C. Nelson, S. Gregory-Evans, R.J. Karnes, R.B. Jenkins, E.A. Klein, and R. Buttyan, *Therapy-induced developmental reprogramming of prostate cancer cells and acquired therapy resistance.* Oncotarget, 2017. **8**(12): p. 18949-18967.
110. Goldman, M., B. Craft, T. Swatloski, M. Cline, O. Morozova, M. Diekhans, D. Haussler, and J. Zhu, *The UCSC Cancer Genomics Browser: update 2015.* Nucleic Acids Res, 2015. **43**(Database issue): p. D812-7.
111. Shkoda, A., J.A. Town, J. Griese, M. Romio, H. Sarioglu, T. Knofel, F. Giehler, and A. Kieser, *The germinal center kinase TNIK is required for canonical NF-kappaB and JNK signaling in B-cells by the EBV oncoprotein LMP1 and the CD40 receptor.* PLoS Biol, 2012. **10**(8): p. e1001376.
112. Leparc, G.G. and R.D. Mitra, *A sensitive procedure to detect alternatively spliced mRNA in pooled-tissue samples.* Nucleic Acids Res, 2007. **35**(21): p. e146.
113. Claessens, F., G. Verrijdt, E. Schoenmakers, A. Haelens, B. Peeters, G. Verhoeven, and W. Rombauts, *Selective DNA binding by the androgen receptor as a mechanism for hormone-specific gene regulation.* J Steroid Biochem Mol Biol, 2001. **76**(1-5): p. 23-30.
114. Le, K.Q., B.S. Prabhakar, W.J. Hong, and L.C. Li, *Alternative splicing as a biomarker and potential target for drug discovery.* Acta Pharmacol Sin, 2015. **36**(10): p. 1212-8.
115. Khemlina, G., S. Ikeda, and R. Kurzrock, *Molecular landscape of prostate cancer: implications for current clinical trials.* Cancer Treat Rev, 2015. **41**(9): p. 761-6.
116. Wang, L., B. Zhu, S. Wang, Y. Wu, W. Zhan, S. Xie, H. Shi, and R. Yu, *Regulation of glioma migration and invasion via modification of Rap2a activity by the ubiquitin ligase Nedd4-1.* Oncol Rep, 2017. **37**(5): p. 2565-2574.
117. Shang, Z., Q. Cai, M. Zhang, S. Zhu, Y. Ma, L. Sun, N. Jiang, J. Tian, X. Niu, J. Chen, Y. Sun, and Y. Niu, *A switch from CD44(+) cell to EMT cell drives the metastasis of prostate cancer.* Oncotarget, 2015. **6**(2): p. 1202-16.
118. Conteduca, V., M. Aieta, D. Amadori, and U. De Giorgi, *Neuroendocrine differentiation in prostate cancer: current and emerging therapy strategies.* Crit Rev Oncol Hematol, 2014. **92**(1): p. 11-24.
119. Yang, X., J. Coulombe-Huntington, S. Kang, G.M. Sheynkman, T. Hao, A. Richardson, S. Sun, F. Yang, Y.A. Shen, R.R. Murray, K. Spirohn, B.E. Begg, M. Duran-Frigola, A. MacWilliams, S.J. Pevzner, Q. Zhong, S.A. Trigg, S. Tam, L. Ghamsari, N. Sahni, S. Yi, M.D. Rodriguez, D. Balcha, G. Tan, M. Costanzo, B. Andrews, C. Boone, X.J. Zhou, K. Salehi-Ashtiani, B. Charloteaux, A.A. Chen, M.A. Calderwood, P. Aloy, F.P. Roth, D.E. Hill, L.M. Iakoucheva, Y. Xia, and M. Vidal, *Widespread Expansion of Protein Interaction Capabilities by Alternative Splicing.* Cell, 2016. **164**(4): p. 805-17.
120. Kelemen, O., P. Convertini, Z. Zhang, Y. Wen, M. Shen, M. Falaleeva, and S. Stamm, *Function of alternative splicing.* Gene, 2013. **514**(1): p. 1-30.

121. Boise, L.H., M. Gonzalez-Garcia, C.E. Postema, L. Ding, T. Lindsten, L.A. Turka, X. Mao, G. Nunez, and C.B. Thompson, *bcl-x, a bcl-2-related gene that functions as a dominant regulator of apoptotic cell death.* Cell, 1993. **74**(4): p. 597-608.
122. Garibyan, L. and N. Avashia, *Polymerase chain reaction.* J Invest Dermatol, 2013. **133**(3): p. e6.
123. Barton, B.E., T.F. Murphy, P. Shu, H.F. Huang, M. Meyenhofer, and A. Barton, *Novel single-stranded oligonucleotides that inhibit signal transducer and activator of transcription 3 induce apoptosis in vitro and in vivo in prostate cancer cell lines.* Mol Cancer Ther, 2004. **3**(10): p. 1183-91.

Appendices

Appendix A Primer sequences

The forward (F) and reverse (R) primer sequences used for qPCR, ChIP assay, PCR cloning, and PCR for detecting transcript variants.

A.1 qPCR primer sequences

Gene Name	Primer sequence (5' → 3')
TNIK	F: CTTGTGGTCTTTGGGTATCAC R: CCACTTCTTAGACTTCAGCC
PSA	F: CACAGCCTGTTTCATCCTGA R: AGGTCCATGACCTTCACAGC
NCAM1	F: GATGCGACCATCCACCTCAA R: TCTCCGGAGGCTTCACAGGTA
NSE	F: GAACTATCCTGTGGTCTCC R: CGACATTGGCTGTGAACTTG
SYP	F: TCAGTTCCGGGTGGTCAAG R: AAGACCCATTGCAGCACCTT
CHGA	F: TCCAAGGCGCCAAGGA R: CATCTTCAAAACCGCTGTGTTTC
GAPDH	F: CGACCTGACCTGCCGTCTAGAA R: GGTGTCGCTGGTGAAGTCGAGAG

A.2 ChIP primer sequences

Gene	Primer sequence (5' → 3')
TNIK +231997/+232096	F: ACAAAGTGACTGGGGACGTTT R: TGCTGTACTATGTCAATGGGGG

A.3 PCR cloning primer sequences

The restriction sites *Xho*I and *Xba*I sites were underlined in the primer sequences.

Insert	Primer sequence (5' → 3')
HA-TNIK	F: TGCTTACTCGAGATGGAATATCCTTATGAC R: TCAGTCTAGATCATTACCAGTTCATCATGG

A.4 PCR primer sequences for detecting each TNIK transcript variant:

TNIK transcript variant	Primer sequence (5' → 3')
Primer A	F: ACAGGAATACATCAGGCGACA
Primer B	R: AATGCCGTCAGATCCTCATCTAT
Primer C	F: GCATGAACAGGAATATAAGCGCAA
Primer D	R: TCAGATCAGCTGGTCGACTG

Appendix B PCR programs

B.1 PCR for cloning HA-TNIK insert from plasmid

PCR for cloning HA-TNIK insert:

Step	Temperature	Time
Initial Denaturation	98˚C	30 sec
30 cycles	98˚C	10 sec
	52˚C	30 sec
	72˚C	2 min
Final Extension	72˚C	2 min
Hold	4˚C	forever

B.2 PCR for detecting TNIK transcript variants

PCR for TNIK transcript variants from cDNA samples:

Step	Temperature	Time
Initial Denaturation	98˚C	30 sec
30 cycles	98˚C	10 sec
	66˚C	30 sec
	72˚C	33 sec
Final Extension	72˚C	2 min
Hold	4˚C	forever

Appendix C Supplementary Figures

C.1 DNA samples after XhoI and XbaI restriction digestion

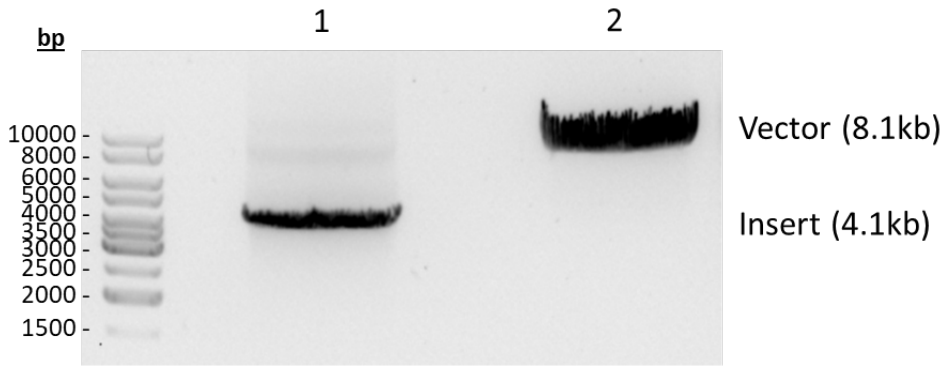

Samples 1: HA-TNIK PCR insert (4.1kb) and 2: pLVX-IRES-Puro vector (8.1kb) were digested by restriction enzymes *Xho*I and *Xba*I overnight, which were separated by agarose gel electrophoresis.

C.2 Plasmid DNA of pLVX-HA-TNIK-IRES-Puro clones

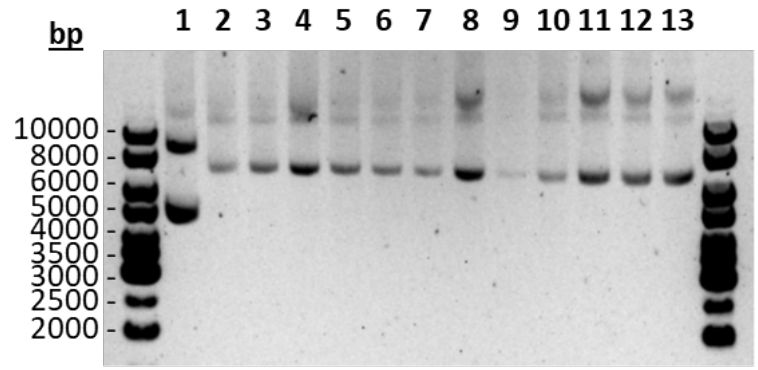

Plasmid DNA in lane 1: pLVX-IRES-Puro and 2-13: pLVX-HA-TNIK-IRES-Puro clones #1-12 were separated by agarose gel electrophoresis.

C.3 PCR for checking orientation of HA-TNIK insert

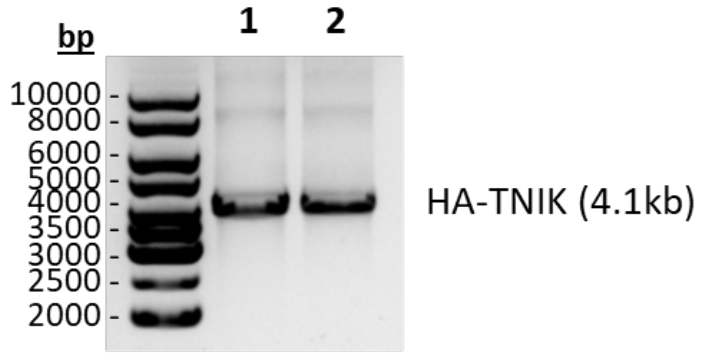

PCR product of HA-TNIK insert from lane 1: pRK5-HA-TNIK and lane 2: pLVX-HA-TNIK-IRES-Puro were separated by agarose gel electrophoresis.

C.4 AR binding site on TNIK gene from publicly available AR ChIP-seq data sets

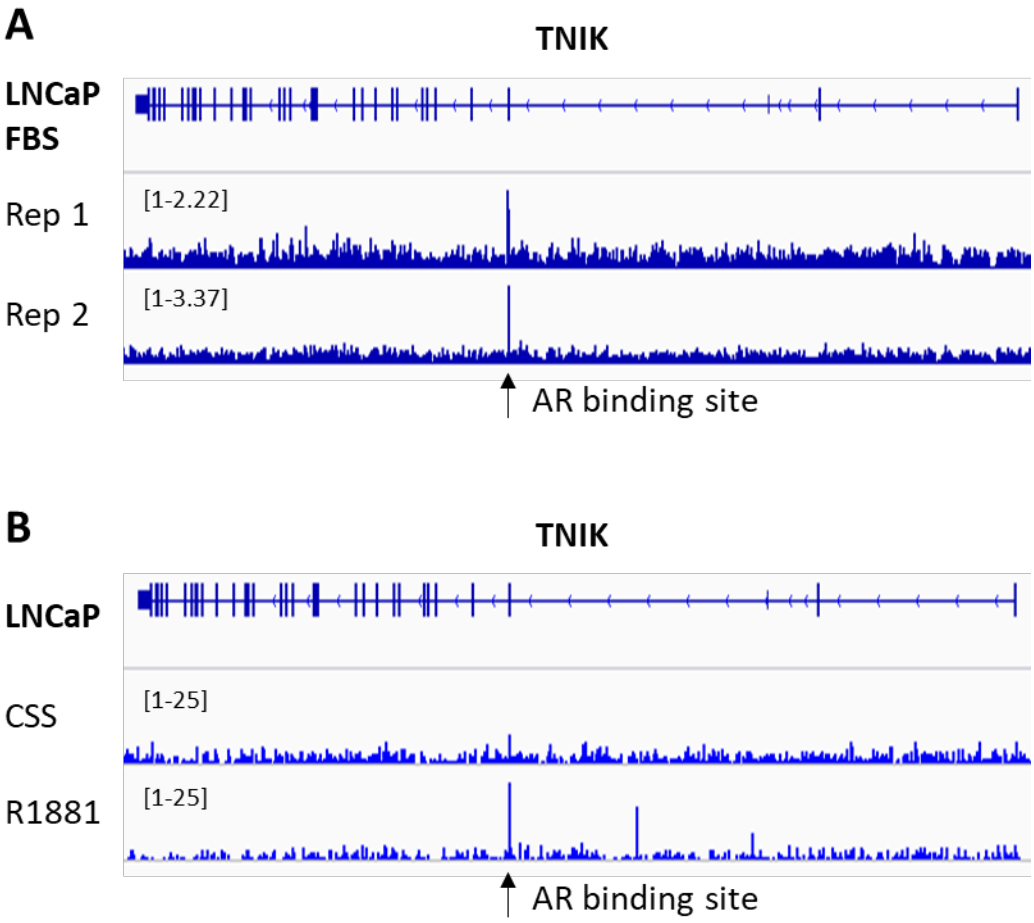

AR binding site on TNIK gene was examined in publicly available AR ChIP-seq data sets in (A) NCBI GEO data sets GSM2122804 and GSM2122804 that are biological replicates of LNCaP cells cultured in media with normal serum (FBS) and (B) NCBI GEO data sets GSM1691153 and GSM1691147 that are LNCaP cells cultured in androgen depleted media (CSS) with or without R1881 stimulation.

C.5 Effect of overexpressing or silencing TNIK on TCF transcriptional activity

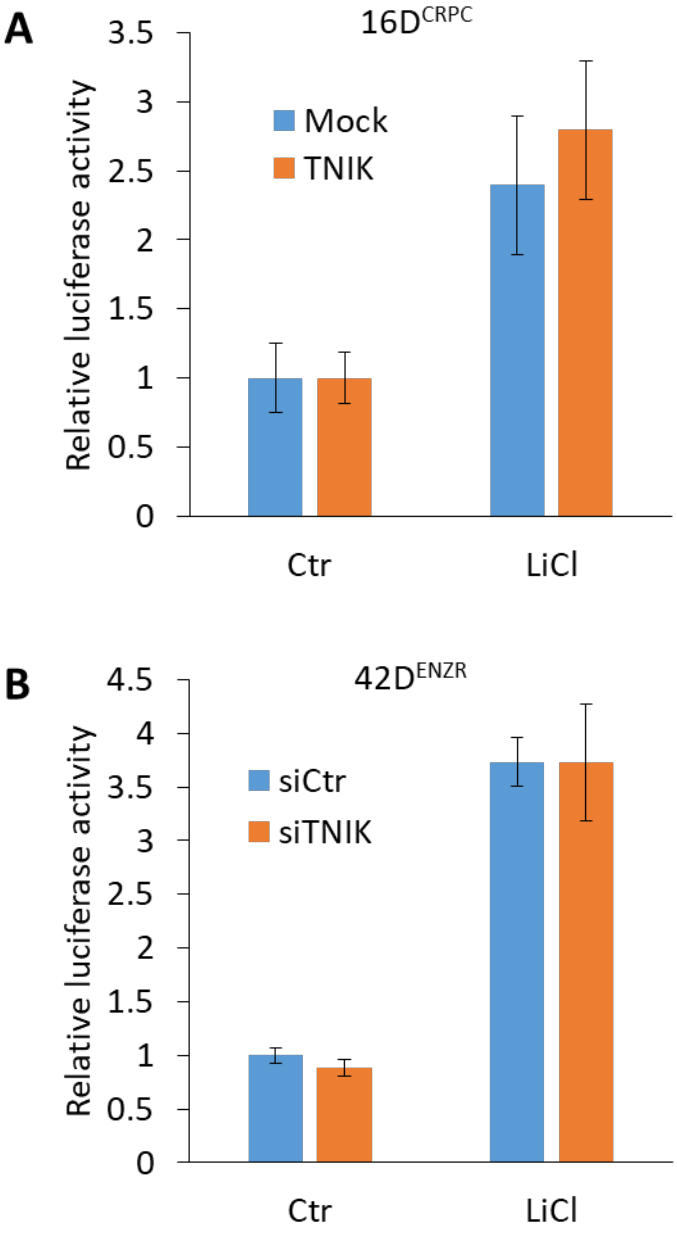

Relative transcriptional activity of TCF in (A) $16D^{TNIK}$ compared to $16D^{Mock}$ and (B) $42D^{ENZR}$ transfected with siTNIK compared to siCtr. Cells were stimulated with 50 mM LiCl for 24 hours.

Appendix D Supplementary Materials and Methods

D.1 Luciferase Assay

For measuring TCF transcriptional activity, 2 x 10^5 cells were seeded in each well in triplicate on a 6-well plate. For each 6-well plate, cells were transiently transfected with 9μg of TCF reporter (pGL3-OT, Addgene) and 1μg of Renilla luciferase reporter (Promega) using TransIT-2020 transfection reagent (Mirus Bio) according to manufacturer's procedure. Luciferase activities were measured using the Dual-Luciferase Reporter Assay System (Promega) using TECAN M200Pro plate reader (Tecan). The Firefly luciferase signal in each sample was normalized with Renilla luciferase signal.